APPLICATIONS OF CONVEX OPTIMIZATION IN NON-ORTHOGONAL MULTIPLE ACCESS SYSTEMS

A Thesis Submitted to The University of Manchester for The Degree of Doctor of Philosophy in the Faculty of Science and Engineering

2021

By

Suhaib M Al Basit

School of Engineering

Department of Electrical and Electronic Engineering

Table of contents

Table of Contents **2**

List of Figures **7**

List of Tables **11**

List of Algorithms **13**

List of Abbreviations **14**

Abstract **18**

Declaration **19**

Copyright **20**

Acknowledgments **22**

1 Introduction **24**

1.1 Background 24

1.1.1 On The Track to Beyond 5G 24

1.1.2 Multiple Access Techniques for Beyond 5G 25

1.1.2.1 Wireless Standardization Overview 25

1.1.2.2 Recent Multiple Access Techniques 27

1.2 Motivation and Contributions 29

1.3 Related Works 32

1.3.1 Non-orthogonal Multiple Access 33

1.3.2 NOMA in Multiple-Antenna systems 34

1.3.3 NOMA and Cooperative Transmission 35

1.4 Dissertation Organization 37

1.5 Author's Publications 38

2 Background Information **39**

2.1 Power Domain Non Orthogonal Multiple Access 39

2.1.1 Basics of NOMA 39

2.1.2 Advantages of NOMA Systems 40

2.1.3 NOMA in Multi-Antenna Systems 41

2.1.4 Cooperative NOMA Transmission 43

2.2 Convex Optimization 44

2.2.1 Quasiconvex Functions 45

2.2.2 Semi-definite Relaxation 47

2.2.3 $\mathcal{S}$-procedure 49

2.2.3.1 Proof of $\mathcal{S}$-procedure 50

3 Joint Beamforming and Power Allocation Design in Downlink Non-Orthogonal Multiple Access Systems 54

3.1 Introduction 54

3.2 System Model and Problem Formulation 55

3.3 Joint Design of Beamforming and Power Allocation 59

3.3.1 Semidefinite Relaxation (SDR) Approach 60

3.3.2 SCA based on AGM Inequality 61

3.4 Simulation Results 65

3.4.1 Sum Rate of Users 65

3.4.2 Convergency Property 67

3.4.3 Rank Results 68

3.5 Summary 70

4 Maximizing SINR for Non-Orthogonal Multiple Access With Bounded Channel Uncertainties **71**

4.1 Introduction 71

4.2 System Model and Problem Formulation 72

4.3 Proposed Optimization Methods 74

4.4 Simulation Result 79

4.5 Summary 83

5 Maximizing Sum Rate for FD/HD Cooperative NOMA System with Jointly Optimizing Beamformer and Relay Power **84**

5.1 Introduction 84

5.2 System Model and Problem Formulation 85

5.3 Proposed Optimization Methods 91

5.3.1 FD/HD Cooperative NOMA Under Perfect CSI Conditions . . . 91

5.3.1.1 FD Cooperative NOMA with MRC and without MRC 91

Alternating Algorithm 92

GP Algorithm 93

Nested Bisection 97

5.3.1.2 HD Cooperative NOMA with MRC and without MRC 98

Alternating Algorithm 99

GP Algorithm 99

Nested Bisection 101

5.3.2 FD/HD Cooperative NOMA Under Imperfect CSI Conditions . 102

5.3.2.1 FD Cooperative NOMA with MRC and without MRC 103

5.3.2.2 HD Cooperative NOMA with MRC and without MRC 107

5.4 Simulation Result 110

5.5 Conclusion 126

6 Conclusions and Directions for Future Work **127**

6.1 Summary 127

6.2 Conclusions 129

6.3 Future Works 130

6.3.1 Extensions of Current Works 130

6.3.2 Promising Future Directions 131

Bibliography **133**

Appendix A **143**

A.1 $\mathcal{S}$-lemma 143

Appendix B **146**

List of Figures

2.1 Basic NOMA transmission schemes [3]. 40

2.2 Beamforming MIMO-NOMA technique [3]. 42

2.3 Downlink broadcast channel in a NOMA system [3]. 42

2.4 Clarification of a quasiconvex function. 45

2.5 Links between different functions sets [69]. 46

3.1 Downlink broadcast channel in a NOMA system. 55

3.2 Comparison of the sum rate of the users in Group 1 versus SNR with $M = 6$ and $K = 4$. 66

3.3 Sum rate of the users in Group 1 versus the iteration index for different SNRs with $M = 6$ and $K = 4$. 67

3.4 Sum rate of the users in Group 1 versus the iteration index for different values of K and M with SNR $= 20$ dB. 68

3.5 The ratio between the largest eigenvalue and the second largest eigenvalue of the optimal beamforming matrix versus the number of antennas with $K = 2$. 69

4.1 Achievable rate for maximized SINR user under different transmitting power with several channel estimation error bound. 80

4.2 Achievable rate for maximized SINR user under different transmitting power and different minimum targeted rate for the other users in the cell R_{Th} number of users in the cell 81

4.3 Achievable rate for maximized SINR user under different transmitting power and different antenna configuration a the Bs 82

4.4 Achievable rate for maximized SINR user under different transmitting power and different number of users in the cell 82

5.1 The downlink FD cooperative NOMA system mode. 86

5.2 The downlink FD cooperative NOMA system mode with MRC at the weak user terminal. 86

5.3 The downlink HD cooperative NOMA system mode. 88

5.4 The downlink HD cooperative NOMA system mode with MRC at the weak user terminal. 89

5.5 The achievable rate for users within the beam with $P_{R_{max}} = 0.2\ W$ and $R_{th} = 0.1\ Bit/s/Hz$ for FD cooperative NOMA system model. 112

5.6 The rate for the far user at different relay power for FD cooperative NOMA. 112

5.7 The achievable rate for the far user at different R_{th} for FD cooperative NOMA system model. 113

5.8 The allocated power of each user within the beam for FD cooperative NOMA system model. 113

5.9 The allocated power of each user within the beam at different R_{th} for FD cooperative NOMA system model. 114

5.10 The achievable rate for users within the beam with $P_{R_{max}} = 0.2$ for FD cooperative NOMA system model considering MRC at the far user. . . 116

5.11 The allocated power of each user within the beam for FD cooperative NOMA system model considering MRC at the far user. 116

5.12 Comparing the power of the relay for FD cooperative NOMA system with and without considering MRC at the far user. 117

5.13 Comparing the near user power for FD cooperative NOMA system with and without considering MRC at the far user. 117

5.14 Comparing the far user power for FD cooperative NOMA system with and without considering MRC at the far user. 118

5.15 The achievable rate for users within the beam with $P_{R_{max}} = 0.2\ W$ and $R_{th} = 0.1\ Bit/s/Hz$ for HD cooperative NOMA system model. 120

5.16 The rate for the far user at different relay power for HD cooperative NOMA. 120

5.17 The achievable rate for the far user at different R_{th} for HD cooperative NOMA system model. 121

5.18 The allocated power of each user within the beam for HD cooperative NOMA system model. 121

5.19 The allocated power of each user within the beam at different R_{th} using AO for HD cooperative NOMA system model. 122

5.20 The allocated power of each user within the beam at different R_{th} using GP for HD cooperative NOMA system model. 122

5.21 The achievable rate for users within the beam with $P_{R_{max}} = 0.2$ for HD cooperative NOMA system model considering MRC at the far user. . . 124

5.22 Comparing the power of the relay for HD cooperative NOMA system with and without considering MRC at the far user. 124

5.23 Comparing the near user power for HD cooperative NOMA system with and without considering MRC at the far user. 125

5.24 Comparing the far user power for HD cooperative NOMA system with and without considering MRC at the far user. 125

6.1 6G performance requirements [1]. 131

List of Tables

3.1 Sum Rate of Users in Group 2 (bps) 65

5.1 The average number of iteration in order to achieve a solution using AO with $R_{th} = 0.1\ Bit/s/Hz$ for FD cooperative NOMA system model. . . 111

5.2 The average number of iteration to achieve a solution using GP with $R_{th} = 0.1\ Bit/s/Hz$ for FD cooperative NOMA system model. 111

5.3 Number of rank one solution for each algorithm in FD cooperative NOMA system model. 111

5.4 Comparing The average number of iteration to achieve a solution $P_{R_{max}} = 0.2\ W\ R_{th} = 0.5\ Bit/s/Hz$ for FD cooperative NOMA system model with and without considering MRC at the weak user. 115

5.5 The average number of iteration in order to achieve a solution using AO with $R_{th} = 0.1\ Bit/s/Hz$ for HD cooperative NOMA system model. . . 119

5.6 The average number of iteration in order to achieve a solution using GP with $R_{th} = 0.1\ Bit/s/Hz$ for HD cooperative NOMA system model. . . 119

5.7 Number of rank one solution for each algorithm in HD cooperative NOMA system model. 123

5.8 Comparing The average number of iteration to achieve a solution $P_{R_{max}} = 0.2\ W\ R_{th} = 0.5\ Bit/s/Hz$ for HD cooperative NOMA system model with and without considering MRC at the weak user. 123

List of Algorithms

1 Proposed AGM Algorithm 63

2 Proposed algorithm design for NOMA beamforming using bisection search. 79

3 Nested Bisection Algorithm for Jointly Optimizing Beamformer and P_R. 97

List of Abbreviations

1G First Generation

2G Second Generation

3G Third Generation

3GPP Third Generation Partnership Project

4G Fourth-Generation

5G Fifth-Generation

AF Amplify-and-Forward

AGM Arithmetic-Geometric Mean

AI Artifcial Intelligent

AMC Adaptive Modulation and Coding

AO Alternating Optimization

AWGN Additive White Gaussian Noise

BF Beamforming

Bs Base Station

CIRs Channel Impulse Responses

CoMP Coordinated Multipoint

CR Cognitive Radio

CSI Channel State Information

CSIT Channel State Information at the transmitter

DF Decode-and-Forward

EVD Eigenvalue decomposition

FD Full-Duplex

GP Geometric Program

GSM Global System of Mobile Communications

HD Half-Duplex

i.i.d. Independent and Identically Distributed

ICSI Imperfect Channel State Information

IDMA Interleave Division Multiple Access

IoT Internet of Things

IRS Intelligent Reflecting Surfaces

ITU International Telecommunication Union

JT Joint-Transmission

LDS Low-density Spreading

LMI Linear Matrix Inequality

MA Multiple Access

MC-CDMA Multi-carrier Code-division Multiple Access

MIMO Multi-Input and Multi-Output

MISO Multiple-Input Single-Output

ML Machin Learning

mmWave Millimeter Wave

MRC Maximal Ratio Combining

NB Nested Bisection

NOMA Non-orthogonal Multiple Access

OFDM Orthogonal Frequency Division Multiplexing

OFDMA Orthogonal Frequency Division Multiple Access

OMA Orthogonal Multiple Access

PCSI Perfect Channel State Information

PDMA Pattern Division Multiple Access

QoS Quality of Service

SCA Successive Convex Approximation

SCMA Sparse Code Multiple Access

SCMA Superposition Coding

SDMA Space Division Multiple Access

SDP Semidefinite Program

SDR Semidefnite Relaxation

SI Self Interference

SIC Successive Interference Cancellation

SINR Signal-to-Interference-Plus-Noise Ratio

SISO Single Input Single Output

SMS Short Message Service

SNR Signal-to-Noise Ratio

SWIPT Simultaneous Wireless Information and Power Transfer

TDMA Time Division Multiple Access

ZF Zero-forcing

ZFBF Zero-forcing Beamforming

Abstract

This thesis contributes to the application of convex optimization in non-orthogonal multiple access systems. In this work, various practical constraints, such as grouping based on their QoS requirements and imperfect channel station information have been taken into consideration. The joint design of beamforming and power allocation in the downlink of the NOMA MIMO multiuser system is investigated, where the users are grouped based on their QoS requirements. The SDR is adopted to approach and showed that the optimal solutions are always rank one using simulation results. Also, a SCA algorithm is proposed based on the AGM inequality to perform the joint design of the beamforming vectors and the power allocation coefficients. Then, the research addressed the worst-case robust beamforming design for the MISO-NOMA downlink systems by taking into account the norm-bounded channel uncertainties. The S-procedure is exploited to reformulate the original non-convex problem into SDP form by recasting the original non-convex constraints into LMI form. Finally, a jointly optimizing beamformer and relay power are investigated for FD/HD cooperative NOMA with several optimization techniques. The study covers both perfect channel state information and the bounded imperfect channel state information. The objective is to maximize the achievable sum-rate for users within the beam. However, the original problem formulation is not convex. Therefore, reformulating the original problem into SDP form is required then several algorithms are applied to find a solution for the optimization problem.

Declaration

No portion of the work referred to in this thesis has been submitted in support of an application for another degree or qualification of this or any other university or other institute of learning.

Copyright

iv. Further information on the conditions under which disclosure, publication and commercialisation of this thesis, the Copyright and any Intellectual Property and/or Reproductions described in it may take place is available in the University IP Policy (see http://www.campus.manchester.ac.uk/ medialibrary/policies/intellectual-property.pdf), in any relevant Thesis restriction declarations deposited in the University Library, The University Library's regulations (see http://www.manchester.ac.uk/library/aboutus/regulations) and in The University's policy on presentation of Theses.

Acknowledgments

First and foremost, I would like to express my sincere gratitude to my supervisors, Prof. Zhiguo Ding and Dr. Emad Alsusa, for their continuous support of my Ph.D research. Special thanks to my main supervisor, Prof. Zhiguo Ding, who provided valuable technical guidance and constructive suggestions on my research works and directions. During the past years, working with Zhiguo is a wonderful experience. His wide knowledge, strong research enthusiasm and hard-working attitude have inspired me during all my PhD period and will have a profound effect on my future career. I am extremely lucky to have such a professional supervisor. I could not have imagined having a better supervisor and mentor for my Ph.D research.

I would like to thank all my collaborators: Dr. Yuanwei Liu, Dr. Xiaofang Sun and Dr. Jingjing Cui for their helpful suggestions and comments on my research. Also, I would like to thank all my colleges and friends in the research group at the University of Manchester and Lancaster University for their constant encouragement and kind help. I really have had wonderful memories in my Ph.D life and study. In the end, I would like to express my deepest gratitude to my beloved family, especially my parents and my wife, who always support me with no limits. Certainly, without my wife backing, this journey wouldn't get success.

To Amal, Yahia and Shaam

Chapter 1

Introduction

1.1 Background

1.1.1 On The Track to Beyond 5G

The vision for the beyond 5G networks are expected to provide a wide coverage which means that all the space-air-ground-sea communication networks will be harmonizing to provide a global-wide coverage. Also, the entire spectrum in addition to mmWave, THz, sub-6 GHz and optical frequency bands should be examined to reach an extremely high data rate. Machine learning (ML) and artificial intelligent (AI) will be applied in order to improve the coming generation networks as well as allow for wider applications. These are considered as the main highlighted view for the next-generation networks beyond the 5G networks [1].

To achieve the frontier of 1 Tbps in a beyond 5G networks as a peak data rate, different categories should be triggered which allow these networks to reach extreme

capacity. A number of enablers at the spectrum, infrastructure and algorithms which includes protocols as well are vital to grasp the planed broadband connectivity goals such as supporting broadband connectivity at railway with speeds likely 1000 km/h and reach a peak data rate up to the Tbps range. Reducing complexity, higher reliability and lower latencies can be realized by improving coding, modulation and waveforms [2].

As the researchers in [2] emphasized that in order to achieve the targeted aims for the beyond 5G networks, should be several enablers applied in different level of the network. These enablers include the infrastructure level based on the evolution of massive multiple-input multiple-output (MIMO), intelligent reflecting surfaces (IRS), and integrated access and backhaul. Also, the designer should include revolutions at the protocol/algorithmic level, waveform, non-orthogonal multiple access (NOMA) and rate splitting and machine learning-aided algorithms.

1.1.2 Multiple Access Techniques for Beyond 5G

1.1.2.1 Wireless Standardization Overview

A limited number of users were to be able to connect for a wireless communication network, for example, in the period between 1957-1967 the Swedish Mobile Telephone System was able to provide connectivity for 125 users to their network [3]. The first generation of wireless networks was implemented in 1980 based on analogue frequency modulation which prevents to apply of error correction codes to the communication system, for this reason, the speech quality was poor. In order to beat the struggles of the first generation networks, the global system of mobile communications (GSM) which considered a second-generation (2G) of communication networks implemented based on digital radio frequency and Time-division multiple access (TDMA) as mul-

tiple access techniques. Moreover, it was the first type of wireless networks provided data service such as short message service (SMS). Shortly, several digital standards developed, such as the advanced mobile phone system (D-AMPS) and IS-95 known as cdmaOne which evolved to the cdma2000 system. The cdma2000 consider as the first standardization for multi-carrier Code-division multiple access (MC-CDMA) system [4].

Within a decade higher data rate transmission was able to be provided by developing the third-generation (3G) networks, that was matured from CDMA to wideband CDMA (WCDMA). Then, the demand of data rate was extremely increased for that, different industrial standardization partner such as 3G partnership project's (3GPP), IEEE 802.11 and IEEE 802.16 had transformed to multi-carrier solutions using orthogonal frequency-division multiplexing (OFDM) and Orthogonal frequency-division multiple access (OFDMA) to overcome the high data throughput demand in fourth-generation (4G) wireless networks [5]. The most effective feature of a multi-carrier system is the flexibility has been provided such as adaptive modulation and coding (AMC) which allow the system to provide different services according to the required quality of service (QoS) [3].

In the past five years, both researchers and industrial communities turned towards evolving the standards of 5G cellular network systems. The aim of the international telecommunication union (ITU) is to complete the whole specifications phases of the 5G standards by the end of 2020 [6]. On the other hand, directed by the extremely accelerated expansion of the wireless capacity needs to be enforced by advanced multimedia applications such as virtual reality and high definition video. Also, developing Internet of Things (IoT) devices and tactile internet resulting in challenges to support the traffic of the large-scale heterogeneous data for the 5G and beyond networks [7].

To overcome the high data rate traffic demands several key enablers should be applied such as a sophisticated MA that has naturally evolved over cellular wireless network generations [8].

In the physical layer, the MA technology considered as a fundamental concept that has matured over the past years for the wireless generations history [9]. The MA technology used for the 1G was frequency division multiple access (FDMA), after that in the 2G TDMA was applied which is based on digital modulation [10]. Then, Qualcomm suggested a CDMA that turned out to be a dominant technology for 3G networks [11]. However, The throughput of data rate was limited in 3G so, in order to enhance the speed of the achievable data rate, OFDMA endorsed in 4G broadband cellular networks [12]. FDMA, TDMA, and OFDMA can be classified as orthogonal multiple access (OMA) since the same time/frequency resource block (RB) can be dedicated only to a single user [7].

1.1.2.2 Recent Multiple Access Techniques

Recently the industrial communities developers have been drawn their attention to utilizing the resource block efficiently. This could be done by enabling NOMA on the resource block either by applying the code-domain, spatial-domain or power-domain [3]. There are several proposed outstanding techniques that represent code-domain NOMA such as sparse code multiple access (SCMA), interleave division multiple access (IDMA), low-density spreading (LDS) and pattern division multiple access (PDMA) [13]. Spatial-domain can utilize the resource block by constructing the channel impulse responses (CIRs) in order to distinguish between users this MA technique is called space division multiple access (SDMA) [14]. For the power-domain NOMA which has proposed to be used on 5G networks [15].

The basic concept of power-domain NOMA can be explained as follows; firstly is to impose superposition coding (SC) at the transmitter side then, a successive interference cancellation (SIC) at the receiver side. This technique is used to guarantee service for multiple users utilizing the same time/frequency RB with different QoS requirements [3]. Moreover, combining the power-domain NOMA with the existing MA paradigms is more likely because it utilizes the new dimension of the power domain [13]. For simplicity in this research, the term NOMA will be referred to as the power-domain NOMA.

1.2 Motivation and Contributions

Motivated by the fundamental work which established the concept of NOMA (see [16–18] and the reference therein), [19] and [20] systematically evaluated the performance of NOMA in downlink and uplink, respectively. Triggered by the unique benefits of multi-antenna systems, the application of the multiple-input multiple-output (MIMO) technique to NOMA has been addressed, e.g., [21–23]. Very recently, [24] proposed a minorization-maximization algorithm to maximize the downlink sum-rate, where the transmit signals of each user is multiplied with a complex precoding vector. Considering the multiuser system where users transmit different numbers of data streams based on their distances away from the BS, [25] solved a minimum power beamforming problem by firstly obtaining the optimal power allocation for given beamforming vectors and then finding beamforming vectors using an iterative algorithm. In our previous work [26], we proposed a mutual information algorithm to design beamforming vectors, in which power allocation only depends on the distances between users and the BS. As an enhanced version of conventional MIMO, [27] proposed a massive-MIMO-NOMA downlink transmission protocol in the presence of limited feedback. The concept of NOMA is evaluated through simulation for full channel state information at the transmitter (CSIT) in the uplink [28] and downlink [29], where the throughput of the system is shown to be on average always better than OMA when considering a fully defined cellular system evaluation. A general framework for multiple-input-multiple-output (MIMO) NOMA system has been developed for both the downlink and the uplink in [30]. The downlink system performance throughput gains are evaluated In [31] by incorporating a complete simulation of an LTE cellular system (3GPP). Kim et. al. [32] developed an optimization problem that finds the power allocation coefficients for a broadcast MIMO NOMA system with N base-station antennas serving simultaneous users.

The assumption of perfect channel state information (CSI) at the transmitter is assumed for most beamforming designs [24]. But, this might not be always valid for practical scenarios because of channel estimation and quantization errors. So, it is important to consider the channel uncertainties particularly in the beamforming design for NOMA networks. In [33], a robust NOMA scheme for the MISO channel to maximize the worst-case achievable sum-rate with a total transmit power constraint has been investigated with developing clustering criteria. However, in [34] study the NOMA scheme applied between all users with a spectrum sharing between all users in the cell. The target in [34] is to tackle the power minimization problem based on a worst-case optimization framework to provide the required quality of service for each user.

In Chapter 3, we focus on the employment of NOMA in the downlink channel of a MIMO multiuser system. In this system, we study a *new* scenario where the users are divided into two groups based on their quality of service (QoS) requirements. Specifically, the users in Group 1 expect to be served with the best efforts, while the users in Group 2 require to reach their own target rates. As such, our work stands as a significant advancement over the existing studies where user grouping is based on their location information. For this scenario, we maximize the sum rate of the users in Group 1 under the constraint of guaranteeing that the users in Group 2 achieve their target rates. Due to its nonconvexity, we first introduce the semidefinite relaxation (SDR) approach [35] to linearize the quadratic form of beamforming vectors. Then a successive convex approximation (SCA) [36] is proposed based on the arithmetic-geometric mean (AGM) inequality to jointly design beamforming matrices and power allocation. Furthermore, the simulation results show a pivotal property that the SDR approach is always tight. An important conclusion is reached that our proposed algorithm outperforms the existing ones in the literature. We also examine the impact of the average signal-to-noise ratio (SNR), the number of antennas at the BS, and the number of users

on the convergence speed of our proposed algorithm.

The objective in Chapter 4 is to maximize the minimum of received signal-to-interference-plus-noise ratios (SINRs) of users, which is not convex in terms of beamforming vectors. The formulated optimization problem is not convex so, to solve the challengeable problem, we first formulate an equivalent optimization problem based on SDP. By applying a rank one relaxation and a linear matrix inequality (LMI) the S-Procedure can be used, which leads to exploiting the bisection algorithm in order to obtain the robust optimal beamforming solution. Finally, simulation results are provided to demonstrate the effectiveness of the proposed robust design.

In Chapter 5, a jointly optimizing beamformer and relay power are studied for FD/HD cooperative NOMA with several optimization techniques. The study covers both perfect channel state information and the bounded imperfect channel state information. The objective is to maximize the achievable sum-rate for users within the beam. However, the original problem formulation is not convex. Therefore, reformulating the original problem into SDP form is required then several algorithms are applied to find a solution for the optimization problem.

1.3 Related Works

As a promising technique that provides superior spectrum efficiency in 5G wireless networks, NOMA has received increasing attention from both academia and industrial communities [37, 38]. Particularly, NOMA is a multi-user multiplexing scheme that realizes multiple access in the power domain. This makes it fundamentally different from the conventional orthogonal multiple access (OMA) schemes, such as TDMA, FDMA, and CDMA, as well as some code-domain non-orthogonal schemes, such as SCMA [39]. With the use of NOMA, the base station (BS) is able to serve multiple users at the same time, frequency, space, and spreading code but at different power levels, which achieves more efficient use of spectrum. Notably, NOMA allocates more power to users with poorer channel quality or ensures some users achieve their target rates, thus striking a balance between network throughput and user fairness.

To realize the benefits of NOMA, successive interference cancellation (SIC) [40] has often been adopted by some users such that they can remove the interference and decode the desired signals in a successive manner. There are several significant and attractive features of NOMA; one of them is the low complexity design and compatibility with other existing MA [15]. Also, power allocation in NOMA provides a reasonable trade-off between system throughput and user fairness. Moreover, the spectrum efficiency from NOMA shows a remarkable difference compared to convectional OMA techniques [41]. In this section, an overview of the recent work of NOMA will be provided in several aspects of the wireless networks.

1.3.1 Non-orthogonal Multiple Access

For the typical OMA techniques, the receivers can easily detect the users' signals based on allocating a unique RB for each user either this RB could be a time, frequency, code or a mixed formation like OFDMA. The gain from orthogonality for the RBs which are provided to the users is to eliminate the interference based on theoretical signal processing concepts [42]. Yet, there is a restriction on the number of users are allowed to be served uses OMA techniques, for this reason, conventional OMA will not be able to provide the required demand for 5G networks devices [43].

There have been conducted wide academic researches efforts for NOMA with a single antenna system on both performance analysis and optimization of the overall NOMA systems. These studies cover downlink/uplink scenarios, power allocation and user fairness. In [41] the power-domain NOMA idea was proposed for cellular future radio access networks by superposing two user signals in the downlink then, implements SIC at the receiver. Results of that study showed improvement on both throughputs of the cell-edge user and overall capacity. the system performance was appraised in [31,44] that considered several design features such as scheduling, error propagation and multi-user pairing. Then, Ding *et al.* [45] inspected the performance of the downlink NOMA cellular scenario by using random users. Their results demonstrated a significant performance in ergodic sum rates compared to conventional OMA.

A different benchmark was introduced by Xu *et al.* [46] based on the information theory aspect to investigate the performance of NOMA over traditional OMA. The benchmark is to compare the individual achievable rate rather than considering only the sum rate which was shown significant outperformance for NOMA over OMA

especially when there is a considerable difference between the channel of users. By taking fairness of the user into account with different channel state information (CSI) criteria such as instantaneous CSI and average CSI, power allocation techniques were examined to assure fairness between users in downlink NOMA system[47].

The transmission of the uplink NOMA scenario was suggested by [48] where the number of users is limited for each sub-carrier in order to maintain complexity at the receiver. Further, for the seek of maximization the total sum-rate of the user's power allocation algorithm was proposed which achieved a bit error rate close to the single-user condition. In addition to that, for enhancing multi-user detector performance the study in [49] proposed an iterative multiuser detection and decoding. A user-pairing for uplink NOMA transmission was suggested in [50] based on the suboptimal algorithm in order to reduce implementing complexity for NOMA.

1.3.2 NOMA in Multiple-Antenna systems

MIMO antenna concept was been applied to NOMA systems in [51, 52] which shows significant enhancement of the ergodic capacity and data rate throughput of the users. In this study [53], according to two types of transmission priority multicast beamforming can be formed by imposing MIMO NOMA. A zero-forcing (ZF) beamforming was used to mitigate inter-cluster interference, then a total transmission power beamforming was minimized in order to formulate the optimal power allocation closed form. Signal alignment idea was enforced in [54] to design different MIMO NOMA uplink/downlink framework. Stochastic geometry was applied to formulate a closed-form so, the performance of this framework was assessed.

Also, pre-coding and detection strategies were proposed in [55] so, can completely make a difference between the users' channel gains. That proposed algorithm allowed NOMA to be applied for MIMO NOMA even in very smiler channel gain conditions especially for IoT devices. Increasing the sum capacity was the goal of the proposed NOMA beamforming scheme in [32]. Where each beam consists of multi-users, they were clustered based on the difference between their channels and with a high correlation among the users. Power allocation of the suggested system was assured enhancing the sum capacity.

Intra-beam superposition coding was suggested by [56] where a pre-coding matrix is managed according to an open loop-type random beamforming. That, controlling criteria provide efficient feedback size information from the user side. Experimental trials for MIMO NOMA systems were operated in order to examine the MIMO NOMA with real scenarios [57]. This study was conducted two main practical experiments the first one 2×2 MIMO with open-loop and the second trial was 4×2 with closed-loop.

1.3.3 NOMA and Cooperative Transmission

Involving NOMA in cooperative communication studies have been started in [58–60]. Cooperative NOMA achieved the same diversity order of regular OMA, yet cooperative NOMA enhances the performance of spectral efficiency for the system. In [58] NOMA downlink cooperative cellular system supported by a half-duplex (HD) amplify-and-forward relay was suggested. Several mathematical tool analyses used to investigate the performance such as the outage performance derived. Another architecture of cooperative MIMO was investigated in [59], where receivers were equipped by MIMO antenna and used maximal ratio combining (MRC). By optimizing the power allocation coefficients it will result in developing the performance of cooperative NOMA as

identified in [60].

Relay selection (RS) criteria impacted on cooperative NOMA in [61], the study investigated and compared two different types of RS max-min and two-stage scheme. Where the two-stage scheme performed better in outage probability and achieved optimal diversity order. In addition to that, two relaying protocols amplify-and-forward (AF) and decode-and-forward (DF) were studied based on different QoS for the users in [62]. Also, the study achieved closed-form expressions to investigate the performance of the system. Improving cooperative NOMA transmission can be done through different approaches such as simultaneous wireless information and power transfer (SWIPT), full-duplex (FD) and cognitive radio (CR) as discussed in [63].

An energy harvesting relay effected in cooperative NOMA was studied in [64] with fixed power allocation and cognitive radio. Characterization tools were used to investigate the performance of the energy harvesting relay. In terms of coordinated multipoint (CoMP) system studies, opportunistic and joint-transmission (JT) approaches were investigated by finding sum-rate and the outage performance in [65].

1.4 Dissertation Organization

The rest of this thesis is organized as follows. Chapter 2 introduces some background concepts such as basic principles of NOMA and convex optimization. Chapter 3 investigates the joint design of beamforming and power allocation in the downlink of the NOMA MIMO multiuser system based on QoS requirements. Chapter 4 studies the worst-case robust beamforming design for the MISO-NOMA downlink systems by taking into account the norm-bounded channel uncertainties. Chapter 5 examines jointly optimizing beamformer and relay power for FD/HD cooperative NOMA with several optimization techniques. The study covers both perfect channel state information and the bounded imperfect channel state information. Chapter 6 concludes the thesis and discusses future research directions.

Notations: Vectors and matrices are denoted by lower-case and upper-case boldface symbols, respectively. $(\cdot)^H$ denotes the Hermitian transpose. $\mathrm{Tr}\,(\cdot)$ denotes the trace operation. $\mathrm{Rank}\,(\cdot)$ denotes the rank, and $\|\cdot\|$ denotes the Euclidean norm, and $|\cdot|$ denotes the absolute value.

1.5 Author's Publications

- X. Sun C. Shen and Y. Xu and **S. M. Al-Basit** and Z. Ding and N. Yang and Z. Zhong, "Joint Beamforming and Power Allocation Design in Downlink Non-Orthogonal Multiple Access Systems,". 2016 IEEE Globecom Workshops.

- **S. M. Al-Basit**, J. Cui, Y. Liu, Z. Ding and P. Fan, "Maximizing SINR for non-orthogonal multiple access with bounded channel uncertainties,". 2017 IEEE/CIC International Conference on Communications in China (ICCC).

- **S. M. Al-Basit** and Z. Ding, "Maximizing Sum Rate for FD/HD Cooperative NOMA System with Jointly Optimizing Beamformer and Relay Power,". 2021 *in preparation.*

Chapter 2

Background Information

2.1 Power Domain Non Orthogonal Multiple Access

2.1.1 Basics of NOMA

A comprehensive illustration for downlink and uplink NOMA transmission schemes are shown in Fig. 2.1, also it shows the basic downlink cooperative NOMA scheme as well. There are two fundamental techniques that power domain NOMA relaying on; SC and SIC. For downlink NOMA, all users' messages are combined through the SC technique and the channel gains of the users are ordered either ascending or descending order. In NOMA, the users with poorer channel condition which are allocated by more power considering the other stronger channel gain users signals as a noise then they decode their messages. On the other hand, the users with stronger channel gain condition they are able to decode the poorer users signals then eliminate them by evoking SIC.

For the uplink scenario, different users receive a controlling signal from the Bs in order to assign the power allocation. After that, several users transmute their signals according to the assigned resource block. Then, the BS applies SIC to decode users information with respect to either ascending or descending decoding order.

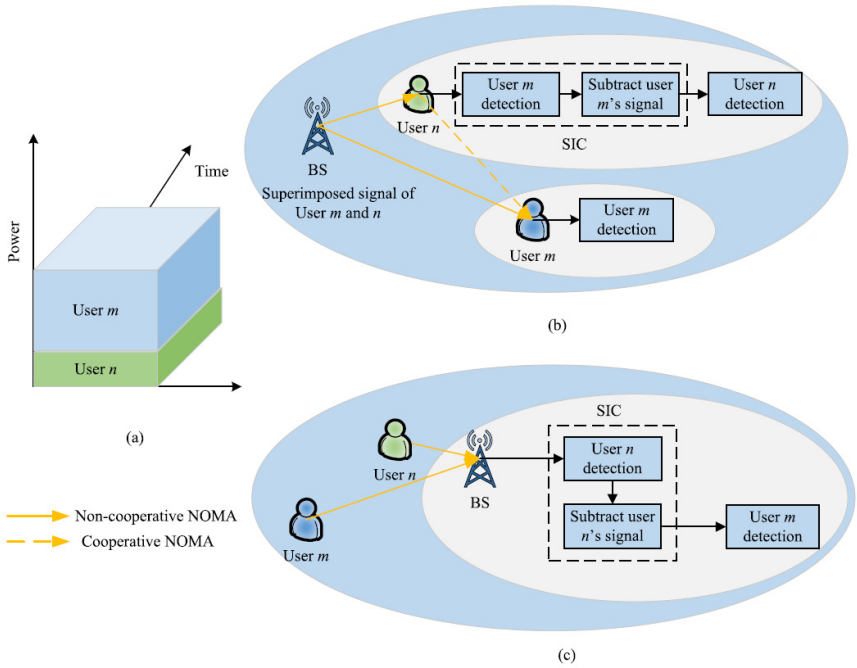

Figure 2.1: Basic NOMA transmission schemes [3].

2.1.2 Advantages of NOMA Systems

NOMA system shows several advantages in different communication aspects such as high bandwidth efficiency, where multiple users can be allowed to share the same resource block wither it is time or frequency, which contributes to improving the overall system throughput [41]. In term of fairness in NOMA, it allocates more power for the poor user. Therefore, NOMA is able to maintain a reasonable trade-off between the fairness within the users according to their throughput [3]. Also, there more practical techniques of guaranteeing fairness for NOMA like the intelligent power allocation poli-

cies in [47] and [66].

Also, ultra-high connectivity is provided from the NOMA system to overcome the high demand for IoT devices in 5G networks [67]. Since the resource block can be utilized by multiple users in NOMA it is a dynamic approach to handle the connectivity task for IoT devices. While in conventional multiple access techniques the same number of resource blocks are required in order to serve the same number of devices [68]. In addition to these advantages, NOMA has a flexible and lower-complexity design in comparison to the other proposed multiple access techniques for beyond 5G networks such as SCMA [3].

2.1.3 NOMA in Multi-Antenna Systems

There are two main configurations to impose MIMO for the NOMA system; the first technique is depicted in Fig. 2.2 where each beamformer is assigned to a dedicated user, therefore, the QoS can be achieved by computing the weights for each beamformer initiated by the most required QoS with a predefined order [3]. This technique is called NOMA with spatial multiplexing (NOMA-SM) since the aim of this scheme is to enhance the throughput by expanding the spatial multiplexing gain employing multiple antennas at both ends between the transmitters and receivers [15]. The attainable rate is investigated in [52], where NOMA-SM based on assumption that it is a consolidation of MIMO and NOMA. With a highly rich scattering surrounding the attainable rate of MIMO channels gains linearly with the minimum of the numbers of transmitting and receiving antennas.

The second setup in order to apply MIMO-NOMA as shown in Fig. 2.3 is called the cluster-based beamformer. Where each beamformer contains multiple users assembling a cluster so, to utilize the power domain NOMA is applied in each individual

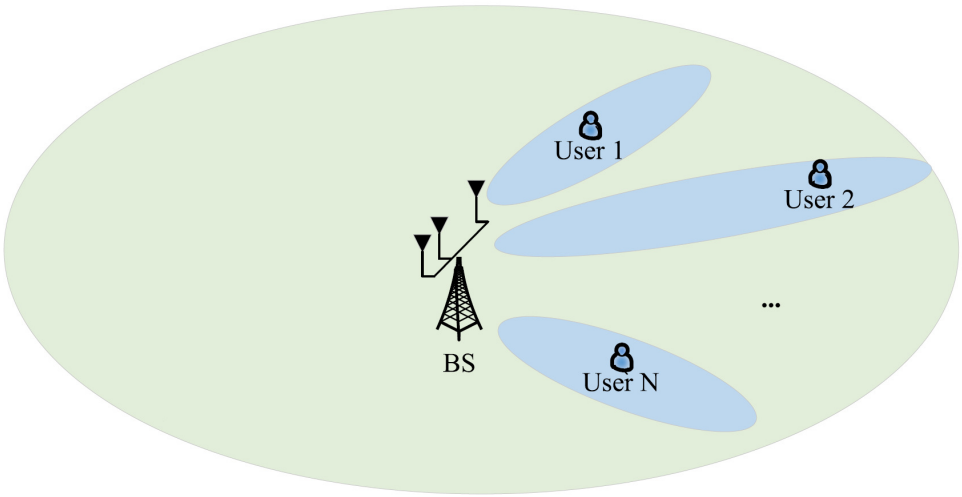

Figure 2.2: Beamforming MIMO-NOMA technique [3].

cluster. This structure enhances the SINR therefore, it improves the spectral efficiency. A high correlation among users spatial channels within the cluster is a condition that must be satisfied in order to apply NOMA efficiently.

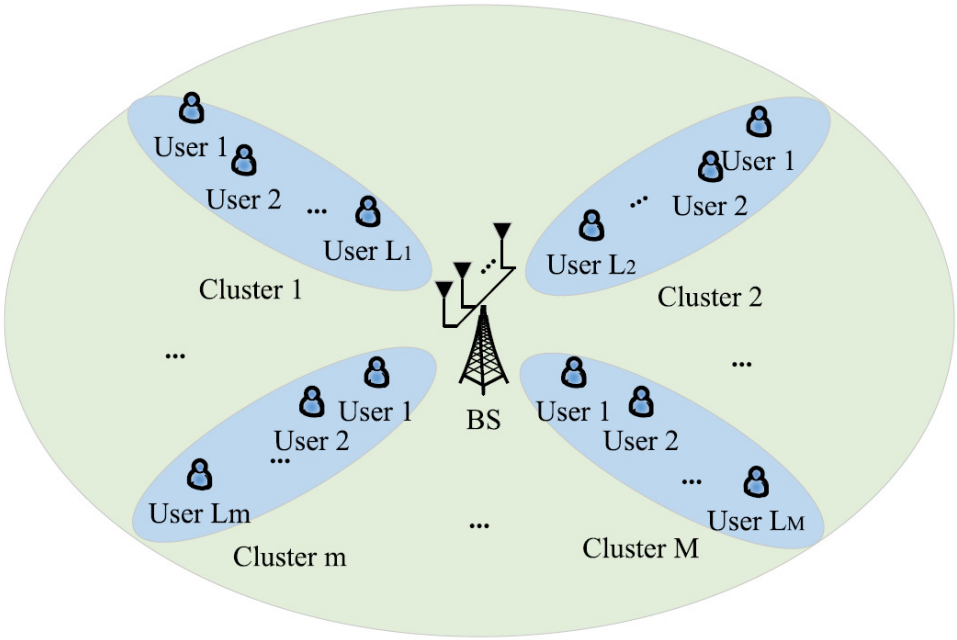

Figure 2.3: Downlink broadcast channel in a NOMA system [3].

On top of employing a powerful transmitter and detector precoder, it turns

feasible to assure that the beamformer link to the specific cluster is orthogonal to the channel vectors of the users in other clusters. So, the intercluster interference can be correctly cancelled [15]. One of the methodologies that can be used to eliminate the intercluster interference is a ZF as it introduced in [53] as a two-stage beamformer approach.

2.1.4 Cooperative NOMA Transmission

The download cooperative NOMA schematic is described in Fig. 2.1. The essential scheme of the cooperative NOMA is to deal with the strong user in the NOMA system as a DF relay intended for providing an aide to the weak user since it decodes its message in the first place. A classical transmission scheme for cooperative NOMA is consist of two stages, direct link transmission and cooperative link transmission. Accordingly, there are two different copies through diverse channels received by the weak user [15]. the relay forwards decoded message in two different strategies which are HF or FD as will be explained later in Chapter 5.

There are various advantages of cooperative NOMA that can be achieved. The first gain point is approach system integration since SIC is applied by the strong user so it is reasonable to regard employing DF protocol to the users required to be supported in the cell edge as a practical example. The second advantage is to improve the fairness because as an important detail for cooperative NOMA about the reliability of weak user with bad channel conditions naturally enhanced. The third point is to get a higher diversity gain that is considered as a powerful way to control the multi-path fading [3].

2.2 Convex Optimization

There are three main mathematical disciplines by combining them they will be forming called convex optimization which are; optimization, convex analysis and numerical computation. Furthermore, convex optimization considers as a powerful tool in engineering since it provides efficient and solid solutions for several practical engineering problems. Implementing convex optimization has been noted from different engineering area such as control, signal processing, communication [69,70], networks, circuit design, information theory and computer science. Also, can be applied in economics, statistics and structural design [71].

An enormous representations of layout engineering problem can be a modelled as constrained optimization problems, based on the form:

$$\begin{aligned} \min \quad & f_0(x) \\ \text{subject to} \quad & f_i(x) \leq 0, \quad i = 1, \ldots, m \\ & h_i(x) = 0, \quad i = 1, \ldots, p \end{aligned} \tag{2.1}$$

where x is a vector of variables, and f_0 is the cost function, f_i is the inequality constraint function and h_i is equality constraint function. Normally, kind of this problem could be extremely difficult to solve specifically when there are many variables of x.There are different causes for this dilemma to find a solutions for this type of problems. One reason is to find a feasible point x that satisfy all constraints could be difficult to get it. Also, a capricious standard of using stopping criteria in commonplace optimization algorithms. Besides to these struggles, the convergence rates by these algorithms are low.

A solid explanation of the theories, applications and algorithms for convex optimization is well explained in [72–74]. In the following sections, there will be a highlighted explanation for the main concepts that will be used in this research to achieve a feasible solution for the proposed problems.

2.2.1 Quasiconvex Functions

As an advantage of a quasiconvex function that the iterations can be minimized from convex optimization problems [71]. A function $f : \mathbb{R}^n \to \mathbb{R}$ is defined as a quasiconvex where the domain of this function and all its α-sublevel sets defined as

$$S_\alpha = \{x \in \mathbf{dom}\ f \mid f(x) \leq \alpha\} \tag{2.2}$$

are convex for each one of α see Fig.2.4.

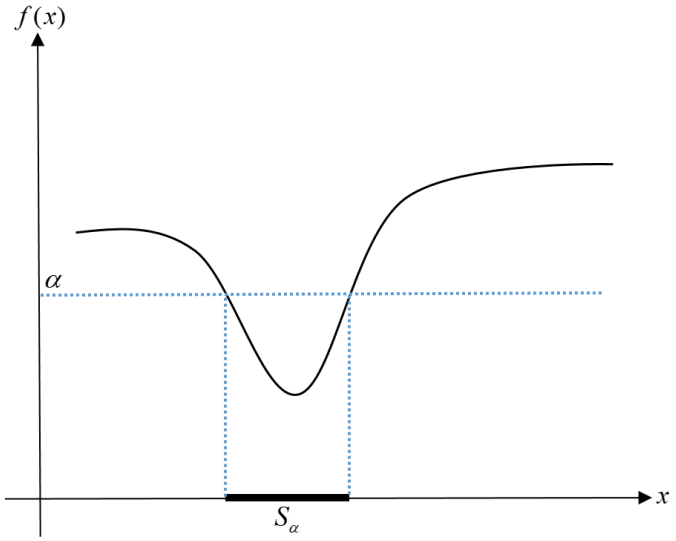

Figure 2.4: Clarification of a quasiconvex function.

There are several notes regarding quasiconvex functions:

- If f is convex function, so it is accordingly a quasiconvex function as well see Fig.2.5.
- Quasiconvex functions could have 'locally flat' areas.
- f is quasiconcave if $-f$ is quasiconvex, especially, superlevel sets $\{x \mid f(x) \geq \alpha\}$ are convex.
- A quasilinear function is termed for functions is quasiconvex and quasiconcave at the same time.

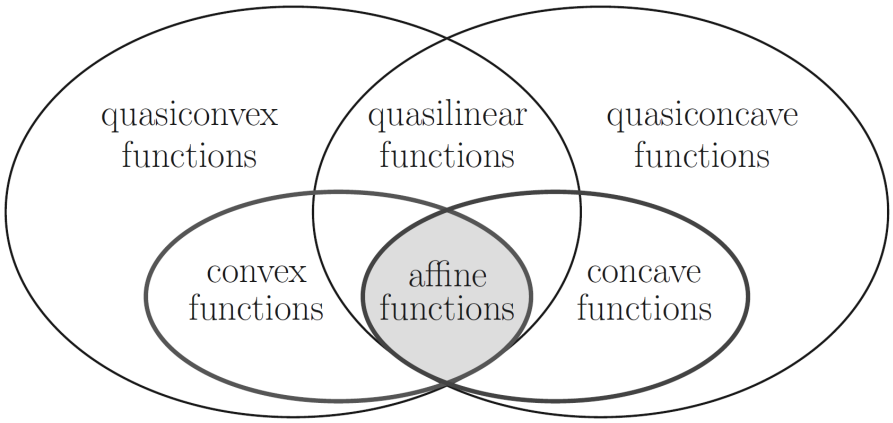

Figure 2.5: Links between different functions sets [69].

There are a few listed examples for quasiconvex, quasiconcave and quasilinear functions [69, 71]:

- $f(x) = \sqrt{(|x|)}$ is quasiconvex on $\mathbb{R}$.
- $f(x) = e^{-x}$ is quasilinear on $\mathbb{R}$.
- $f(x) = \log(x)$ is quasilinear on $\mathbb{R}_{++}$.
- Ceiling function:

$$\lceil x \rceil = \inf\{z \in \mathbb{Z} \mid z \geq x\},$$

is lower semi-continuous, nonconvex but it is quasiconvex and quasiconcave so it is quasilinear.

- Linear-fractional function
$$f(\mathbf{x}) = \frac{\mathbf{a^T x} + b}{\mathbf{c^T x} + d},$$
is quasiconvex on $\{\mathbf{x} \mid \mathbf{c^T x} + \mathbf{d} > \mathbf{0}\}$. It could be demonstrated that a linear-fractional function is also quasiconcave, thus it is quasilinear.

- $f(\mathbf{X}) = \mathbf{rank}(\mathbf{X})$ is a quasiconcave on on $\mathbb{S}^n_+$.

- $f(x) = \frac{\|x-a\|_2}{\|x-b\|_2}$ is quasiconvex on the halfspace $\{x \mid \|x-a\|_2 \leq \|x-b\|_2\}$.

2.2.2 Semi-definite Relaxation

Semidefinite relaxation (SDR) is a robust and computationally efficient approximation approach, where has been applied on a wide wireless communications and signal processing optimization problems to realize an approximate solution to a non-convex problem that is very significant. SDR can be imposed specifically for numerous non-convex quadratically constrained quadratic programs (QCQPs) problems. For example, the real-valued homogeneous QCQP is written as follows:

$$\begin{aligned} \min_{\mathbf{x}\in\mathbb{R}^2} \quad & \mathbf{x}^T\mathbf{C}\mathbf{x} \\ s.t. \quad & \mathbf{x}^T\mathbf{A}_i\mathbf{x} \trianglerighteq_i b_i \quad i = 1, \ldots, m. \end{aligned} \tag{2.3}$$

"$\trianglerighteq_i$" means either "$\leq$", "$\geq$" or "$=$". $\mathbf{C}$ and $\mathbf{A}_i \in \mathbb{S}^n$, where $\mathbb{S}^n$ stands for the set of all real symmetric $n \times n$ matrices; and $b_i \in \mathbb{R}$. The first important stage in inferring an SDR of (2.3) is to look at both the objective function and constraints are linear in the

matrix $\mathbf{x}^T\mathbf{x}$ where

$$\mathbf{x}^T\mathbf{C}\mathbf{x} = \mathrm{Tr}(\mathbf{x}^T\mathbf{C}\mathbf{x}) = \mathrm{Tr}(\mathbf{C}\mathbf{x}^T\mathbf{x}) \text{ and}$$
$$\mathbf{x}^T\mathbf{A}_i\mathbf{x} = \mathrm{Tr}(\mathbf{x}^T\mathbf{A}_i\mathbf{x}) = \mathrm{Tr}(\mathbf{A}_i\mathbf{x}^T\mathbf{x}).$$

So, by proposing a new variable $\mathbf{X} = \mathbf{x}^\mathbf{T}\mathbf{x}$ where, $\mathbf{X}$ is a rank one symmetric positive semidefinite (PSD) matrix. Then, an equivalent representation of (2.3):

$$\begin{aligned} \min_{\mathbf{X}\in\mathbb{S}^n} \quad & \mathrm{Tr}(\mathbf{C}\mathbf{X}) \\ s.t. \quad & \mathrm{Tr}(\mathbf{A}_i\mathbf{X}) \trianglerighteq_i b_i \quad i = 1, \ldots, m, \\ & \mathbf{X} \succcurlyeq 0 \\ & \mathrm{rank}(\mathbf{X}) = 1. \end{aligned} \tag{2.4}$$

At this step the problem (2.3) converts to a convex problem except the rank one constraint $\mathrm{rank}(\mathbf{X}) = 1$. So, the following relaxed formulation:

$$\begin{aligned} \min_{\mathbf{X}\in\mathbb{S}^n} \quad & \mathrm{Tr}(\mathbf{C}\mathbf{X}) \\ s.t. \quad & \mathrm{Tr}(\mathbf{A}_i\mathbf{X}) \trianglerighteq_i b_i \quad i = 1, \ldots, m, \\ & \mathbf{X} \succcurlyeq 0. \end{aligned} \tag{2.5}$$

Problem (2.5) is recognized as a SDR of (2.3) and the outcome of this relaxed formulation is can be solved by using the convex optimization toolbox CVX in the MATLAB. . Then, the algorithm returns a solution that is optimal for the original problem. Moreover, when $m \leq 2$ there will be a $\mathrm{rank}(\mathbf{X}^*) \leq 1$ at any time that (2.5) is feasible [75].

As an extension of QCQP a separable QCQPs form:

$$\begin{aligned} \min_{\mathbf{x}_1,\ldots,\mathbf{x}_k \in \mathbb{C}^n} \quad & \sum_{i=1}^{k} \mathbf{x}_i^H \mathbf{C}_i \mathbf{x}_i \\ s.t. \quad & \sum_{l=1}^{k} \mathbf{x}_l^H \mathbf{A}_{i,l} \mathbf{x}_l \trianglerighteq_i b_i \quad i = 1, \ldots, m. \end{aligned} \tag{2.6}$$

This problem (2.6) is used in downlink transmit beamforming optimization problems [76]. Also, can be rewritten in SDR form:

$$\begin{aligned} \min_{\mathbf{X}_1,\ldots,\mathbf{X}_k \in \mathbb{H}^n} \quad & \sum_{i=1}^{k} \mathrm{Tr}(\mathbf{X}_i \mathbf{C}_i) \\ s.t. \quad & \sum_{l=1}^{k} \mathrm{Tr}(\mathbf{X}_i \mathbf{A}_{i,l}) \trianglerighteq_i b_i \quad i = 1, \ldots, m, \\ & \mathbf{X}_1 \succcurlyeq 0, \ldots, \mathbf{X}_k \succcurlyeq 0. \end{aligned} \tag{2.7}$$

Next, as prove in [77] a solution $\{\mathbf{X_i^*}\}_{\mathbf{i=1}}^{\mathbf{k}}$ occurs when ranks fulfil

$$\sum_{i=1}^{k} \mathrm{rank}(\mathbf{X_i^*})^2 \leq m.$$

2.2.3 $\mathcal{S}$-procedure

$\mathcal{S}$-procedure or $\mathcal{S}$-lemma as it is termed as well, it is introduced a useful way to transform many quadratic constraints into a linear matrix inequality (LMI) constraint. In fact, it turns multiple quadratic constraints into a single semidefinite matrix inequality with an additional unknown nonnegative parameter. Lately, this mathematical technique has been applied in robust transmit beamforming in MIMO wireless communications especially, in imperfect channel state information (CSI) environments [78].

$\mathcal{S}$-procedure is stated as following [69]:

Let $\mathbf{A_1}$, $\mathbf{A_2} \in \mathbb{H}^n$, $\mathbf{b_1}$, $\mathbf{b_2} \in \mathbb{C}^n$, h_1, $h_2 \in \mathbb{R}$. The following implication

$$\underbrace{\mathbf{x}^H\mathbf{A}_1\mathbf{x} + 2\mathrm{Re}\{\mathbf{b}_1^H\mathbf{x}\} + h_1 \leq 0}_{2.8a} \Rightarrow \underbrace{\mathbf{x}^H\mathbf{A}_2\mathbf{x} + 2\mathrm{Re}\{\mathbf{b}_2^H\mathbf{x}\} + h_2 \leq 0}_{2.8b} \tag{2.8}$$

i.e.,$\left\{\mathbf{x} \in \mathbb{H}^n \,\middle|\, \mathbf{x}^H\mathbf{A}_1\mathbf{x} + 2\mathrm{Re}\{\mathbf{b}_1^H\mathbf{x}\} + h_1 \leq 0\right\} \subseteq \left\{\mathbf{x} \in \mathbb{H}^n \,\middle|\, \mathbf{x}^H\mathbf{A}_2\mathbf{x} + 2\mathrm{Re}\{\mathbf{b}_2^H\mathbf{x}\} + h_2 \leq 0\right\}$, holds true if and only if there exists a $\lambda \geq 0$ such that

$$\begin{bmatrix} \mathbf{A}_2 & \mathbf{b}_2 \\ \mathbf{b}_2^H & h_2 \end{bmatrix} \preceq \lambda \begin{bmatrix} \mathbf{A}_1 & \mathbf{b}_1 \\ \mathbf{b}_1^H & h_1 \end{bmatrix} \tag{2.9}$$

provided that there exists a point $\hat{\mathbf{x}}$ with $\hat{\mathbf{x}}^H\mathbf{A}_1\hat{\mathbf{x}} + 2\mathrm{Re}\{\mathbf{b}_1^H\hat{\mathbf{x}}\} + h_1 < 0$.

An other clarification for $\mathcal{S}$-procedure, that is crucial in how to basically address $\mathcal{S}$-procedure. Presume that there exists a point $\hat{\mathbf{x}}$ fulfilling $\hat{\mathbf{x}}^H\mathbf{A}_1\hat{\mathbf{x}} + 2\mathrm{Re}\{\mathbf{b}_1^H\hat{\mathbf{x}}\} + h_1 < 0$. The statement, that the second-order inequality (2.8b) is true for all $\mathbf{x}$ fulfilling the second-order inequality (2.8a), is true if and only if (2.9) is true for some $\lambda \geq 0$. It is worth to mention that opposing to the semidefinite matrix inequality given by the Schur complement, the correspondent semidefinite matrix inequality given by (2.9) never involves $\mathbf{x}$. It is only puts in an additional unknown variable λ under nonnegative constraint in the redefined optimization problem [69].

2.2.3.1 Proof of $\mathcal{S}$-procedure

In order to prove the $\mathcal{S}$-procedure where, (2.8) and (2.9) are strong substitute each other let $\mathbf{A_1}$, $\mathbf{A_2}$, $\mathbf{Q_1}$ and $\mathbf{Q_2} \in \mathbb{S}^n$, $\mathbf{b_1}$, $\mathbf{b_2} \in \mathbb{R}^n$, h_1, $h_2 \in \mathbb{R}$. Consider the following inequality system

$$\lambda \geq 0, \ \lambda\mathbf{Q}_1 + \mathbf{Q}_2 \succeq \mathbf{0}. \tag{2.10}$$

This equation can also be rewritten as following

$$\mathbb{F}(\lambda) = \lambda\mathbf{F} + \mathbf{G} \preceq \mathbf{0}, \tag{2.11}$$

where

$$\mathbf{F} = \mathbf{DIAG}(-1, -\mathbf{Q}_1) \in \mathbb{S}^{n+1}, \mathbf{G} = \mathbf{DIAG}(0, -\mathbf{Q}_2) \in \mathbb{S}^{n+1}. \tag{2.12}$$

Also, consider the following system

$$\mathbf{Z} \triangleq \begin{bmatrix} z & \mathbf{a}^T \\ \mathbf{a} & \mathbf{X} \end{bmatrix} \succeq \mathbf{0}, \mathrm{Tr}(\mathbf{GZ}) > 0, \mathrm{Tr}(\mathbf{FZ}) = 0. \tag{2.13}$$

Note that (2.11) and (2.13) are strong alternatives. Then, substitute (2.12) into (2.13) brings in

$$\mathbf{X} \succeq \mathbf{0}, \mathrm{Tr}(\mathbf{XQ}_2) < 0, \mathrm{Tr}(\mathbf{XQ}_1) \leq 0. \tag{2.14}$$

Then, (2.14) can be expressed as

$$x^T\mathbf{Q}_2 x < 0, x^T\mathbf{Q}_1 x \leq 0, x \in \mathbb{R}^n. \tag{2.15}$$

So, the result that (2.10) and (2.15) must be strong alternatives, provided that $\mathbf{F}$ given in (2.12) is indefinite by

$$\sum_{i=1}^{n} \upsilon_i \mathbf{F}_i \succeq 0 \Rightarrow \sum_{i=1}^{n} \upsilon_i \mathbf{F}_i = 0. \tag{2.16}$$

When the assumption of $\mathbf{Q}_1$ must have a negative eigenvalue at least holds true, strong alternatives occurs between (2.10) and (2.15). Let $\mathbf{Q}_1$ and $\mathbf{Q}_2$ be partitioned in the

following forms

$$\mathbf{Q}_1 = \begin{bmatrix} \mathbf{A}_1 & \mathbf{b}_1 \\ \mathbf{b}_1^T & h_2 \end{bmatrix}, \ \mathbf{Q}_2 = -\begin{bmatrix} \mathbf{A}_2 & \mathbf{b}_2 \\ \mathbf{b}_2^T & h_2 \end{bmatrix}. \tag{2.17}$$

Substituting (2.17) into (2.10) brings on

$$\begin{bmatrix} \mathbf{A}_2 & \mathbf{b}_2 \\ \mathbf{b}_2^T & h_2 \end{bmatrix} \preceq \lambda \begin{bmatrix} \mathbf{A}_1 & \mathbf{b}_1 \\ \mathbf{b}_1^T & h_1 \end{bmatrix}, \ \lambda \geq 0. \tag{2.18}$$

Furthermore, it can be demonstrated (see Remark 2.2.1) that

$$\begin{cases} \mathbf{x}^T\mathbf{A}_1\mathbf{x} + 2\mathbf{b}_1^T\mathbf{x} + h_1 \leq 0 \\ \mathbf{x}^T\mathbf{A}_2\mathbf{x} + 2\mathbf{b}_2^T\mathbf{x} + h_2 > 0 \end{cases} \text{where } \mathbf{x} \in \mathbb{R}^{n-1}, \tag{2.19}$$

and (2.15) are feasibility equivalent, As long as the assumption of $\mathbf{Q}_1$ must have a negative eigenvalue at least holds true, particularly, there exists an $\hat{\mathbf{x}}$ such that

$$\hat{\mathbf{x}}^T\mathbf{A}_1\hat{\mathbf{x}} + 2\mathbf{b}_1^T\hat{\mathbf{x}} + h_1 < 0. \tag{2.20}$$

So, (2.19) and (2.18) are strong alternatives under the premise (2.20). Furthermore, the infeasibility of (2.19) implies that the following implication is true:

$$\mathbf{x}^T\mathbf{A}_1\mathbf{x} + 2\mathbf{b}_1^T\mathbf{x} + h_1 \leq 0 \Rightarrow \mathbf{x}^T\mathbf{A}_2\mathbf{x} + 2\mathbf{b}_2^T\mathbf{x} + h_2 \leq 0. \tag{2.21}$$

Especially, the system given by (2.21) remains true if and only if there exists a λ satisfying the system given by (2.18) provided that (2.20) is true. By this the proof of the $\mathcal{S}$-procedure is completed.

Remark 2.2.1 *(Proof the feasibility equivalence of (2.15) and (2.19))*

Replacing (2.17) and $x = (\mathbf{v}, w) \in \mathbb{R}^n$ into (2.15) becomes

$$\begin{cases} q_1(\tilde{\mathbf{v}}) \triangleq \tilde{\mathbf{v}}^T \mathbf{A}_1 \tilde{\mathbf{v}} + 2\mathbf{b}_1^T \tilde{\mathbf{v}} + h_1 \leq 0 \\ q_2(\tilde{\mathbf{v}}) \triangleq \tilde{\mathbf{v}}^T \mathbf{A}_2 \tilde{\mathbf{v}} + 2\mathbf{b}_2^T \tilde{\mathbf{v}} + h_2 > 0 \end{cases} \quad \text{if} w \neq 0 \text{ and } \tilde{\mathbf{v}} = \mathbf{v}/w, \tag{2.22a}$$

$$\begin{cases} \mathbf{v}^T \mathbf{A}_1 \mathbf{v} \leq 0 \\ \mathbf{v}^T \mathbf{A}_2 \mathbf{v} > 0 \end{cases} \quad \text{if } w = 0. \tag{2.22b}$$

So, (2.15) is feasible, if and only if either (2.22a) or (2.22b) is feasible.

Replacing $\tilde{\mathbf{v}}$ in (2.22a) with $\mathbf{x} = \hat{\mathbf{x}} + t\mathbf{v} \in \mathbb{R}^{n-1}$ becomes

$$\begin{aligned} q_1(\mathbf{x}) &= q_1(\hat{\mathbf{x}}) + t^2 \mathbf{v}^T \mathbf{A}_1 \mathbf{v} + 2t(\mathbf{A}_1 \hat{\mathbf{x}} + \mathbf{b}_1)^T \mathbf{v} \\ &\leq q_1(\hat{\mathbf{x}}) + 2t(\mathbf{A}_1 \hat{\mathbf{x}} + \mathbf{b}_1)^T \mathbf{v} \ (by\ (2.22b)), \end{aligned} \tag{2.23}$$

$$q_2(\mathbf{x}) = q_2(\hat{\mathbf{x}}) + t^2 \mathbf{v}^T \mathbf{A}_2 \mathbf{v} + 2t(\mathbf{A}_2 \hat{\mathbf{x}} + \mathbf{b}_2)^T \mathbf{v}. \tag{2.24}$$

Suppose that $(\mathbf{A}_1 \hat{\mathbf{x}} + \mathbf{b}_1)^T \mathbf{v} \neq 0$. By letting $t \to \pm\infty$ in both (2.23) and (2.24) (depending on the sign of $(\mathbf{A}_1 \hat{\mathbf{x}} + \mathbf{b}_1)^T \mathbf{v}$), through applying (2.22b) to (2.24), It can be derived that

$$\begin{cases} \mathbf{x}^T \mathbf{A}_1 \mathbf{x} + 2\mathbf{b}_1^T \mathbf{x} + h_1 \leq 0 \\ \mathbf{x}^T \mathbf{A}_2 \mathbf{x} + 2\mathbf{b}_2^T \mathbf{x} + h_2 > 0 \end{cases} \tag{2.25}$$

must be feasible if (2.22b) under the assumption (2.20). Also, when $(\mathbf{A}_1 \hat{\mathbf{x}} + \mathbf{b}_1)^T \mathbf{v} = 0$, (2.23) reduces to $q_1(\mathbf{x}) \leq q_1(\hat{\mathbf{x}}) < 0$. So, (2.22a) is feasible for this case. Accordingly, the proof that (2.19) is feasible if and only if (2.15) is feasible, provided that (2.20) is true [69].

Chapter 3

Joint Beamforming and Power Allocation Design in Downlink Non-Orthogonal Multiple Access Systems

3.1 Introduction

In this part the joint design of beamforming and power allocation in the downlink of the NOMA MIMO multiuser system, where the users are grouped based on their QoS requirements. The problem formulation where the sum rate of the users who expect to be served with the best efforts is maximized under the rate constraints of the users with strict QoS requirements and the maximum transmit power constraint at the BS. SDR approach is proposed to solve the non-convex optimization problem and SCA has intended an algorithm based on the AGM inequality to perform the joint

design of the beamforming vectors and the power allocation coefficients. Simulation results are presented to show the performance advantage of the proposed algorithm over existing algorithms and the impact of system parameters on the convergence speed of the proposed algorithm.

3.2 System Model and Problem Formulation

We consider a downlink wireless broadcast channel in a MIMO multiuser system, as illustrated in Fig. 3.1, where an M-antenna base station (BS) serves several single-antenna users simultaneously. In this system, we consider the employment of NOMA to improve spectrum efficiency. We assume that the fading coefficients keep invariant during the channel coherence time and the channel state information (CSI) is known at the BS.

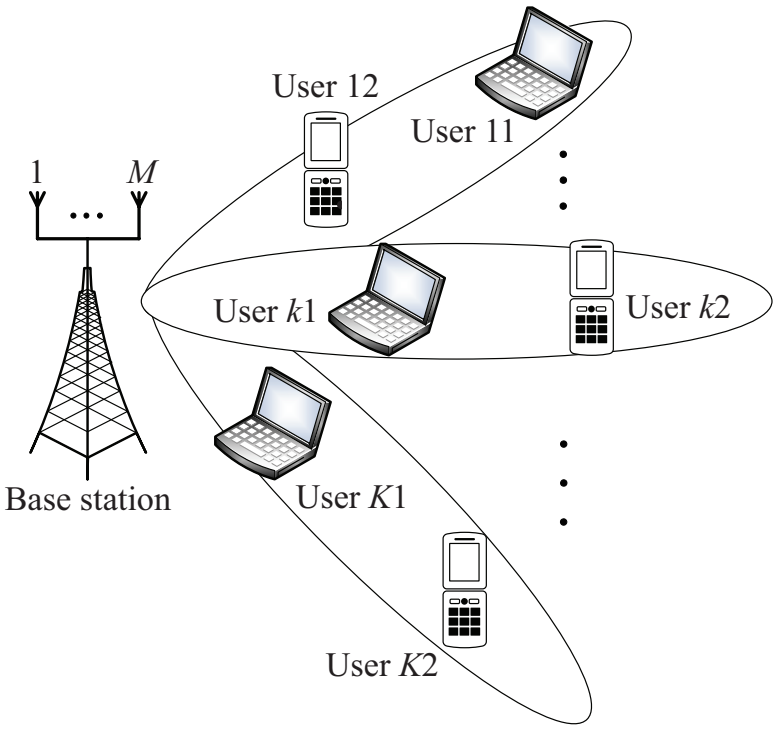

Figure 3.1: Downlink broadcast channel in a NOMA system.

In this work, we address a *new* scenario where the users in this system are divided into two groups, depending upon their QoS requirements. Group 1 contains the users that expect to be served with the best efforts, e.g., the users which are downloading with flexible delay-tolerant tasks. Differently, Group 2 contains the users that need a target rate such that they can carry out phone calls or other types of real-time tasks. Without loss of generality, we assume that each group has K users. We denote user $k1$, $k \in \{1, \cdots, K\}$, as the users in Group 1 and denote user $k2$ as the users in Group 2. We also assume that user $k1$ and user $k2$ are randomly paired. We further assume that the number of antennas at the BS is no less than the number of user pairs, i.e., $M \geq K$. Finally, we clarify that it is not necessary to order users according to their channel conditions in this work since the order of SIC is only determined by their QoS requirements.

We now formulate the problem to be tackled in the considered system. As per the rules of NOMA, we first express the information bearing vector, $\mathbf{s} \in \mathbb{C}^{K\times 1}$, as

$$\mathbf{s} = \left[\sqrt{a_1}s_{11}+\sqrt{b_1}s_{12},\ \cdots,\ \sqrt{a_K}s_{K1}+\sqrt{b_K}s_{K2}\right]^T, \tag{3.1}$$

where s_{k1} is the signal intended to user $k1$, s_{k2} is the signal intended to user $k2$, the allocated power to user $k1$ is a_k, and the allocated power to user $k2$ is b_k. Here, the allocated power needs to satisfy the condition that $a_k + b_k = 1$, $\forall k$.

An $M\times K$ beamforming matrix $\mathbf{P}$ is adopted at the BS to facilitate multiuser broadcasting. Mathematically, we express $\mathbf{P}$ as $\mathbf{P} = [\mathbf{p}_1, \cdots, \mathbf{p}_K]$, where $\mathbf{p}_k$ is the beamforming vector designed for the k-th user pair, containing user $k1$ and user $k2$. Suppose that user $k1$ expects to be served with the best efforts. To achieve this, the beamforming matrix is designed to guarantee that user $k1$ receives no interference from other user pairs. Motivated by this, zero-forcing (ZF) beamforming can be applied by leveraging the available CSI at the BS. Moreover, we note that user $k2$ has a strict QoS

requirement. This implies that user $k2$ can be treated as a primary user in cognitive radio networks and thus, it is important to ensure that the interference temperature experienced by user $k2$ is carefully controlled. It follows that the beamforming matrix needs to be designed such that user $k2$ receives no interference from other user pairs. To fulfill the aforementioned requirements, we define a new $M\times(K-1)$ matrix $\tilde{\mathbf{G}}_k$, where $\tilde{\mathbf{G}}_k=[\mathbf{g}_1,\cdots,\mathbf{g}_{k-1},\mathbf{g}_{k+1},\cdots,\mathbf{g}_K]$, and $\mathbf{g}_k\in\mathbb{C}^M$ is the Rayleigh fading channel vector from BS to user $k1$. As such, $\tilde{\mathbf{G}}_k$ contains the channel vectors from the BS to all users in Group 1, except for those from the BS to user $k1$. We decompose the beamforming vector $\mathbf{p}_k$ as $\mathbf{p}_k=\mathbf{U}_k\mathbf{q}_k$, where $\mathbf{U}_k$ is normalized and lies in the null space of $\tilde{\mathbf{G}}_k$, and $\mathbf{q}_k$ aims to improve the rates of users in Group 1 and guarantee the users in Group 2 to reach the target rate.

Based on the definition of $\mathbf{U}_k$ and $\tilde{\mathbf{G}}_k$, we confirm that $\mathbf{U}_k$ lies in the null space of $\tilde{\mathbf{G}}_k$. Applying the singular value decomposition, we decompose $\tilde{\mathbf{G}}_k$ as

$$\tilde{\mathbf{G}}_k=\left[\mathbf{A}_k^{(K-1)},\mathbf{A}_k^{(M-K+1)}\right]\mathbf{D}_k\mathbf{B}_k^H, \tag{3.2}$$

where $\mathbf{A}_k^{(K-1)}$ is the first $K-1$ left eigenvectors of $\tilde{\mathbf{G}}_k$, which form an orthogonal basis of $\tilde{\mathbf{G}}_k$, and $\mathbf{A}_k^{(M-K+1)}$ corresponding the zero eigenvalues represents the last $M-K+1$ left eigenvectors of $\tilde{\mathbf{G}}_k$, which form an orthogonal basis of the null space of $\tilde{\mathbf{G}}_k$. Therefore, $\mathbf{U}_k$ is given by $\mathbf{U}_k=\mathbf{A}_k^{(M-K+1)}$.

We assume that the SIC is employed at user $k1$ to remove the interference caused by s_{k2}. Under this assumption, s_{k2} can be correctly decoded and completely cancelled at user $k1$ if the actual rate of s_{k2} is larger than or equal to its target rate at user $k1$. With the aid of ZF beamforming, the received signal at user $k1$, y_{k1}, is written as

$$y_{k1}=\sqrt{a_k}\mathbf{g}_k^H\mathbf{U}_k\mathbf{q}_k s_{k1}+n_{k1}, \tag{3.3}$$

where $n_{k1} \sim \mathcal{CN}(0, \sigma_{k1}^2)$ denotes the circularly symmetric complex Gaussian noise at user $k1$ with zero mean and variance σ_{k1}^2. Based on (3.3), the SNR of the desired message at user $k1$ is obtained as

$$\mathrm{SNR}_{k1} = a_k \left| \tilde{\mathbf{g}}_k^H \mathbf{U}_k \mathbf{q}_k \right|^2, \tag{3.4}$$

where $\tilde{\mathbf{g}}_k = \mathbf{g}_k / \sigma_{k1}$ for all k.

We next focus on user $k2$. We note that neither the inter-beam interference nor the intra-beam interference can be completely canceled at user $k2$. As such, the received signal at user $k2$, y_{k2}, is written as

$$\begin{aligned} y_{k2} =& \sqrt{b_k} \mathbf{h}_k^H \mathbf{U}_k \mathbf{q}_k s_{k2} + \sqrt{a_k} \mathbf{h}_k^H \mathbf{U}_k \mathbf{q}_k s_{k1} \\ &+ \sum_{i \neq k} \mathbf{h}_k^H \mathbf{U}_i \mathbf{q}_i \left(\sqrt{a_i} s_{i1} + \sqrt{b_i} s_{i2} \right) + n_{k2}, \end{aligned} \tag{3.5}$$

where $\mathbf{h}_k \in \mathbb{C}^{M \times 1}$ is the Rayleigh fading channel vector from the BS to user $k2$ and $n_{k2} \sim \mathcal{CN}(0, \sigma_{k2}^2)$ denotes the circularly symmetric complex Gaussian noise at user $k2$ with zero mean and variance σ_{k2}^2. It is seen from (3.5) that the first item in the right-hand side is the desired signal at user $k2$ and the remaining items are the received interference and noise. Based on (3.5), the decoded signal-to-interference-plus-noise ratio (SINR) of user $k2$ is obtained as

$$\mathrm{SINR}_{k2} = \frac{b_k |\tilde{\mathbf{h}}_k^H \mathbf{U}_k \mathbf{q}_k|^2}{a_k |\tilde{\mathbf{h}}_k^H \mathbf{U}_k \mathbf{q}_k|^2 + \sum_{i \neq k} |\tilde{\mathbf{h}}_k^H \mathbf{U}_i \mathbf{q}_i|^2 + 1}, \tag{3.6}$$

where $\tilde{\mathbf{h}}_k = \mathbf{h}_k / \sigma_{k2}$. In addition, using (3.3) and (3.5), the decoded SINR of user $k2$ at user $k1$ is obtained as

$$\overline{\mathrm{SINR}}_{k2} = \frac{b_k |\tilde{\mathbf{g}}_k^H \mathbf{U}_k \mathbf{q}_k|^2}{a_k |\tilde{\mathbf{g}}_k^H \mathbf{U}_k \mathbf{q}_k|^2 + 1}. \tag{3.7}$$

In the considered system, the strict QoS requirement of user $k2$ is demanded not only at its own receiver, but also at the other user within the same user pair, i.e., user $k1$, for the purpose of SIC. Therefore, both the allocated power and the

designed beamforming matrix need to meet the target rate R_0, i.e., $\log\left(1+\mathrm{SINR}_{k2}\right)\geq R_0$ and $\log\left(1+\overline{\mathrm{SINR}}_{k2}\right)\geq R_0$ [79]. Under this constraint, the goal of our design in the considered system is to maximize the sum rate of the users in Group 1, since user $k1$ expects to be served with the best efforts. Mathematically, the optimization problem, denoted by **P1**, is formulated as

$$\mathbf{P1} \quad \max_{\{a_k,b_k,\mathbf{q}_k\}_{k=1}^K} \sum_{k=1}^{K} \log\left(1+\mathrm{SNR}_{k1}\right) \tag{3.8a}$$

$$\text{s.t.} \quad \log\left(1+\mathrm{SINR}_{k2}\right)\geq R_0,\ \forall k, \tag{3.8b}$$

$$\log\left(1+\overline{\mathrm{SINR}}_{k2}\right)\geq R_0,\ \forall k, \tag{3.8c}$$

$$\sum_{k=1}^{K}\mathrm{Tr}\left(\mathbf{q}_k\mathbf{q}_k^H\right)\leq P_{\max}, \tag{3.8d}$$

$$a_k+b_k=1,\ \forall k, \tag{3.8e}$$

$$a_k\geq 0, b_k\geq 0,\ \forall k, \tag{3.8f}$$

where (3.8d) indicates that the BS is subject to the maximum transmit power $P_{\max}$.

It can be seen from **P1** that the sum rate of the users in Group 1 and the achievable rates of the users in Group 2 depend on $\{\mathbf{q}_k\}$ and $\{a_k\}$. In the following section, we will jointly design beamforming vectors and power allocation coefficients to solve **P1**.

3.3 Joint Design of Beamforming and Power Allocation

In this section, we aim to solve **P1** given in (3.8). To this end, we first employ the SDR approach [35] to linearize the beamforming vectors. Then we apply the successive convex approximation based on the AGM inequality to perform the joint design of

beamforming vectors and power allocation coefficients.

3.3.1 Semidefinite Relaxation (SDR) Approach

We first note that the optimization problem **P1** is a quadratically constrained quadratic program and non-convex with respect to the beamforming vectors $\mathbf{q}_k$. Hence, in this subsection, we introduce the SDR approach to linearize the beamforming vectors such that for any given $\{a_k\}$, the beamforming design can be reformulated as a convex problem with linear matrix inequalities (LMIs).

Specifically, we find that both the objective function and the constraints in **P1** are linear with the matrix $\mathbf{q}_k\mathbf{q}_k^H$. As such, we introduce an $(M-K+1)\times(M-K+1)$ positive semidefinite matrix, $\mathbf{Q}_k$, into the optimization problem to replace $\mathbf{q}_k\mathbf{q}_k^H$. If $\mathbf{Q}_k$ is a rank-one matrix, the optimization problem with $\mathbf{Q}_k$ is equivalent to the original optimization problem **P1**. We then note that the introduced constraint $\text{Rank}(\mathbf{Q}_k)=1$, $\forall k$, is non-convex. To address this issue, we drop this constraint to obtain the relaxed optimization problem **P2**, which reads

$$\mathbf{P2} \quad \max_{\{a_k,\mathbf{Q}_k\}_{k=1}^K} R \triangleq \sum_{k=1}^{K} \log\left(1+a_k \,\text{Tr}\left(\mathbf{G}_k\mathbf{Q}_k\right)\right) \tag{3.9a}$$

$$\text{s.t.} \quad a_k \,\text{Tr}\left(\mathbf{H}_{kk}\mathbf{Q}_k\right) \le \Delta_1,\ \forall k, \tag{3.9b}$$

$$a_k \,\text{Tr}\left(\mathbf{G}_k\mathbf{Q}_k\right) \le \Delta_2,\ \forall k, \tag{3.9c}$$

$$\mathbf{Q}_k \succeq 0,\ \forall k, \tag{3.9d}$$

$$\sum_{k=1}^{K} \text{Tr}\left(\mathbf{Q}_k\right) \le P_{\max}, \tag{3.9e}$$

$$0 \le a_k \le 1,\ \forall k, \tag{3.9f}$$

where, for the sake of clarity, we apply the properties of matrix trace and define $\mathbf{H}_{ki} = \mathbf{U}_i^H\tilde{\mathbf{h}}_k\tilde{\mathbf{h}}_k^H\mathbf{U}_i$ and $\mathbf{G}_k = \mathbf{U}_k^H\tilde{\mathbf{g}}_k\tilde{\mathbf{g}}_k^H\mathbf{U}_k$ for $i \in \{1,\cdots,K\}$, and

$$\Delta_1 = \frac{1}{\gamma}\operatorname{Tr}\left(\mathbf{H}_{kk}\mathbf{Q}_k\right) - \frac{\gamma}{\gamma+1}\sum_{i\neq k}^{K}\operatorname{Tr}\left(\mathbf{H}_{ki}\mathbf{Q}_i\right) - \frac{\gamma}{\gamma+1},$$
$$\Delta_2 = \frac{1}{\gamma+1}\operatorname{Tr}\left(\mathbf{G}_k\mathbf{Q}_k\right) - \frac{\gamma}{\gamma+1},$$

with $\gamma = 2^{R_0} - 1$ being the SINR target of user $k2$.

By introducing a set of slack variables $\{s_k\}$, **P2** is equivalent to

$$\mathbf{P3} \quad \max_{\{a_k,\mathbf{Q}_k,s_k\}_{k=1}^{K}} \quad \sum_{k=1}^{K}\log\left(1+s_k\right) \tag{3.11a}$$
$$\text{s.t.} \quad a_k\operatorname{Tr}\left(\mathbf{G}_k\mathbf{Q}_k\right) \geq s_k, \forall k, \tag{3.11b}$$
$$(3.9\text{b}) - (3.9\text{f}).$$

Here we remark that for any fixed power allocation scheme, the problem **P3** is concave, and for any fixed beamforming matrices, **P3** is also concave. However, it can be easily shown that $a_k\operatorname{Tr}(\mathbf{G}_k\mathbf{Q}_k)$, as well as $a_k\operatorname{Tr}(\mathbf{H}_{kk}\mathbf{Q}_k)$, are concave in a_k and $\mathbf{Q}_k$ since their Hessian matrices are negative semidefinite. Henceforth, the problem **P3** is nonconvex due to the constraints (3.9b) and (3.9c).

3.3.2 SCA based on AGM Inequality

In view of the nonconvexity of **P3**, we now consider the suboptimal design of the power allocation coefficients a_k and the beamforming matrices $\mathbf{Q}_k$ under the constraints given by (3.9b) and (3.9c). It is noted that the functions in the left-hand side of (3.9b) and (3.9c) are concave while functions in the right-hand side of (3.9b) and (3.9c) are linear. To resolve (3.9b) and (3.9c) by their structure, we apply the AGM inequality to approximate the concave function by a convex function. Specifically, the AGM inequality says that $2xy \leq x^2 + y^2$ holds true for any two positive numbers x and y with the equality holds true if and only if $x = y$.

Thus we define two quadratic functions as

$$\mu\left(a_k, \mathbf{Q}_k\right) \triangleq \frac{1}{2}\left(a_k^2 + \left(\mathrm{Tr}\left(\mathbf{H}_{kk}\mathbf{Q}_k\right)\right)^2\right), \tag{3.12}$$

$$\nu\left(a_k, \mathbf{Q}_k\right) \triangleq \frac{1}{2}\left(a_k^2 + \left(\mathrm{Tr}\left(\mathbf{G}_k\mathbf{Q}_k\right)\right)^2\right). \tag{3.13}$$

Note that $a_k \,\mathrm{Tr}\left(\mathbf{H}_{kk}\mathbf{Q}_k\right) \leq \mu\left(a_k, \mathbf{Q}_k\right)$ and $a_k \,\mathrm{Tr}\left(\mathbf{G}_k\mathbf{Q}_k\right) \leq \nu\left(a_k, \mathbf{Q}_k\right)$, while both $\mu\left(a_k, \mathbf{Q}_k\right)$ and $\nu\left(a_k, \mathbf{Q}_k\right)$ are convex with respect to a_k and $\mathbf{Q}_k$. Hence, (3.9b) and (3.9c) can be conservatively guaranteed by two convex constraints $\mu\left(a_k, \mathbf{Q}_k\right) \leq \Delta_1$ and $\nu\left(a_k, \mathbf{Q}_k\right) \leq \Delta_2$.

However, there is a gap between $a_k \,\mathrm{Tr}\left(\mathbf{H}_{kk}\mathbf{Q}_k\right)$ and $\mu\left(a_k, \mathbf{Q}_k\right)$, also between $a_k \,\mathrm{Tr}\left(\mathbf{G}_k\mathbf{Q}_k\right)$ and $\nu\left(a_k, \mathbf{Q}_k\right)$. In order to reduce the approximation gaps, we introduce a series of factors, c_{ki}, where $k = 1, \cdots, K$ and $i = 1, 2$, as follows

$$2a_k \,\mathrm{Tr}\left(\mathbf{H}_{kk}\mathbf{Q}_k\right) \leq \left(a_k c_{k1}\right)^2 + \left(\frac{\mathrm{Tr}\left(\mathbf{H}_{kk}\mathbf{Q}_k\right)}{c_{k1}}\right)^2, \tag{3.14a}$$

$$2a_k \,\mathrm{Tr}\left(\mathbf{G}_k\mathbf{Q}_k\right) \leq \left(a_k c_{k2}\right)^2 + \left(\frac{\mathrm{Tr}\left(\mathbf{G}_k\mathbf{Q}_k\right)}{c_{k2}}\right)^2, \tag{3.14b}$$

where the equalities hold true if and only if

$$c_{k1} = \sqrt{\frac{\mathrm{Tr}(\mathbf{H}_{kk}\mathbf{Q}_k)}{a_k}} \text{ and } c_{k2} = \sqrt{\frac{\mathrm{Tr}(\mathbf{G}_k\mathbf{Q}_k)}{a_k}}, \ \forall k. \tag{3.15}$$

With proper choice of c_{ki}, the conservatism of the approximation to (3.9b) and (3.9c) by (3.14) can thus be reduced.

With the AGM inequality based constraints (3.14), the optimization problem

Algorithm 1 Proposed AGM Algorithm

Initialize $c_{k1}^{(1)} = c_{k2}^{(1)} = 1, \forall k$, $R^{(0)} = -\infty, \epsilon = 1$
Set iteration index $t = 1$
while $\epsilon \geq 0.01$ **do**
  Update $\{\mathbf{Q}_k^{(t)}, a_k^{(t)}\}$ with $c_{k1}^{(t)}$ and $c_{k2}^{(t)}$ by solving (3.16);
  Update the sum rate of users in Group 1, $R^{(t)}$ by (3.9a);
  Update $c_{k1}^{(t+1)}$ and $c_{k2}^{(t+1)}$ based on (3.17);
  Update $\epsilon = \left(R^{(t)} - R^{(t-1)}\right)/R^{(t-1)}$;
  $t := t + 1$;
end while
Output $\{\mathbf{Q}_k^{(t-1)}, a_k^{(t-1)}\}$

P3 is then conservatively approximated by

$$\mathbf{P4} \max_{\{a_k, \mathbf{Q}_k, s_k\}} \sum_{k=1}^{K} \log\left(1 + s_k\right) \tag{3.16a}$$

$$\text{s.t.} \quad a_k \operatorname{Tr}\left(\mathbf{G}_k \mathbf{Q}_k\right) \geq s_k, \forall k, \tag{3.16b}$$

$$\left(a_k c_{k1}\right)^2 + \left(\frac{\operatorname{Tr}\left(\mathbf{H}_{kk}\mathbf{Q}_k\right)}{c_{k1}}\right)^2 \leq 2\Delta_1, \forall k, \tag{3.16c}$$

$$\left(a_k c_{k2}\right)^2 + \left(\frac{\operatorname{Tr}\left(\mathbf{G}_k\mathbf{Q}_k\right)}{c_{k2}}\right)^2 \leq 2\Delta_2, \forall k, \tag{3.16d}$$

$$(3.9\text{d}) - (3.9\text{f}),$$

which is a convex problem for any fixed factors c_{ki}, and thus can be solved by off-the-shelf solvers, e.g., `CVX` [80].

By applying the idea of SCA [36], we iteratively approximate the feasible set of **P3** by updating c_{ki} in **P4** with

$$c_{k1}^{(t+1)} = \sqrt{\frac{\operatorname{Tr}(\mathbf{H}_{kk}\mathbf{Q}_k^{(t)})}{a_k^{(t)}}}, \; c_{k2}^{(t+1)} = \sqrt{\frac{\operatorname{Tr}(\mathbf{G}_k\mathbf{Q}_k^{(t)})}{a_k^{(t)}}}, \tag{3.17}$$

where t is the iteration index. The iteration process to **P3**, called *AGM Algorithm*, is then detailed in **Algorithm 1**.

The proposed AGM algorithm in this work continuously decreases the gap between the reformed optimization problem and the original optimization problem.

Specifically, this decrease is achieved by iteratively updating c_{k1} and c_{k2}, $\forall k$, until the sum rate of the users in Group 1 converges. We can draw the following lemma, whose proof is omitted due to the space limits.

Lemma 1 *Every limit point of the sequence generated by Algorithm 1 is a stationary point of problem* ***P2****.*

We remark that $\mathbf{q}_k\mathbf{q}_k^H$ is relaxed to a positive semidefinite matrix $\mathbf{Q}_k$ in $\mathbf{P4}$ by the SDR technique. However, the optimal solution of $\mathbf{Q}_k$ to $\mathbf{P4}$ is not guaranteed to be of rank one, which mandates the use of the Gaussian randomization procedure or the rank-one approximation [35].

Table 3.1: Sum Rate of Users in Group 2 (bps)

SNR	10 dB	20 dB	30 dB	40 dB	50 dB
Required QoS	1.0521	1.0521	1.0521	1.0521	1.0521
AGM	1.0526	1.0540	1.0557	1.0571	1.0573
AO	1.0523	1.0521	1.0521	1.0521	1.0521
Unjoint	0.8439	0.9816	1.0357	1.0541	1.0601

3.4 Simulation Results

In this section, we present Monte Carlo simulation results to evaluate the performance of the proposed joint beamforming and power allocation design, referred to as the AGM algorithm, in the downlink channel of a NOMA-based MIMO multiuser system. To this end, we generate the entries of $\mathbf{g}_k$ and $\mathbf{h}_k$ using the independent circularly symmetric complex Gaussian distribution with zero mean and unit variance. Moreover, we assume the total transmit power at the BS is normalized to unity, i.e., $P_{\max} = 1$ watt. Without loss of generality, we further assume that the noise level at users is the same, i.e., $\sigma_{k1}^2 = \sigma_{k2}^2 = \sigma^2$, $\forall k$. Accordingly, the SNR used in this section refers to the average SNR which is defined as $\text{SNR} = P_{\max}/\sigma^2$. The target SINR requirement of the users in Group 2 is set to be 0.2, i.e., $\gamma = 0.2$.

3.4.1 Sum Rate of Users

Fig. 3.2 depicts the sum rate of the users in Group 1 versus SNR. In this figure, we compare our proposed AGM algorithm to the alternating optimization (AO) algorithm, the unjoint algorithm [81], and the OMA algorithm. Here, the AO algorithm updates the beamforming matrix with fixed allocated power and updates the allocated power with the fixed beamforming matrix alternatively, while the unjoint algorithm adopts the ZF beamforming and allocates power accordingly to reach the target rate. From Fig. 3.2,

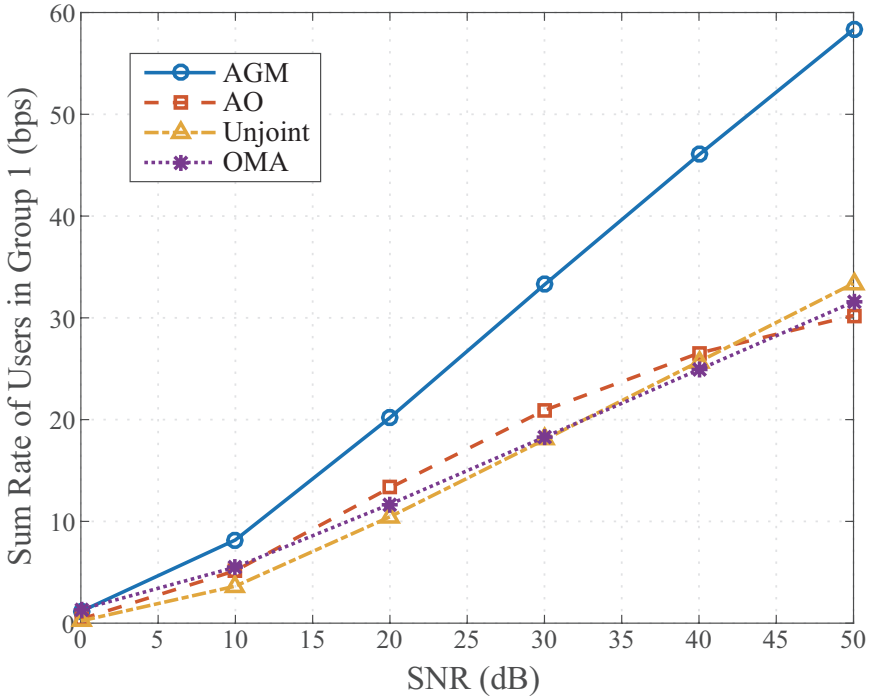

Figure 3.2: Comparison of the sum rate of the users in Group 1 versus SNR with $M = 6$ and $K = 4$.

we observe that the proposed design achieves a significant performance advantage over other algorithms, especially in the high SNR regime. This is due to the joint design of the beamforming matrix and power allocation in our proposed algorithm.

We then compare the sum rate of the users in Group 2 of different algorithms in Table 3.1. It can be clearly observed that our proposed algorithm achieves a higher sum rate than both the AO algorithm and the unjoint algorithm. Moreover, we observe that our algorithm always guarantees the required QoS requirement over the whole SNR regime, while the unjoint algorithm does not. Both observations demonstrate the benefits of our proposed algorithm for the users in Group 2 relative to the existing algorithms.

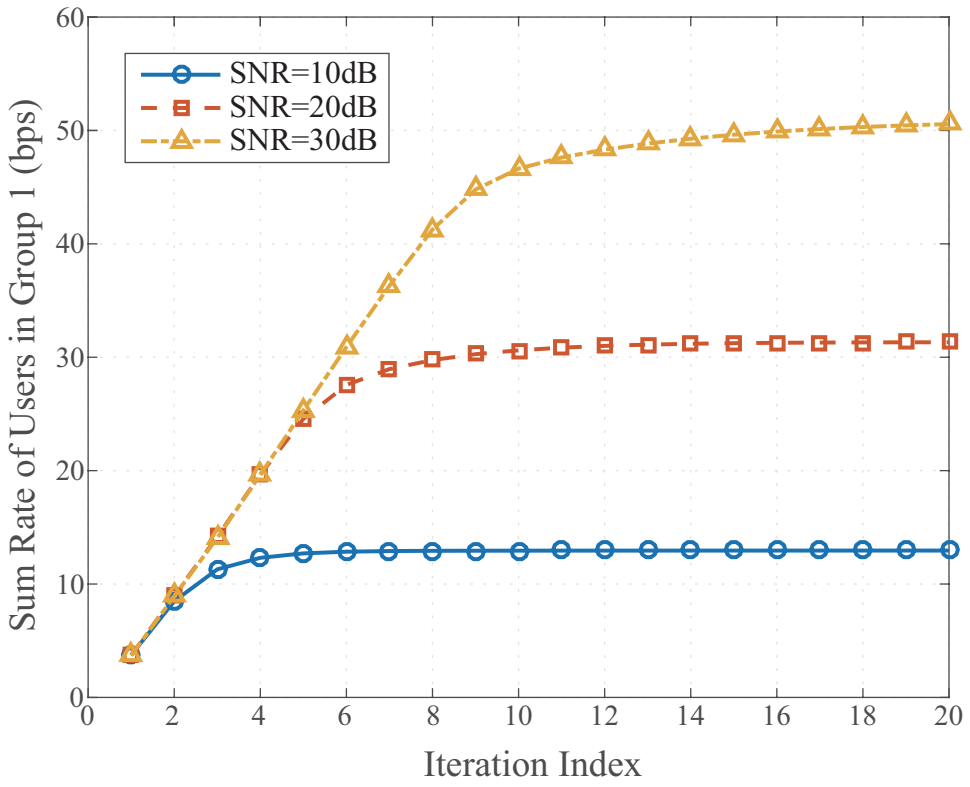

Figure 3.3: Sum rate of the users in Group 1 versus the iteration index for different SNRs with $M = 6$ and $K = 4$.

3.4.2 Convergency Property

Figs. 3.3 and 3.4 depict the convergence of the AGM algorithm versus the iteration index, which allows us to examine the impact of system parameters on the convergence rate of our proposed algorithm. From Fig. 3.3, we observe that the convergence rate of our proposed AGM algorithm becomes lower when the SNR increases. This is due to the fact that the gap between a_k and $\mathrm{Tr}\,(\mathbf{G}_k\mathbf{Q}_k)$ and the gap between a_k and $\mathrm{Tr}\,(\mathbf{H}_{kk}\mathbf{Q}_k)$ increase when the noise level decreases. From Fig. 3.4, we observe that the convergence rate of the AGM algorithm becomes lower when $M-K$ increase. This is because there are $(M-K+1)^2$ independent variables in each of the K beamforming matrices to be optimized.

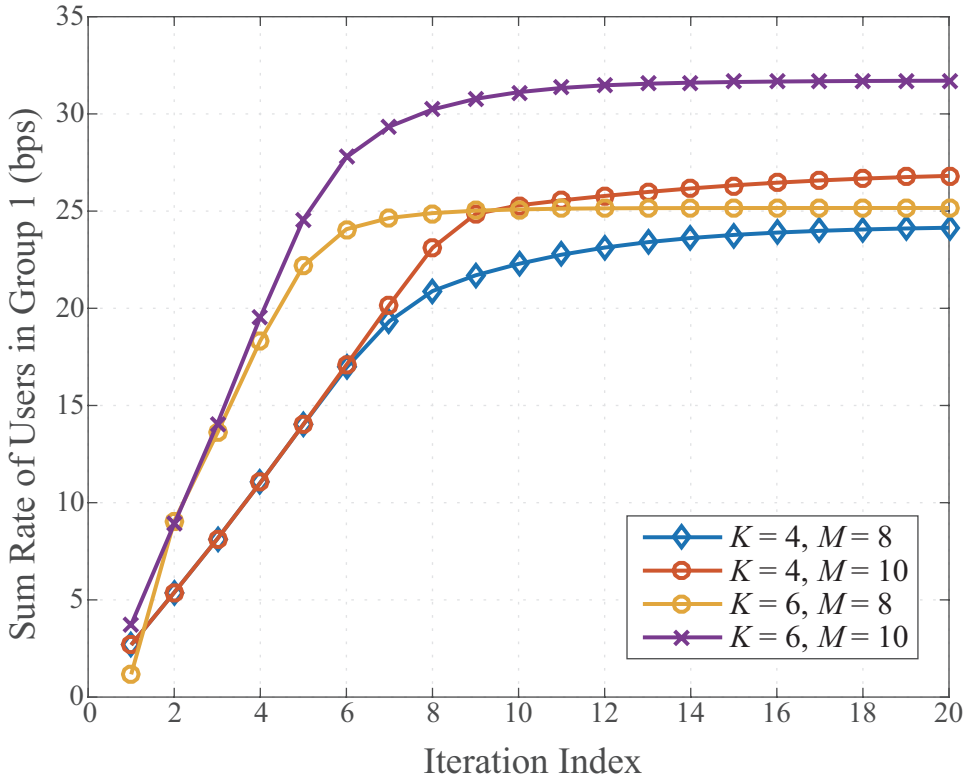

Figure 3.4: Sum rate of the users in Group 1 versus the iteration index for different values of K and M with SNR = 20 dB.

3.4.3 Rank Results

Fig. 3.5 depicts the ratio between the largest eigenvalue and the second largest eigenvalue of the optimal beamforming matrix, denoted by R_λ, versus the number of antennas for $2,000$ independent Rayleigh channel realizations. Due to the quadratic form of $\mathbf{Q}_k$ in (3.16c) and (3.16d), as well as the nonlinear objective function, the rank one optimality of **P4** can not be drawn directly by applying the lemma in [82]. This makes the rank analysis very challenging and thus motivates us to use simulation results to demonstrate the rank of the obtained solution. It can be seen from Fig. 3.5, that if problem **P4** is feasible, then it always yields a sufficiently large R_λ, implying that the AGM algorithm admits a rank-one optimal solution $\{\mathbf{Q}_k\}$ when it converges in all simulation cases.

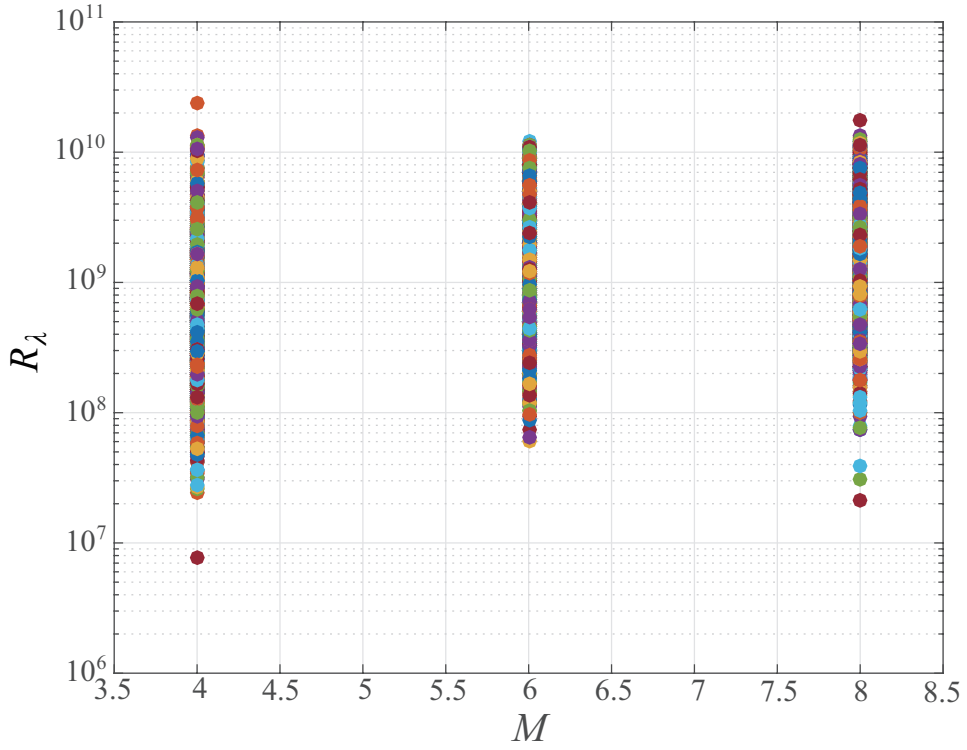

Figure 3.5: The ratio between the largest eigenvalue and the second largest eigenvalue of the optimal beamforming matrix versus the number of antennas with $K = 2$.

3.5 Summary

The joint design of beamforming and power allocation in the downlink of the NOMA MIMO multiuser system is investigated, where the users are grouped based on their QoS requirements. For the sake of practicality, the problem is formulated where the sum rate of the users who expect to be served with the best efforts is maximized under the rate constraints of the users with strict QoS requirements and the maximum transmit power constraint at the BS. We then eliminated the inter-beam interference by applying the ZF beamforming. To solve the non-convex optimization problem, the SDR is adopted to approach and showed that the optimal solutions are always rank one using simulation results. Also, a SCA algorithm is proposed based on the AGM inequality to perform the joint design of the beamforming vectors and the power allocation coefficients. Simulation results were presented to show the performance advantage of our proposed algorithm over existing algorithms and the impact of system parameters on the convergence speed of our proposed algorithm

Chapter 4

Maximizing SINR for Non-Orthogonal Multiple Access With Bounded Channel Uncertainties

4.1 Introduction

In this chapter the worst-case robust beamforming design for the MISO-NOMA downlink systems by taking into account the norm-bounded channel uncertainties are investigated. The objective is to balance the users SINRs with the constraints of the total transmit power of the other users and the received interference power at the users. However, the original robust problem formulation is not convex due to the imperfect CSI. The S-procedure is exploited to reformulate the original non-convex problem into the SDP form by recasting the original non-convex constraints into the LMI form.

4.2 System Model and Problem Formulation

The system model is based on multiple-input single-output (MISO-NOMA) downlink systems, where the base station is equipped with M antennas and sends different messages to K users denoted as $U_1, U_2, \ldots, U_K$. Each user is equipped with a single antenna. The channel between the BS and the k^{th} user U_k is denoted by $\mathbf{h}_k$ and $\mathbf{w}_k$ represents the corresponding beamforming vector of the k^{th} user U_k. The received signal at U_k is given by

$$y_k = \mathbf{h}_k^H \mathbf{w}_k s_k + \sum_{m \neq k} \mathbf{h}_k^H \mathbf{w}_m s_m + n_k, \forall k \tag{4.1}$$

where s_k denotes the symbol intended for U_k and $n_k \sim \mathcal{CN}(0, \sigma_k^2)$ represents a zero-mean additive white Gaussian noise with variance represents a zero-mean additive white Gaussian noise with variance σ_k^2. The power of the symbol $s_k$is assumed to be unity, i.e. $\mathbb{E}\left[|s_k|^2\right] = 1$. In practical scenarios, there are difficulties to have perfect CSI at the transmitter due to channel estimation and quantization errors. Therefore, we consider a robust beamforming design to overcome these channel uncertainties. In particular, we incorporate norm bounded channel uncertainties in the design as

$$\mathbf{h}_k = \hat{\mathbf{h}}_k + \Delta\hat{\mathbf{h}}, \left\|\Delta\hat{\mathbf{h}}\right\|_2 = \left\|\mathbf{h}_k - \hat{\mathbf{h}}_k\right\|_2 \leq \epsilon, \tag{4.2}$$

where $\hat{\mathbf{h}}_k, \Delta\hat{\mathbf{h}}$ and $\epsilon \geq 0$ denote the estimate of $\mathbf{h}_k$,the norm-bounded channel estimation error and the channel estimation error bound, respectively.

In NOMA scheme, user multiplexing is performed in power domain and the SIC approach is employed at receivers to separate signals between different users. In

this scheme, users are sorted based on the norm of their channels, i.e., $\left\|\hat{\mathbf{h}}_1\right\|_2 \leq \left\|\hat{\mathbf{h}}_2\right\|_2 \leq \ldots \leq \left\|\hat{\mathbf{h}}_K\right\|_2$ where the channels have been ordered inversely with the path loss ,for example, the k_{th} user locates to the closest distance to the Bs decodes the signals intended for the users from U_1 to U_{k-1} through SIC approach whereas the signals intended for the rest of the users i.e., $(U_{k+1}, \ldots, U_K)$ are treated as the interference at the k^{th} user. Based on this SIC approach, the l^{th} user can detect and remove the k^{th} users signals for $1 \leq k \leq l$. Hence, the signal at l^{th} the user after removing the first $k-1$ users signals to detect k^{th} user is represented as

$$y_l^k = \mathbf{h}_l^H \mathbf{w}_k s_k + \sum_{m=1}^{k-1} \Delta\hat{\mathbf{h}}_l \mathbf{w}_m s_m + \sum_{m=k+1}^{K} \mathbf{h}_l^H \mathbf{w}_m s_m + n_k, \forall k, l \in \{k, k+1, \ldots K\} \tag{4.3}$$

where the first term is the desired signal to detect s_k and the second term is due to imperfect CSI at the receivers during the SIC process. Due to the channel uncertainties, the signals intended for the users $U_1, \ldots, U_{k-1}$ cannot be completely removed by the l^{th} user. The third term is the interference introduced by the signals intended to the users $U_{k+1}, \ldots, U_K$. According to the NOMA scheme, the l^{th} user should be able to detect all k^{th} $(k < l)$ user signals.

$$y_l^l = \mathbf{h}_l^H \mathbf{w}_l s_l + \sum_{m=1}^{l-1} \Delta\hat{\mathbf{h}}_l \mathbf{w}_m s_m + \sum_{m=l+1}^{K} \mathbf{h}_l^H \mathbf{w}_m s_m + n_l. \quad \forall k, l \in \{k, k+1, \ldots K\} \tag{4.4}$$

The instantaneous received SINR at the l^{th} user can be expressed as

$$\mathrm{SINR}_l^l = \frac{\mathbf{h}_l^{\mathrm{H}} \mathbf{w}_l \mathbf{w}_l^{\mathrm{H}} \mathbf{h}_l}{\sum_{m=1}^{l-1} \Delta\hat{\mathbf{h}}_l^{\mathrm{H}} \mathbf{w}_m \mathbf{w}_m^{\mathrm{H}} \Delta\hat{\mathbf{h}}_l + \sum_{m=l+1}^{K} \mathbf{h}_l^{\mathrm{H}} \mathbf{w}_m \mathbf{w}_m^{\mathrm{H}} \mathbf{h}_l + \sigma_l^2}. \tag{4.5}$$

4.3 Proposed Optimization Methods

The SINR basically determines the quality of service (QoS) of the users. Therefore, robust SINR maximization has been investigated by incorporating channel uncertainties to assure the required SINR at each user. The worst-case SINR of each user is considered in this study and the optimization problem is formulated as follow:

$$\mathbf{P1} \quad \max \min_{\|\Delta\hat{\mathbf{h}}_l\|_2 \leq \epsilon} \mathrm{SINR}_l^l, \tag{4.6a}$$

$$s.t. \quad \min_{\|\Delta\hat{\mathbf{h}}_i\|_2 \leq \epsilon} \left(\min_{i \in \{l+1,\ldots,K\}} \mathrm{SINR}_l^i \right) \geq \gamma_i^{min}, \forall i \tag{4.6b}$$

$$\sum_{l=1}^{K} \|\mathbf{w}_l\|^2 \leq P_T, \tag{4.6c}$$

considering in the problem formulation a minimum required SINRs for the remaining users in the cell (4.6b) and limited by transmitted power P_T. This problem **P1** is not convex in fact it's quasi-convex. In order to solve this quasi-convex problem, by employing the classical bisection method [72]. Based on the above idea, first, recast **P1** in the epigraph form by introducing a new variable $t \geq 0$, where t is an auxiliary variable for scaling the SINR. Also, the solution of **P1** can ensure the perfect case under

the assumption of perfect CSI is assumed.

$$\mathbf{P2} \quad \max t, \tag{4.7a}$$

$$s.t. \quad \min_{\|\Delta\hat{\mathbf{h}}_l\|_2 \leq \epsilon} \mathrm{SINR}_l^l \geq t, \forall l \tag{4.7b}$$

$$\min_{\|\Delta\hat{\mathbf{h}}_i\|_2 \leq \epsilon} (\min_{i \in \{l+1,\ldots,K\}} \mathrm{SINR}_l^i) \geq \gamma_i^{min}, \forall i \tag{4.7c}$$

$$\sum_{l=1}^{K} \|\mathbf{w}_l\|^2 \leq P_T. \tag{4.7d}$$

Given a set of target SINR levels $\gamma = [\gamma_i^{min}, \ldots, \gamma_K]$ with $\gamma_i^{min} = (2^{R_i^{min}} - 1)$ denoting the target minimum required SINR to achieve a target rate of the ith user, where $i = l+1, \ldots, K$. The equivalent transformations of $(4.7c)$ can be obtained as ϖ_{il} as follows:

$$\begin{cases} \min\limits_{\|\Delta\hat{\mathbf{h}}_{l+1}\|_2 \leq \epsilon} \gamma_i^{min}(\sum\limits_{m=1}^{i-1} \Delta\mathbf{h}_{l+1}^H \mathbf{w}_m \mathbf{w}_m^H \Delta\hat{\mathbf{h}}_{l+1} + \\ \sum\limits_{m=i+1}^{K} \mathbf{h}_{l+1}^H \mathbf{w}_m \mathbf{w}_m^H \mathbf{h}_{l+1} + \sigma_{l+1}^2) \leq \mathbf{h}_{l+1}^H \mathbf{w}_{l+1} \mathbf{w}_{l+1}^H \mathbf{h}_{l+1} \\ \vdots \\ \min\limits_{\|\Delta\hat{\mathbf{h}}_K\|_2 \leq \epsilon} \gamma_i^{min}(\sum\limits_{m=1}^{i-1} \Delta\mathbf{h}_K^H \mathbf{w}_m \mathbf{w}_m^H \Delta\hat{\mathbf{h}}_K \\ + \sum\limits_{m=i+1}^{K} \mathbf{h}_K^H \mathbf{w}_m \mathbf{w}_m^H \mathbf{h}_K + \sigma_K^2) \leq \mathbf{h}_K^H \mathbf{w}_K \mathbf{w}_K^H \mathbf{h}_K \end{cases}$$

$$\Leftrightarrow \min_{\|\Delta\hat{\mathbf{h}}_i\|_2 \leq \epsilon} (\sum_{m=1}^{i-1} \Delta\mathbf{h}_i^H \mathbf{w}_m \mathbf{w}_m^H \Delta\hat{\mathbf{h}}_i + \sum_{m=i+1}^{K} \mathbf{h}_i^H \mathbf{w}_m \mathbf{w}_m^H \mathbf{h}_i + \sigma_i^2) \leq \frac{1}{\gamma_i^{min}} (\mathbf{h}_i^H \mathbf{w}_i \mathbf{w}_i^H \mathbf{h}_i) \triangleq \varpi_i. \tag{4.8}$$

The problem formulation in (4.7) still not convex and the optimal solution cannot be obtained directly. To tackle this issue, we introduce a new matrix variable $\mathbf{W_l} = \mathbf{w_l w_l^H}$ and reformulate the original robust problem in (4.7) into the following

form:

$$\mathbf{P3} \quad \max_{\mathbf{W}_l \in \mathbb{C}^{M\times M}} t, \tag{4.9a}$$

$$s.t. \quad \min_{\|\Delta\hat{\mathbf{h}}_l\|_2 \leq \epsilon} \frac{\mathbf{h}_l^{\mathrm{H}} \mathbf{W}_l \mathbf{h}_l}{\sum\limits_{m=1}^{l-1} \Delta\hat{\mathbf{h}}_l^{\mathrm{H}} \mathbf{W}_m \Delta\hat{\mathbf{h}}_l + \sum\limits_{m=l+1}^{K} \mathbf{h}_l^{\mathrm{H}} \mathbf{W}_m \mathbf{h}_l + \sigma_l^2} \geq t, \forall l \tag{4.9b}$$

$$\varpi_{il}, \forall i = l+1, \ldots, K \tag{4.9c}$$

$$\sum_{l=1}^{K} \mathrm{Tr}(\mathbf{W}_l) \leq P_T, \tag{4.9d}$$

$$\mathbf{W}_l \succeq 0, \forall l, \tag{4.9e}$$

$$\mathrm{rank}(\mathbf{W}_l) = 1. \forall l \tag{4.9f}$$

To incorporate the channel uncertainties in the robust optimization framework, we exploit the following S-procedure *Lemma 1* to convert the non-convex constraint into LMI form.

Lemma 1 *S-procedure [83]*

Let $f_k(\mathbf{x}), k = 1, 2,$, *be defined as*

$$f_k(\mathbf{x}) = \mathbf{x}^H \mathbf{A}_k \mathbf{x} + 2\Re\{\mathbf{b}_k^H \mathbf{x}\} + c_k, \tag{4.10}$$

where $\mathbf{A}_k = \mathbf{A}_k^H \in \mathbb{C}^{n\times n}$,$\mathbf{b}_k = \mathbb{C}^n$ *and* $c_k \in \mathbb{R}$. *The implication* $f_1(\mathbf{x}) \geq 0 \Longrightarrow f_2(\mathbf{x})$ *holds if and only if there exists* $\alpha \geq 0$ *such that*

$$\begin{bmatrix} \mathbf{A}_2 & \mathbf{b}_2 \\ \mathbf{b}_2^H & c_2 \end{bmatrix} - \alpha \begin{bmatrix} \mathbf{A}_1 & \mathbf{b}_1 \\ \mathbf{b}_1^H & c_1 \end{bmatrix} \succeq 0, \tag{4.11}$$

provided there exists a point $\widetilde{\mathbf{x}}$ *with* $f_1(\widetilde{\mathbf{x}}) > 0$.

By applying S-procedure the constraints (4.9*b*) and (4.9*c*) are derived as

$$\Delta\hat{\mathbf{h}}_l^{\mathrm{H}} \underbrace{\mathbf{I}}_{\mathbf{A_1}} \Delta\hat{\mathbf{h}}_l - \underbrace{\epsilon^2}_{c_1} \leq 0, \tag{4.12}$$

$$\begin{aligned} \Rightarrow \Delta\hat{\mathbf{h}}_l^{\mathrm{H}} \underbrace{(\sum_{m\neq l}^{K} \mathbf{W}_m - \frac{\mathbf{W}_l}{t})}_{\mathbf{A_2}} \Delta\hat{\mathbf{h}}_l \\ + 2\mathrm{Re}\{\hat{\mathbf{h}}_l^{\mathrm{H}} \underbrace{\left(-\frac{\mathbf{W}_l}{t} + \sum_{m=l+1}^{K} \mathbf{W}_m\right)}_{\mathbf{b_2}} \Delta\hat{\mathbf{h}}_l\} \\ \underbrace{+ \hat{\mathbf{h}}_l^{\mathrm{H}}(\sum_{m=l+1}^{K} \mathbf{W}_m - \frac{\mathbf{W}_l}{t})\hat{\mathbf{h}}_l + t\sigma_l^2}_{c_2} \leq 0. \end{aligned} \tag{4.13}$$

To clarify how the S-procedure has been applied equations 4.12 and 4.13 are mapped by underbrace to the variables which are mentioned in Lemma 1 equation 4.11. Then, the constraint (4.9*b*) can be reformulated with $\lambda_l \geq 0$ as the following semidefinite constraint as follow

$$\mathbf{C}_l = \begin{bmatrix} \lambda_l \mathrm{I} + \frac{\mathbf{W}_l}{t} - \sum_{m\neq l}^{K} \mathbf{W}_m & (\frac{\mathbf{W}_l}{t} - \sum_{m=l+1}^{K} \mathbf{W}_m)\hat{\mathbf{h}}_l \\ \hat{\mathbf{h}}_l^H(\frac{\mathbf{W}_l}{t} - \sum_{m=l+1}^{K} \mathbf{W}_m) & \hat{\mathbf{h}}_l^H(\frac{\mathbf{W}_l}{t} - \sum_{m=l+1}^{K} \mathbf{W}_m)\hat{\mathbf{h}}_l - \upsilon_l \end{bmatrix} \succeq 0, \tag{4.14}$$

where $\upsilon_l = t\sigma_l^2 + \lambda_l\epsilon^2$. The reformulation for the constraint (4.9*c*) can be written as

$$\mathbf{D}_{il} = \begin{bmatrix} \lambda_i \mathrm{I} + \frac{\mathbf{W}_i}{\gamma_i} - \sum_{m \neq i}^{K} \mathbf{W}_m & (\frac{\mathbf{W}_i}{\gamma_i} - \sum_{m=i+1}^{K} \mathbf{W}_m)\hat{\mathbf{h}}_i \\ \hat{\mathbf{h}}_i^H (\frac{\mathbf{W}_i}{\gamma_i} - \sum_{m=i+1}^{K} \mathbf{W}_m) & \hat{\mathbf{h}}_i^H (\frac{\mathbf{W}_i}{\gamma_i} - \sum_{m=i+1}^{K} \mathbf{W}_m)\hat{\mathbf{h}}_i - \upsilon_i \end{bmatrix} \succeq 0, \tag{4.15}$$

where $\upsilon_i = \gamma_i^{min}\sigma_i^2 + \lambda_i \epsilon^2$. As a result, combine (4.14) and (4.15) the equivalent formulation of the original optimization problem (4.7) becomes:

$$\mathbf{P4} \qquad \max_{\substack{\mathbf{W}_l \in^{M \times M} \\ \lambda_l \geq 0 \\ \lambda_{il} \geq 0}} t,$$

$$s.t. \qquad \begin{cases} \mathbf{C}_l \succeq 0, \\ \mathbf{D}_{il} \succeq 0, \\ \sum_{\mathrm{l}=1}^{\mathrm{K}} \mathrm{Tr}(\mathbf{W}_l) \leq P_T, \\ \mathbf{W}_l \succeq 0, \\ \mathrm{rank}(\mathbf{W}_l) = 1. \forall l \end{cases} \tag{4.16}$$

Despite of that the constraints have been reformulated into SDP form, the problem is still not convex due to the rank-1 constraints on the beamforming matrices and also the dependence of with other variables [34]. To prove the fact the problem (4.16) exists a rank-one solution,the following *Proposition* 1 is given in the Appendix B, by using the *Proposition* 1 the following *Lemma* 2 about exist of rank one.

Lemma 2 *Provided the problem in (*4.16*) is feasible, there always exists a rank-one optimal solution* $\mathbf{W}_l^*$*.*

Now, an algorithm to solve the optimization problem (4.16) is proposed in Algorithm 2. This algorithm is based on bisection search it is described as follows

Algorithm 2 Proposed algorithm design for NOMA beamforming using bisection search.

Input: $\mathbf{h}_l$ $\mathbf{h}_i$ γ_i^{min} P_T ϵ
Input: t_{LB} t_{UB} ε
1: **while** $t_{UB} - t_{LB} \leq \varepsilon$ **do**
2: Update $t = (t_{LB} + t_{UB})/2$;
3: Calculate $\mathbf{W}_l$ with the constraints in (4.16), by solving the convex problem;
4: **if** feasible **then**
5: $\mathbf{W}_l^* = \mathbf{W}_l$; $SINR_{max} = t$
6: Update $t_{LB} = t$
7: **else**
8: Update $t_{UB} = t$
9: **end if**
10: **end while**
11: Extract the beamforming solution $\mathbf{w}_l$ from $\mathbf{W}_l$ by matrix decomposition.
Output: $SINR_{max}$ and $\mathbf{w}_l^*$

In line 4 of Algorithm 2, it requires discovering the feasibility of a convex SDP problem, this can be done by checking if there exist any feasible solution of the SDP. After the algorithm converges, if the final beamforming solution is a rank-1, then it is guaranteed to be optimal. But if the beamforming solution is not a tank-1 the randomization method will be used that achieves the largest t.

4.4 Simulation Result

To evaluate the performance of the proposed robust beamforming approach, A single-cell downlink transmission is considered where a multi-antenna BS serves randomly distributed single antenna users within a one-kilometre radius. In the simulations, it is assumed that the BS is equipped with four antennas ($M = 4$) and it serves four users ($K = 4$). The channel coefficients between the BS and the users are generated as $\mathbf{h}_l = \chi_l \sqrt{d_l^{-\beta}}$ where $\chi_l \sim \mathcal{CN}(0, I)$,$\beta = 2$ is the path-loss exponent and d_k is the distance between U_l and the BS.

Fig. 4.1 shows a comparison of different channel estimation error bound versus the transmitted power from the Bs. The noise power is assumed to be $\sigma_l^2 = 0$ dB. The dash-dot curves represent the case with error bound imperfect channel estimation (ICSI) NOMA, while the solid curves represent the perfect CSI (PCSI) NOMA case. One can observe that the PCSI NOMA achieves a very high performance compares to the ICSI NOMA. However, achieving a perfect CSI condition is very difficult to get it. Fig. 4.1 demonstrates the performance of several errors bound and as the bound increased the achieved rate decreased because the SINR for the user will be decreased as well.

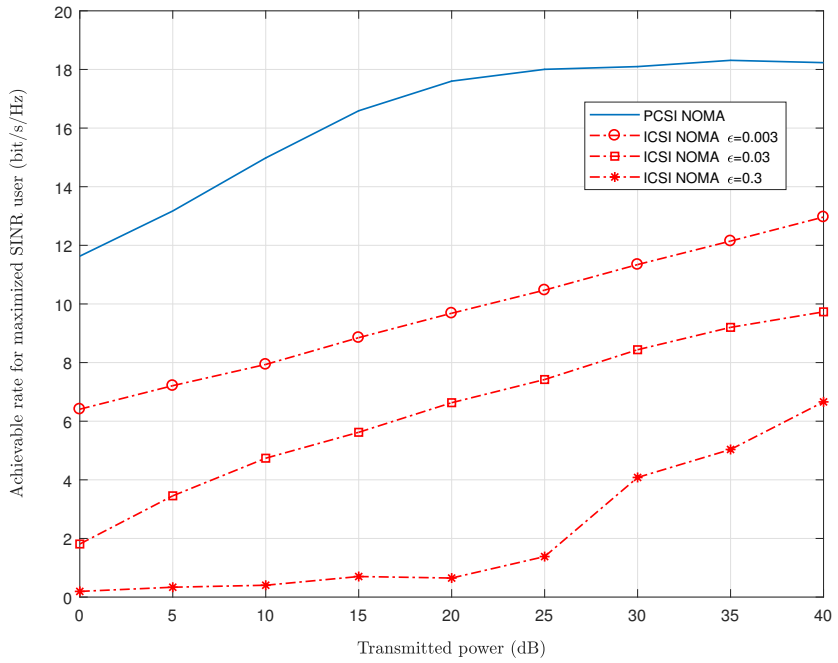

Figure 4.1: Achievable rate for maximized SINR user under different transmitting power with several channel estimation error bound.

In Fig. 4.2 provides the impact of R_{Th} on the PCSI NOMA and the ICSI NOMA in order to guarantee minimum rate constraint for other users. As shown there will be a gap as this rate is increased. Fig. 4.3 plots the effect of changing the antenna configuration at the Bs. It can be observed for the PCSI NOMA there will be a slight

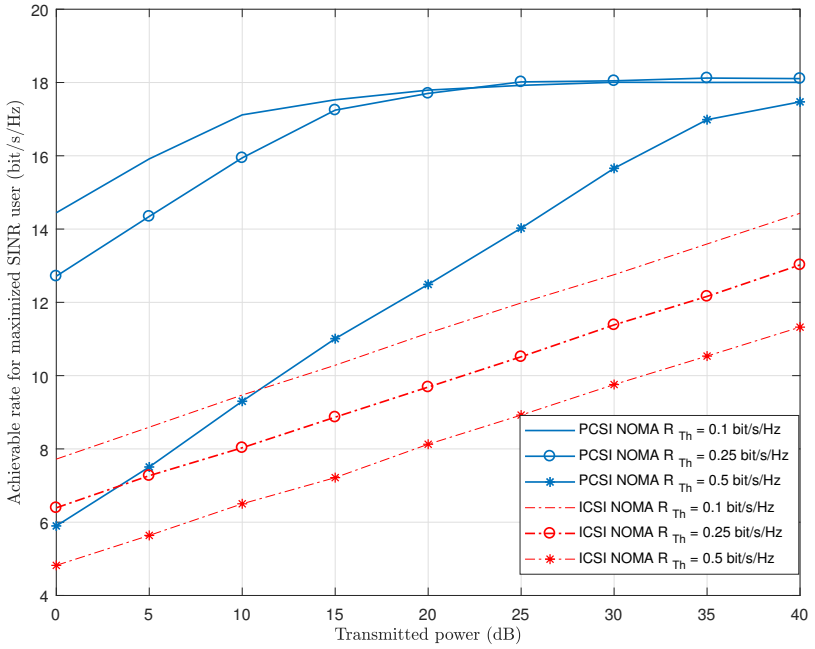

Figure 4.2: Achievable rate for maximized SINR user under different transmitting power and different minimum targeted rate for the other users in the cell R_{Th} number of users in the cell

effect as the number of antennas are increased in the low transmission power. However, for the ICSI there will be a noticeable gap as the number of antennas are decreased at the Bs. In Fig. 4.4 shows as the number decreased in the cell the maximized user SINR will be increased for both PCSI and ICSI. Moreover, as the number increased in the cell the performance of the system will be close especially at high transmitted power.

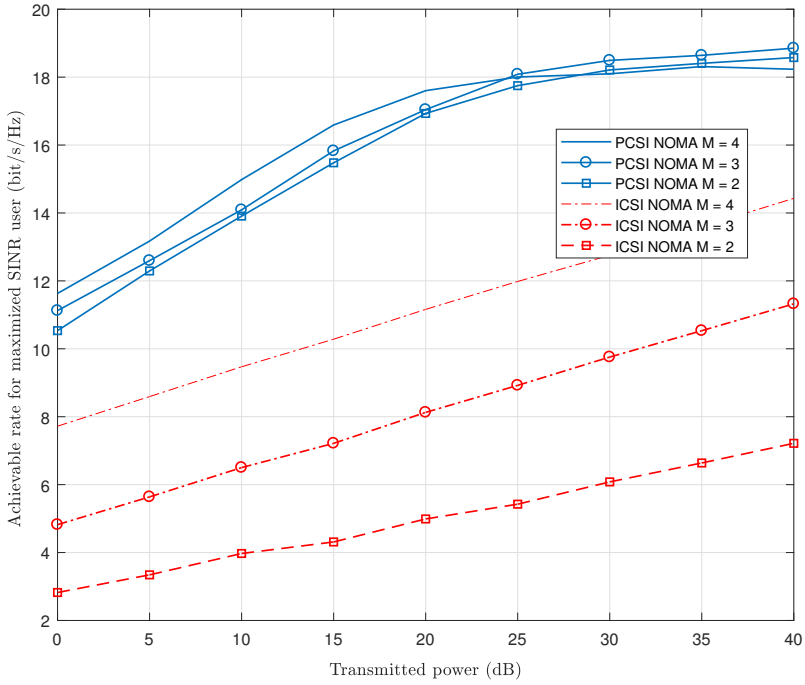

Figure 4.3: Achievable rate for maximized SINR user under different transmitting power and different antenna configuration a the Bs

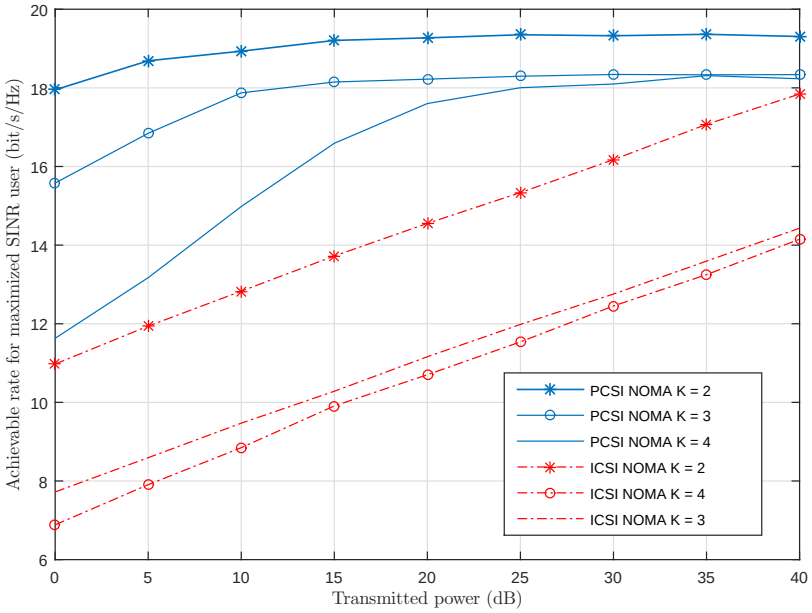

Figure 4.4: Achievable rate for maximized SINR user under different transmitting power and different number of users in the cell

4.5 Summary

This chapter has addressed the worst-case robust beamforming design for the MISO-NOMA downlink systems by taking into account the norm-bounded channel uncertainties. The objective was to balance the users SINRs with the constraints of the total transmit power of the other users and the received interference power at the users. However, the original robust problem formulation is not convex due to the imperfect CSI. To tackle the non-convexity with this challenge, the S-procedure is exploited to reformulate the original non-convex problem into the SDP form by recasting the original non-convex constraints into the LMI form. A bisection based algorithm has been devised to obtain robust beamforming solutions with rank relaxation.

Chapter 5

Maximizing Sum Rate for FD/HD Cooperative NOMA System with Jointly Optimizing Beamformer and Relay Power

5.1 Introduction

In this chapter, a jointly optimizing beamformer and relay power are studied for FD/HD cooperative NOMA with several optimization techniques. The study covers both perfect channel state information and the bounded imperfect channel state information. The objective is to maximize the achievable sum-rate for users within the beam. However, the original problem formulation is not convex. Therefore, reformulating the original problem into SDP form is required then several algorithms are applied to find a solution for the optimization problem.

5.2 System Model and Problem Formulation

The system model of a cooperative non-orthogonal multiple access is described as following: The BS is equipped with multiple antennas wherein the cell there are two users far and near users. The far user is assisted by the near user via sending another copy of its signal. This can be implemented by Half-Duplex (HD) or Full-Duplex (FD) scenarios. This study considers different set-ups such as includes maximum ratio combing (MRC) at the weak user terminal. Furthermore, imperfect channel state information is investigated as well in the formulated optimization problem.

In Fig. 5.1, it shows a two-user with FD cooperative NOMA system, which consists of a transmitter i.e. Bs equipped with M antennas, a near user and a cell-edge user. Each user is equipped with a single transmitter antenna and a single receiver antenna. The near user acts as a DF relay to transmit information to the cell-edge user. For the FD scenario there is an effect of self-interference SI on the system performance due to time-varying channels and carrier offsets [84]. The residual SI channel h_R can be modelled as independent identically distributed (i.i.d) Gaussian random entries [85].

The cell-edge user is either received his signal from the relay only or take the advantage of MRC to merge the direct link signals from the Bs based on the assumption that both signals can be fully resolved at the cell-edge user as shown in Fig. 5.2. The achievable sum rate of the FD NOMA system is given by:

$$R = \underbrace{\log_2(1+\mathrm{SINR}_2^{FD})}_{\text{Achievable rate for the near user}} + \underbrace{\min\{\log_2(1+\mathrm{SINR}_1^{2,FD}), \log_2(1+\mathrm{SNR}_R)\}}_{\text{Achievable rate for the cell-edge user}} \quad (5.1)$$

If MRC is processed at the cell-edge user the achievable sum rate of the system

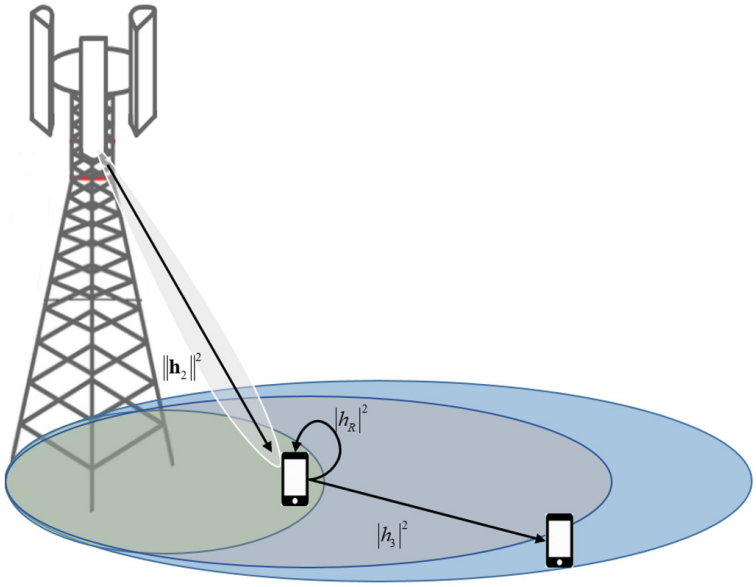

Figure 5.1: The downlink FD cooperative NOMA system mode.

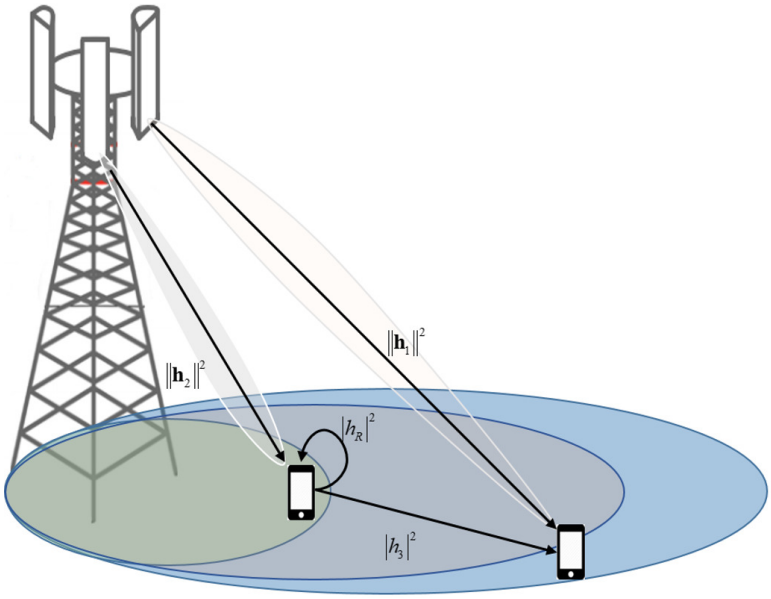

Figure 5.2: The downlink FD cooperative NOMA system mode with MRC at the weak user terminal.

will be:

$$R = \log_2(1 + \mathrm{SINR}_2^{FD}) + \min\{\log_2(1 + \mathrm{SINR}_1^{2,FD}), \log_2(1 + \mathrm{SNR}_R + \mathrm{SINR}_1^{FD})\}. \quad (5.2)$$

It is assumed that the resolvability of the signals i.e. by introducing a processing delay

to combine the signals received from the terminal user UE2 and the BS by MRC [86,87]. Where, $\mathrm{SINR}_1^{2,FD}$ is the received signal-to-interference-plus-noise-ratio at the near user to detect the cell-edge user message x_1. x_1 and x_2 are the i.i.d. information bearing signal for two users with normalized power, i.e., $\mathbb{E}|x_1|^2 = \mathbb{E}|x_2|^2 = 1$.

$$\mathrm{SINR}_1^{2,FD} = \frac{\rho_2 \mathbf{h}_2^{\mathrm{H}} \mathbf{w}_1 \mathbf{w}_1^{\mathrm{H}} \mathbf{h}_2}{\rho_2 \mathbf{h}_2^{\mathrm{H}} \mathbf{w}_2 \mathbf{w}_2^{\mathrm{H}} \mathbf{h}_2 + \rho_2 |h_R|^2 P_R + 1}. \tag{5.3}$$

After using the SIC technique, the received SINR at the near user to detect its own information can be shown as

$$\mathrm{SINR}_2^{FD} = \frac{\rho_2 \mathbf{h}_2^{\mathrm{H}} \mathbf{w}_2 \mathbf{w}_2^{\mathrm{H}} \mathbf{h}_2}{\rho_2 |h_R|^2 P_R + 1}. \tag{5.4}$$

$\mathbf{h}_n \in \mathbb{C}^{M \times 1}$ where $n = 1, 2$ is the channel coefficient between the transmitter and the users, $\mathbf{w}_1$ and $\mathbf{w}_2$ are the corresponding transmit beamforming, P_R is the transmit power to forward information at the relay and $\rho_n = 1/\sigma_n^2$ where $n_n \sim \mathcal{CN}(0, \sigma_n^2)$. The SNR from the cooperative link is

$$\mathrm{SNR}_R = \rho_{1,R} |h_3|^2 P_R. \tag{5.5}$$

Where, $\rho_{1,R} = 1/\sigma_{1,R}^2$ $n_{1,R} \sim \mathcal{CN}(0, \sigma_{1,R}^2)$ and $h_3 \in \mathbb{C}$ is the channel coefficient between the relay and the cell-edge user. If the system mode in Fig. 5.2 SINR for the cell-edge user should be considered as following:

$$\mathrm{SINR}_1^{FD} = \frac{\rho_1 \mathbf{h}_1^{\mathrm{H}} \mathbf{w}_1 \mathbf{w}_1^{\mathrm{H}} \mathbf{h}_1}{\rho_1 \mathbf{h}_1^{\mathrm{H}} \mathbf{w}_2 \mathbf{w}_2^{\mathrm{H}} \mathbf{h}_1 + 1}. \tag{5.6}$$

The other mode for the cooperative is HD mode which is depicted in Fig. 5.3, so the transmission occurs in two time slots.

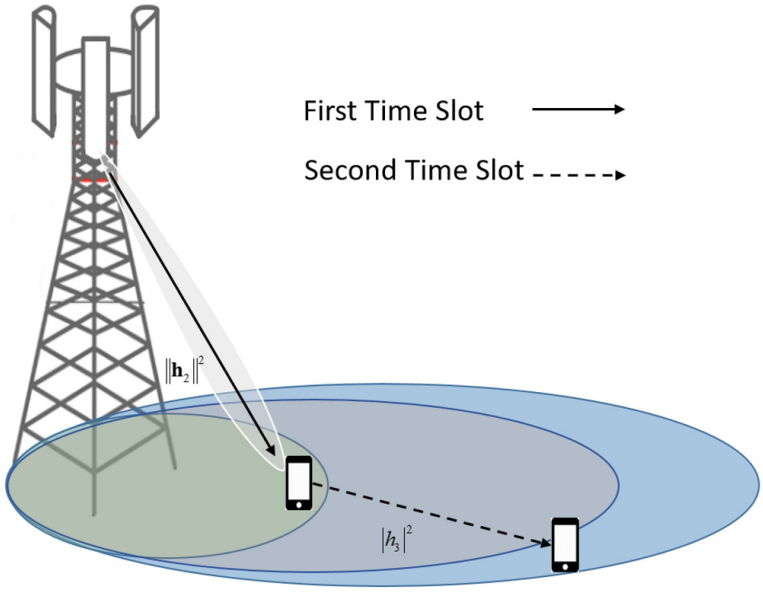

Figure 5.3: The downlink HD cooperative NOMA system mode.

The achievable sum rate of the HD NOMA system is given by:

$$R = \frac{1}{2}\log_2(1+\mathrm{SNR}_2^{HD}) + \frac{1}{2}\min\{\log_2(1+\mathrm{SINR}_1^{2,HD}), \log_2(1+\mathrm{SNR}_R)\}. \tag{5.7}$$

If MRC is processed at the cell-edge user as shown in Fig. 5.4 the achievable sum rate of the system will be:

$$R = \frac{1}{2}\log_2(1+\mathrm{SNR}_2^{HD}) + \frac{1}{2}\min\{\log_2(1+\mathrm{SINR}_1^{2,HD}), \log_2(1+\mathrm{SNR}_R+\mathrm{SINR}_1^{HD})\}. \tag{5.8}$$

Where,

$$\mathrm{SINR}_1^{2,HD} = \frac{\rho_2 \mathbf{h}_2^{\mathrm{H}} \mathbf{w}_1 \mathbf{w}_1^{\mathrm{H}} \mathbf{h}_2}{\rho_2 \mathbf{h}_2^{\mathrm{H}} \mathbf{w}_2 \mathbf{w}_2^{\mathrm{H}} \mathbf{h}_2 + 1}. \tag{5.9}$$

When SIC is applied, the received SNR at the near user is

$$\mathrm{SINR}_2^{HD}=\rho_2\mathbf{h}_2^{\mathrm{H}}\mathbf{w}_2\mathbf{w}_2^{\mathrm{H}}\mathbf{h}_2, \tag{5.10}$$

and SINR for the cell-edge user should be

$$\mathrm{SINR}_1^{\mathrm{HD}}=\frac{\rho_1\mathbf{h}_1^{\mathrm{H}}\mathbf{w}_1\mathbf{w}_1^{\mathrm{H}}\mathbf{h}_1}{\rho_1\mathbf{h}_1^{\mathrm{H}}\mathbf{w}_2\mathbf{w}_2^{\mathrm{H}}\mathbf{h}_1+1}. \tag{5.11}$$

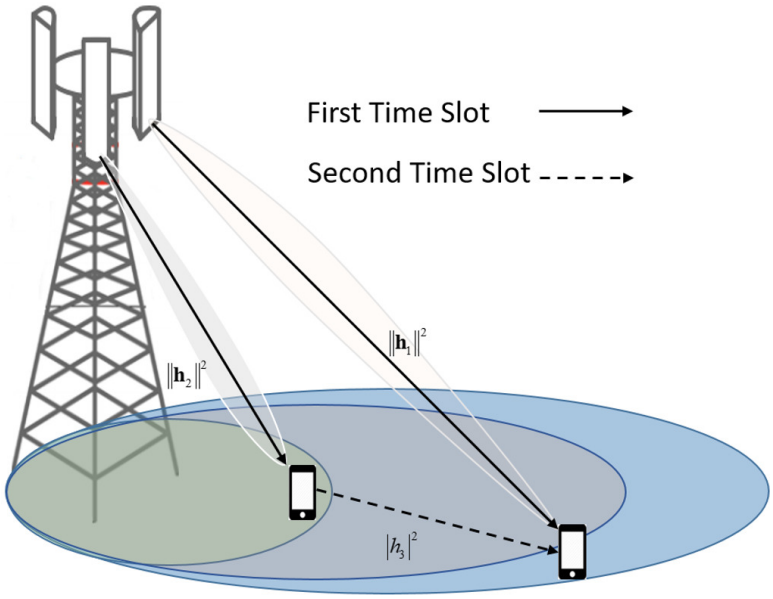

Figure 5.4: The downlink HD cooperative NOMA system mode with MRC at the weak user terminal.

The target is to maximize the sum-rate of the system by optimizing the beamforming together with the power of the relay for FD/HD cooperative NOMA. Taking into account several scenarios such as with MRC and without MRC under perfect CSI and imperfect CSI conditions. While guaranteeing the minimum required target rate of the cell-edge user and the successful decoding rate for the near user. So, the formulation of the problem is expressed as follows:

$$\mathbf{P1}: \quad \max R \tag{5.12a}$$

$$s.t. \quad \mathrm{SINR}_2 \geq \gamma_2, \tag{5.12b}$$

$$\mathrm{SINR}_1^2 \geq \gamma_1, \tag{5.12c}$$

$$\mathrm{SNR}_R \geq \gamma_1, \tag{5.12d}$$

$$R_1^2 \geq R_{min}, \tag{5.12e}$$

$$\|\mathbf{w}_1\|^2 + \|\mathbf{w}_2\|^2 \leq P_{max}, \tag{5.12f}$$

$$P_R \leq P_{R_{\max}}, \tag{5.12g}$$

where γ_2,γ_1 are the needed SINR for the near user and the cell-edge user, R_{min}, P_{max} and $P_{R_{\max}}$ indicate the minimum required target rate, maximum available transmit power,and maximum available transmit power from the relay consecutively.

It's worth noting that as highlighted in [88], the proposed two-user for cooperative NOMA scheme can be expanded to a multi-user scenario by using the matching theory [89]. Especially, by applying one-to-one matching, $2K$ users can be divided into K groups, and two users are paired in each group.

5.3 Proposed Optimization Methods

5.3.1 FD/HD Cooperative NOMA Under Perfect CSI Conditions

5.3.1.1 FD Cooperative NOMA with MRC and without MRC

Problem **P1** is not convex caused by fractional and coupling variables. In order to solve the non-convexity of the problem transforming the problem to a amenable one, then propose an efficient iterative algorithm is required. After defining positive semidefinite (PSD) matrices, $\mathbf{H} = \mathbf{h}\mathbf{h}^H$ and $\mathbf{W}_n = \mathbf{w}_n\mathbf{w}_n^H$, there are three proposed way to transform this problem will be discussed in this research.

$$\mathbf{P2}: \max_{t,\gamma_2,\gamma_1,\mathbf{W}_1,\mathbf{W}_2,P_R} t \tag{5.13a}$$

$$s.t. \quad \log_2(1+\gamma_2) + \log_2(1+\gamma_1) \geq t \tag{5.13b}$$

$$\rho_2 \mathrm{Tr}(\mathbf{H}_2\mathbf{W}_2) - \gamma_2(\rho_2|h_3|^2 P_R + 1) \geq 0, \tag{5.13c}$$

$$\rho_2 \mathrm{Tr}(\mathbf{H}_2\mathbf{W}_1) - \gamma_1\rho_2 \mathrm{Tr}(\mathbf{H}_2\mathbf{W}_2) - \gamma_1(\rho_2|h_3|^2 P_R + 1) \geq 0, \tag{5.13d}$$

$$\rho_{1,R}|h_3|^2 P_R \geq \gamma_1, \tag{5.13e}$$

$$\rho_2 \mathrm{Tr}(\mathbf{H}_2\mathbf{W}_1) - \delta^{FD}\rho_2 \mathrm{Tr}(\mathbf{H}_2\mathbf{W}_2) - \delta^{FD}\rho_2|h_3|^2 P_R \geq \delta^{FD}, \tag{5.13f}$$

$$\mathrm{Tr}(\mathbf{W}_1 + \mathbf{W}_2) \leq P_{max}, \tag{5.13g}$$

$$P_R \leq P_{R_{\max}}, \tag{5.13h}$$

$$\mathrm{rank}(\mathbf{W}_n) = 1. \tag{5.13i}$$

Where $\delta^{FD} = 2^{R_{min}} - 1$ and $n = 1, 2$. The following constraints are introduced in **P3** in order to include MRC to the cell-edge user into the problem formulation as following

$$\mathbf{P3}: \max_{t,\gamma_2,\gamma_1,u_1,u_2,\mathbf{W}_1,\mathbf{W}_2,P_R} (5.13a),$$

$$s.t. \quad (5.13b), (5.13c), (5.13d),$$

$$u_1 + u_2 \geq \gamma_1, \tag{5.14a}$$

$$\rho_{1,R}|h_3|^2 P_R \geq u_1, \tag{5.14b}$$

$$\rho_1 \mathrm{Tr}(\mathbf{H}_1\mathbf{W}_1) - u_2(\rho_1 \mathrm{Tr}(\mathbf{H}_1\mathbf{W}_2)+1) \geq 0 \tag{5.14c}$$

$$(5.13f), (5.13g), (5.13h), (5.13i).$$

Alternating Algorithm

One approach is to apply the Taylor series in constraints 5.13c and 5.13d. Then the problem **P2** will be written as following:

$$\mathbf{P4}: \max_{t,\gamma_2,\gamma_1,\mathbf{W}_1,\mathbf{W}_2,P_R} t \tag{5.15a}$$

$$s.t. \quad \log_2(1+\gamma_2) + \log_2(1+\gamma_1) \geq t \tag{5.15b}$$

$$\rho_2 \mathrm{Tr}(\mathbf{H}_2\mathbf{W}_2) - \gamma_2^{(k)}(\rho_2|h_3|^2 P_R^{(k)} + 1) - (\rho_2|h_3|^2 P_R^{(k)} + 1)(\gamma_2 - \gamma_2^{(k)})$$
$$- \gamma_2^{(k)}\rho_2|h_3|^2(P_R - P_R^{(k)}) \geq 0, \tag{5.15c}$$

$$\rho_2 \mathrm{Tr}(\mathbf{H}_2\mathbf{W}_1) - \gamma_1^{(k)}\rho_2 \mathrm{Tr}(\mathbf{H}_2\mathbf{W}_2^{(k)}) - \rho_2 \mathrm{Tr}(\mathbf{H}_2\mathbf{W}_2^{(k)})(\gamma_1 - \gamma_1^{(k)})$$
$$- \gamma_1^{(k)}\rho_2 \mathrm{Tr}(\mathbf{H}_2(\mathbf{W}_2 - \mathbf{W}_2^{(k)})) - \gamma_1^{(k)}(\rho_2|h_3|^2 P_R^{(k)} + 1)$$
$$- (\rho_2|h_3|^2 P_R^{(k)} + 1)(\gamma_1 - \gamma_1^{(k)}) - \gamma_1^{(k)}\rho_2|h_3|^2(P_R - P_R^{(k)}) \geq 0, \tag{5.15d}$$

$$\rho_{1,R}|h_3|^2 P_R \geq \gamma_1, \tag{5.15e}$$

$$\rho_2 \mathrm{Tr}(\mathbf{H}_2\mathbf{W}_1) - \delta^{FD}\rho_2 \mathrm{Tr}(\mathbf{H}_2\mathbf{W}_2) - \delta^{FD}\rho_2|h_3|^2 P_R \geq \delta^{FD}, \tag{5.15f}$$

$$\mathrm{Tr}(\mathbf{W}_1 + \mathbf{W}_2) \leq P_{max}, \tag{5.15g}$$

$$P_R \leq P_{R_{\max}}, \tag{5.15h}$$

$$\mathrm{rank}(\mathbf{W}_n) = 1. \tag{5.15i}$$

The process of the alternating optimization algorithm is started by initializing the values of $\gamma_2^{(k)}, \gamma_1^{(k)}, \mathbf{W_2^{(k)}}$**and** $\mathbf{P_R^{(k)}}$ then update the values iteratively till the convergence threshold is satisfied. For the MRC case Taylor series expansion is required to be applied for (5.14c)

$$\begin{aligned}
\mathbf{P5}: \quad & \max_{t,\gamma_2,\gamma_1,u_1,u_2,\mathbf{W}_1,\mathbf{W}_2,P_R} (5.15a), \\
s.t. \quad & (5.15b), (5.15c), (5.15d), (5.14a), (5.14b) \\
& \rho_1 \mathrm{Tr}(\mathbf{H}_1\mathbf{W}_1) - u_2^{(k)}(\rho_1 \mathrm{Tr}(\mathbf{H}_1\mathbf{W}_2^{(k)}) + 1) - (\rho_1 \mathrm{Tr}(\mathbf{H}_1\mathbf{W}_2^{(k)}) + 1)(u_2 - u_2^{(k)}) \\
& -u_2^{(k)}\rho_1 \mathrm{Tr}(\mathbf{H}_1(\mathbf{W}_1 - \mathbf{W}_2^{(k)})) \geq 0 \qquad (5.16a) \\
& (5.15f), (5.15g), (5.15h), (5.15i).
\end{aligned}$$

GP Algorithm

Another way to transform the problem to convex is to use GP by introducing several variables to the constraints 5.13c and 5.13d. Then the constraint can be redefined as

$$\ln(\rho_2 \mathrm{Tr}(\mathbf{H}_2\mathbf{W}_2)) \geq a + b, \qquad (5.17a)$$

$$\ln(\rho_2 \mathrm{Tr}(\mathbf{H}_2\mathbf{W}_1)) \geq b + c + d, \qquad (5.17b)$$

$$\gamma_2 \leq \exp(a), \qquad (5.17c)$$

$$\rho_{1,R}|h_3|^2 P_R + 1 \leq \exp(b) \qquad (5.17d)$$

$$\gamma_1 \leq \exp(c) \qquad (5.17e)$$

$$\rho_2 \mathrm{Tr}(\mathbf{H}_2\mathbf{W}_2) \leq \exp(d), \qquad (5.17f)$$

where a, b, c and d are auxiliary variables. Then replace LHS for 5.17c-5.17f by their first-order Taylor expansions based on the SCA method, which targets to iteratively

approximate the non-convex problem by a convex one.

$$\gamma_2 \leq \exp(a^{(k)})(1 + a - a^{(k)}), \tag{5.18a}$$

$$\rho_{1,R}|h_3|^2 P_R + 1 \leq \exp(b^{(k)})(1 + b - b^{(k)}), \tag{5.18b}$$

$$\gamma_1 \leq \exp(c^{(k)})(1 + c - c^{(k)}), \tag{5.18c}$$

$$\rho_2 \mathrm{Tr}(\mathbf{H}_2\mathbf{W}_2) \leq \exp(d^{(k)})(1 + d - d^{(k)}). \tag{5.18d}$$

So, **P2** can be reframed as the following problem based on the transformation and approximation in 5.17 and 5.18.

$$\mathbf{P6}: \quad \max_{t,\gamma_2,\gamma_1,\mathbf{W}_1,\mathbf{W}_2,P_R} \quad t \tag{5.19a}$$

$$s.t. \quad \log_2(1+\gamma_2) + \log_2(1+\gamma_1) \geq t, \tag{5.19b}$$

$$\ln(\rho_2 \mathrm{Tr}(\mathbf{H}_2\mathbf{W}_2)) \geq a + b, \tag{5.19c}$$

$$\ln(\rho_2 \mathrm{Tr}(\mathbf{H}_2\mathbf{W}_1)) \geq b + c + d, \tag{5.19d}$$

$$\rho_{1,R}|h_3|^2 P_R \geq \gamma_1, \tag{5.19e}$$

$$\rho_2 \mathrm{Tr}(\mathbf{H}_2\mathbf{W}_1) - \delta^{FD}\rho_2 \mathrm{Tr}(\mathbf{H}_2\mathbf{W}_2) - \delta^{FD}\rho_2|h_3|^2 P_R \geq \delta^{FD}, \tag{5.19f}$$

$$\gamma_2 \leq \exp(a^{(k)})(1 + a - a^{(k)}), \tag{5.19g}$$

$$\rho_{1,R}|h_3|^2 P_R + 1 \leq \exp(b^{(k)})(1 + b - b^{(k)}), \tag{5.19h}$$

$$\gamma_1 \leq \exp(c^{(k)})(1 + c - c^{(k)}), \tag{5.19i}$$

$$\rho_2 \mathrm{Tr}(\mathbf{H}_2\mathbf{W}_2) \leq \exp(d^{(k)})(1 + d - d^{(k)}), \tag{5.19j}$$

$$\mathrm{Tr}(\mathbf{W}_1 + \mathbf{W}_2) \leq P_{max}, \tag{5.19k}$$

$$P_R \leq P_{R_{\max}}, \tag{5.19l}$$

$$\mathrm{rank}(\mathbf{W}_n) = 1. \tag{5.19m}$$

Then, iteratively update the variables in 5.20, the iteration operation will stop when the predefined standard is attained.

$$a^{(k)} = \ln(\gamma_2^{(k)}), \tag{5.20a}$$

$$b^{(k)} = \ln(\rho_{1,R}|h_3|^2 P_R^{(k)} + 1), \tag{5.20b}$$

$$c^{(k)} = \ln(\gamma_1^{(k)}), \tag{5.20c}$$

$$d^{(k)} = \ln(\rho_2 \mathrm{Tr}(\mathbf{H}_2 \mathbf{W}_2^{(k)})). \tag{5.20d}$$

For MRC the constraint 5.14c can be reformulated as

$$\ln(\rho_1 \mathrm{Tr}(\mathbf{H}_1 \mathbf{W}_1)) \geq e + f, \tag{5.21a}$$

$$u_2 \leq \exp(e), \tag{5.21b}$$

$$\rho_1 \mathrm{Tr}(\mathbf{H}_1 \mathbf{W}_2) + 1 \leq \exp(f). \tag{5.21c}$$

Where e and f are auxiliary variables. After that, LHS for 5.21b and 5.21c be changed by their Taylor expansions

$$u_2 \leq \exp(e^{(k)})(1 + e - e^{(k)}), \tag{5.22a}$$

$$\rho_1 \mathrm{Tr}(\mathbf{H}_1 \mathbf{W}_2) + 1 \leq \exp(f^{(k)})(1 + f - f^{(k)}). \tag{5.22b}$$

$$\begin{aligned}
\mathbf{P7}: \quad & \max_{t,\gamma_2,\gamma_1,u_1,u_2,\mathbf{W}_1,\mathbf{W}_2,P_R} (5.19a), \\
s.t. \quad & (5.19b), (5.19c), (5.19d), (5.14a), (5.14b) \\
& \ln(\rho_1 \mathrm{Tr}(\mathbf{H}_1 \mathbf{W}_1)) \geq e + f, && (5.23a) \\
& (5.19f), (5.19g), (5.19h), (5.19i), (5.19j), \\
& u_2 \leq \exp(e^{(k)})(1 + e - e^{(k)}), && (5.23b) \\
& \rho_1 \mathrm{Tr}(\mathbf{H}_1 \mathbf{W}_2) + 1 \leq \exp(f^{(k)})(1 + f - f^{(k)}), && (5.23c) \\
& (5.19k), (5.19l), (5.19m).
\end{aligned}$$

Also, it is required to update the variables in 5.24 iteratively till the solution is converge to the specific criteria

$$e^{(k)} = \ln(u_2^{(k)}), \tag{5.24a}$$

$$f^{(k)} = \ln(\rho_1 \mathrm{Tr}(\mathbf{H}_1 \mathbf{W}_2^{(k)}) + 1). \tag{5.24b}$$

Algorithm 3 Nested Bisection Algorithm for Jointly Optimizing Beamformer and P_R.

Initialize: $\gamma_1, \gamma_2, \hat{\gamma}_1, \hat{\gamma}_2$ randomly in $[0, \gamma_n^{(u)}]$
while $\left\| [\gamma_1, \gamma_2]^T - [\hat{\gamma}_1, \hat{\gamma}_2]^T \right\| \geq \xi$ **do**
  Set $\hat{\gamma}_1 = \gamma_1, \hat{\gamma}_2 = \gamma_2$
Initialize: $\gamma_1^{(u)}, \gamma_1^{(l)}$
  while $\gamma_1^{(u)} - \gamma_1^{(l)} \geq \xi$ **do**
    $\gamma_1 = \frac{\gamma_1^{(u)} + \gamma_1^{(l)}}{2}$,
    Solve **P2**,
    if P2 gets a feasible solution **then**
      $\gamma_1^{(l)} = \gamma_1$
    else
      $\gamma_1^{(u)} = \gamma_1$
    end if
  end while
Initialize: $\gamma_2^{(u)}, \gamma_2^{(l)}$
  while $\gamma_2^{(u)} - \gamma_2^{(l)} \geq \xi$ **do**
    $\gamma_2 = \frac{\gamma_2^{(u)} + \gamma_2^{(l)}}{2}$,
    Solve **P2**,
    if P2 gets a feasible solution **then**
      $\gamma_2^{(l)} = \gamma_2$
    else
      $\gamma_2^{(u)} = \gamma_2$
    end if
  end while
end while
Extract the beamforming solution $\mathbf{w}_n$ from $\mathbf{W}_n$ by matrix decomposition.
Output: P_R^* and $\mathbf{w}_n^*$

Nested Bisection

When MRC is considered the NB **Algorithm 3** applied according to do bisection search by initializing γ_1,γ_2 and u_2.

5.3.1.2 HD Cooperative NOMA with MRC and without MRC

Regarding the HD transmission scheme, the optimization problem can be worked out as follows:

$$\mathbf{P8}: \quad \max_{t,\gamma_2,\gamma_1,\mathbf{W}_1,\mathbf{W}_2,P_R} \; t \tag{5.25a}$$

$$s.t. \quad \log_2(1+\gamma_2)+\log_2(1+\gamma_1) \geq 2t \tag{5.25b}$$

$$\rho_2 \mathrm{Tr}(\mathbf{H}_2\mathbf{W}_2) \geq \gamma_2, \tag{5.25c}$$

$$\rho_2 \mathrm{Tr}(\mathbf{H}_2\mathbf{W}_1) - \gamma_1\rho_2 \mathrm{Tr}(\mathbf{H}_2\mathbf{W}_2) \geq \gamma_1, \tag{5.25d}$$

$$\rho_{1,R}|h_3|^2 P_R \geq \gamma_1, \tag{5.25e}$$

$$\rho_2 \mathrm{Tr}(\mathbf{H}_2\mathbf{W}_1) - \delta^{HD}\rho_2 \mathrm{Tr}(\mathbf{H}_2\mathbf{W}_2) \geq \delta^{HD}, \tag{5.25f}$$

$$\mathrm{Tr}(\mathbf{W}_1+\mathbf{W}_2) \leq P_{max}, \tag{5.25g}$$

$$P_R \leq P_{R_{\max}}, \tag{5.25h}$$

$$\mathrm{rank}(\mathbf{W}_n) = 1. \tag{5.25i}$$

Where $\delta^{HD} = 2^{2R_{min}} - 1$ and $n = 1, 2$.

If MRC is included in the problem formulation there will be additional constraint added two maintain the achievable SINR for the cell-edge user as shown next.

$$\mathbf{P9}: \quad \max_{t,\gamma_2,\gamma_1,u_1,u_2,\mathbf{W}_1,\mathbf{W}_2,P_R} (5.25a),$$

$$s.t. \quad (5.25b), (5.25c), (5.25d),$$

$$u_1 + u_2 \geq \gamma_1, \tag{5.26a}$$

$$\rho_{1,R}|h_3|^2 P_R \geq u_1, \tag{5.26b}$$

$$\rho_1 \mathrm{Tr}(\mathbf{H}_1\mathbf{W}_1) - u_2(\rho_1 \mathrm{Tr}(\mathbf{H}_1\mathbf{W}_2)+1) \geq 0 \tag{5.26c}$$

$$(5.25f), (5.25g), (5.25h), (5.25i).$$

Alternating Algorithm

When AO is applied for this problem is required to replace some constraints such as 5.25d with their Taylor series expansion. Then, the problem will be

$$\begin{aligned}
\mathbf{P10}: \quad & \max_{t,\gamma_2,\gamma_1,\mathbf{W}_1,\mathbf{W}_2,P_R} (5.25a), \\
& s.t. \quad (5.25b), (5.25c), \\
& \rho_2 \mathrm{Tr}(\mathbf{H}_2\mathbf{W}_1) - \gamma_1^{(k)}\rho_2 \mathrm{Tr}(\mathbf{H}_2\mathbf{W}_2^{(k)}) - \rho_2 \mathrm{Tr}(\mathbf{H}_2\mathbf{W}_2^{(k)})(\gamma_1 - \gamma_1^{(k)}) \\
& -\gamma_1^{(k)}\rho_2 \mathrm{Tr}(\mathbf{H}_2(\mathbf{W}_2 - \mathbf{W}_2^{(k)})) \geq 0, \qquad (5.27a) \\
& (5.25e), (5.25f), (5.25g), (5.25h), (5.25i).
\end{aligned}$$

For MRC case also 5.26c constrain is needed to be replaced then the problem will be

$$\begin{aligned}
\mathbf{P11}: \quad & \max_{t,\gamma_2,\gamma_1,u_1,u_2,\mathbf{W}_1,\mathbf{W}_2,P_R} (5.25a), \\
& s.t. \quad (5.25b), (5.25c), (5.27a), (5.26a), (5.26b) \\
& \rho_1 \mathrm{Tr}(\mathbf{H}_1\mathbf{W}_1) - u_2^{(k)}(\rho \mathrm{Tr}(\mathbf{H}_1\mathbf{W}_2^{(k)}) + 1) - (\rho_1 \mathrm{Tr}(\mathbf{H}_1\mathbf{W}_2^{(k)}) + 1)(u_2 - u_2^{(k)}) \\
& - u_2^{(k)}\rho_1 \mathrm{Tr}(\mathbf{H}_1(\mathbf{W}_1 - \mathbf{W}_2^{(k)})) \geq 0 \qquad (5.28a) \\
& (5.25f), (5.25g), (5.25h), (5.25i).
\end{aligned}$$

GP Algorithm

By introducing variables a, b to the constraint 5.25d. Then the problem can be redefined

as

$$\mathbf{P12}: \max_{t,\gamma_2,\gamma_1,\mathbf{W}_1,\mathbf{W}_2,P_R} (5.25a),$$

$$s.t. \quad (5.25b), (5.25c),$$

$$\ln(\rho_2 \mathrm{Tr}(\mathbf{H}_2\mathbf{W}_1)) \geq \exp(a+b), \tag{5.29a}$$

$$\gamma_1 \leq \exp(a^{(k)})(1+a-a^{(k)}), \tag{5.29b}$$

$$\rho_2 \mathrm{Tr}(\mathbf{H}_2\mathbf{W}_2)+1 \leq \exp(b^{(k)})(1+b-b^{(k)}), \tag{5.29c}$$

$$(5.25e), (5.25f), (5.25g), (5.25h), (5.25i).$$

It is required to update the variables in 5.30 iteratively till the solution is converged.

$$a^{(k)} = \ln(\gamma_1^{(k)}), \tag{5.30a}$$

$$b^{(k)} = \ln(\rho_2 \mathrm{Tr}(\mathbf{H}_2\mathbf{W}_2^{(k)})). \tag{5.30b}$$

In HD cooperative NOMA with MRC scheme, to apply GP to the problem there will be more variables to be introduced c, d to the constraint 5.26c. Then the problem can be redefined as

$$\mathbf{P13}: \max_{t,\gamma_2,\gamma_1,u_1,u_2,\mathbf{W}_1,\mathbf{W}_2,P_R} (5.25a),$$

$$s.t. \quad (5.25b), (5.25c), (5.29a), (5.29b), (5.29c),$$

$$\ln(\rho_1 \mathrm{Tr}(\mathbf{H}_1\mathbf{W}_1)) \geq c+d, \tag{5.31a}$$

$$u_2 \leq \exp(c^{(k)})(1+c-c^{(k)}), \tag{5.31b}$$

$$\rho_1 \mathrm{Tr}(\mathbf{H}_1\mathbf{W}_2)+1 \leq \exp(d^{(k)})(1+d-d^{(k)}), \tag{5.31c}$$

$$(5.25f), (5.25g), (5.25h), (5.25i).$$

It is required to update the variables in 5.30 and iteratively till the solution is converged.

$$c^{(k)} = \ln(u_2^{(k)}), \tag{5.32a}$$

$$d^{(k)} = \ln(\rho_1 \mathrm{Tr}(\mathbf{H}_1\mathbf{W}_2^{(k)})+1). \tag{5.32b}$$

Nested Bisection

Also, the bisection algorithm can be applied for **P8** where the search based on the achievable SINR for the cell-edge user. On the other hand, when the MRC processed by the cell-edge user in **P9** the NB algorithm will be applied to find the solution. Where, γ_1, and u_2 are the two-component conducting bisection search alternative till the solution is converged.

5.3.2 FD/HD Cooperative NOMA Under Imperfect CSI Conditions

The deterministic error bound approach is used to model imperfect CSI. Where the actual channel between the Bs and the terminals within the cell can be described as shown

$$\mathbf{h}_1 = \hat{\mathbf{h}}_1 + \Delta\hat{\mathbf{h}}_1, \qquad \Delta\hat{\mathbf{h}}_1^{\mathrm{H}}\Delta\hat{\mathbf{h}}_1 \leq \varepsilon_1^2, \tag{5.33a}$$

$$\mathbf{h}_2 = \hat{\mathbf{h}}_2 + \Delta\hat{\mathbf{h}}_2, \qquad \Delta\hat{\mathbf{h}}_2^{\mathrm{H}}\Delta\hat{\mathbf{h}}_2 \leq \varepsilon_2^2, \tag{5.33b}$$

where $\hat{\mathbf{h}}_1$ and $\hat{\mathbf{h}}_2$ represent the estimated channels, $\Delta\hat{\mathbf{h}}_1$ and $\Delta\hat{\mathbf{h}}_2$ denote the uncertainty region for the error that is bounded by ε_1 and ε_2 where they represent the radius of the norm bound.

5.3.2.1 FD Cooperative NOMA with MRC and without MRC

Then the problem will formulated as following:

$$\mathbf{P14}: \max_{t,\gamma_2,\gamma_1,\mathbf{W}_1,\mathbf{W}_2,P_R} t \tag{5.34a}$$

$$s.t. \quad \log_2(1+\gamma_2)+\log_2(1+\gamma_1)\geq t, \tag{5.34b}$$

$$\min_{\Delta\hat{\mathbf{h}}_2^H\mathbf{I}\Delta\hat{\mathbf{h}}_2\leq\varepsilon_2^2} -\rho_2\Delta\hat{\mathbf{h}}_2^H\frac{\mathbf{W}_2}{\gamma_2}\Delta\hat{\mathbf{h}}_2-2\rho_2\mathrm{Re}\{\Delta\hat{\mathbf{h}}_2^H\frac{\mathbf{W}_2}{\gamma_2}\hat{\mathbf{h}}_2\}-\rho_2\hat{\mathbf{h}}_2^H\frac{\mathbf{W}_2}{\gamma_2}\hat{\mathbf{h}}_2$$

$$+\rho|h_3|^2P_R+1\leq 0, \tag{5.34c}$$

$$\min_{\Delta\hat{\mathbf{h}}_2^H\mathbf{I}\Delta\hat{\mathbf{h}}_2\leq\varepsilon_2^2} \rho_2\Delta\hat{\mathbf{h}}_2^H(\mathbf{W}_2-\frac{\mathbf{W}_1}{\gamma_1})\Delta\hat{\mathbf{h}}_2+2\rho_2\mathrm{Re}\{\Delta\hat{\mathbf{h}}_2^H(\mathbf{W}_2-\frac{\mathbf{W}_1}{\gamma_1})\hat{\mathbf{h}}_2\}$$

$$+\rho_2\hat{\mathbf{h}}_2^H(\mathbf{W}_2-\frac{\mathbf{W}_1}{\gamma_1})\hat{\mathbf{h}}_2+\rho_2|h_3|^2P_R+1\leq 0, \tag{5.34d}$$

$$\rho_{1,R}|h_3|^2P_R\geq\gamma_1, \tag{5.34e}$$

$$\min_{\Delta\hat{\mathbf{h}}_2^H\mathbf{I}\Delta\hat{\mathbf{h}}_2\leq\varepsilon_2^2} \rho_2\Delta\hat{\mathbf{h}}_2^H(\delta^{FD}\mathbf{W}_2-\mathbf{W}_1)\Delta\hat{\mathbf{h}}_2+2\rho_2\mathrm{Re}\{\Delta\hat{\mathbf{h}}_2^H(\delta^{FD}\mathbf{W}_2-\mathbf{W}_1)\hat{\mathbf{h}}_2\}$$

$$+\rho_2\hat{\mathbf{h}}_2^H(\delta^{FD}\mathbf{W}_2-\mathbf{W}_1)\hat{\mathbf{h}}_2+\rho_2\delta^{FD}|h_3|^2P_R+\delta^{FD}\leq 0, \tag{5.34f}$$

$$\mathrm{Tr}(\mathbf{W}_1+\mathbf{W}_2)\leq P_{\max}, \tag{5.34g}$$

$$P_R\leq P_{R_{\max}}, \tag{5.34h}$$

$$\mathrm{rank}(\mathbf{W}_n)=1. \tag{5.34i}$$

Moreover, when the MRC is prossessed at the cell-edge user then the problem can be described as shown

$$\mathbf{P15}: \max_{t,\gamma_2,\gamma_1,u_1,u_2,\mathbf{W}_1,\mathbf{W}_2,P_R} (5.34a),$$

$$s.t. \quad (5.34b), (5.34c), (5.34d),$$

$$u_1 + u_2 \geq \gamma_1, \tag{5.35a}$$

$$\rho_{1,R}|h_3|^2 P_R \geq u_1, \tag{5.35b}$$

$$\min_{\Delta\hat{\mathbf{h}}_1^H \mathbf{I} \Delta\hat{\mathbf{h}}_1 \leq \varepsilon_1^2} \rho_1 \Delta\hat{\mathbf{h}}_1^H (\mathbf{W}_2 - \frac{\mathbf{W}_1}{u_2}) \Delta\hat{\mathbf{h}}_1 + 2\rho_1 \mathrm{Re}\{\Delta\hat{\mathbf{h}}_1^H (\mathbf{W}_2 - \frac{\mathbf{W}_1}{u_2}) \hat{\mathbf{h}}_1\}$$
$$+ \rho_1 \hat{\mathbf{h}}_1^H (\mathbf{W}_2 - \frac{\mathbf{W}_1}{u_2}) \hat{\mathbf{h}}_1 + 1 \leq 0, \tag{5.35c}$$

$$(5.34f), (5.34g), (5.34h), (5.34i).$$

Then the $\mathcal{S}$-procedure which is explained in Section 2.2.3, will be applied at the constraints in **P14** and **P15** that contains uncertainty terms in order to transform these

constraints from quadratic form to a LMI equations.

$$\mathbf{P16}: \max_{t,\gamma_2,\gamma_1,\mathbf{W}_1,\mathbf{W}_2,P_R,\lambda_1,\lambda_2,\lambda_3} \quad t \tag{5.36a}$$

$$s.t. \quad \log_2(1+\gamma_2)+\log_2(1+\gamma_1)\geq t, \tag{5.36b}$$

$$\begin{bmatrix} -\rho_2\frac{\mathbf{W}_2}{\gamma_2}-\lambda_1\mathbf{I} & -\rho_2\frac{\mathbf{W}_2}{\gamma_2}\hat{\mathbf{h}}_2 \\ -\hat{\mathbf{h}}_2^H\rho_2\frac{\mathbf{W}_2}{\gamma_2} & -\rho_2\hat{\mathbf{h}}_2^H\frac{\mathbf{W}_2}{\gamma_2}\hat{\mathbf{h}}_2+\rho|h_3|^2P_R+1+\lambda_1\varepsilon_2^2 \end{bmatrix}\preceq 0, \tag{5.36c}$$

$$\begin{bmatrix} \rho_2(\mathbf{W}_2-\frac{\mathbf{W}_1}{\gamma_1})-\lambda_2\mathbf{I} & \rho_2(\mathbf{W}_2-\frac{\mathbf{W}_1}{\gamma_1})\hat{\mathbf{h}}_2 \\ \hat{\mathbf{h}}_2^H\rho_2(\mathbf{W}_2-\frac{\mathbf{W}_1}{\gamma_1}) & \rho_2\hat{\mathbf{h}}_2^H(\mathbf{W}_2-\frac{\mathbf{W}_1}{\gamma_1})\hat{\mathbf{h}}_2+\rho_2|h_3|^2P_R+1+\lambda_2\varepsilon_2^2 \end{bmatrix}\preceq 0, \tag{5.36d}$$

$$\rho_{1,R}|h_3|^2P_R\geq\gamma_1, \tag{5.36e}$$

$$\begin{bmatrix} \rho_2(\delta^{FD}\mathbf{W}_2-\mathbf{W}_1)-\lambda_3\mathbf{I} & \rho_2(\delta^{FD}\mathbf{W}_2-\mathbf{W}_1)\hat{\mathbf{h}}_2 \\ \hat{\mathbf{h}}_2^H\rho_2(\delta^{FD}\mathbf{W}_2-\mathbf{W}_1) & \rho_2\hat{\mathbf{h}}_2^H(\delta^{FD}\mathbf{W}_2-\mathbf{W}_1)\hat{\mathbf{h}}_2+\rho_2|h_3|^2P_R+1+\lambda_3\varepsilon_2^2 \end{bmatrix}\preceq 0 \tag{5.36f}$$

$$\mathrm{Tr}(\mathbf{W}_1+\mathbf{W}_2)\leq P_{\max}, \tag{5.36g}$$

$$P_R\leq P_{R_{\max}}, \tag{5.36h}$$

$$\mathrm{rank}(\mathbf{W}_n)=1. \tag{5.36i}$$

Also, reformatting **P15** then it will be as following:

$$\mathbf{P17}: \max_{t,\gamma_2,\gamma_1,u_1,u_2,\mathbf{W}_1,\mathbf{W}_2,P_R,\lambda_1,\lambda_2,\lambda_3,\lambda_4} (5.36a),$$

$$s.t. \quad (5.36b), (5.36c), (5.36d),$$

$$u_1 + u_2 \geq \gamma_1, \tag{5.37a}$$

$$\rho_{1,R}|h_3|^2 P_R \geq u_1, \tag{5.37b}$$

$$\begin{bmatrix} \rho_1(\mathbf{W}_2 - \frac{\mathbf{W}_1}{u_2}) - \lambda_4\mathbf{I} & \rho_1(\mathbf{W}_2 - \frac{\mathbf{W}_1}{u_2})\hat{\mathbf{h}}_1 \\ \hat{\mathbf{h}}_1^H\rho_1(\mathbf{W}_2 - \frac{\mathbf{W}_1}{u_2}) & \rho_1\hat{\mathbf{h}}_1^H(\mathbf{W}_2 - \frac{\mathbf{W}_1}{u_2})\hat{\mathbf{h}}_1 + 1 + \lambda_4\varepsilon_1^2 \end{bmatrix} \preceq 0, \tag{5.37c}$$

$$(5.36f), (5.36g), (5.36h), (5.36i).$$

Next, there are two different approaches to achieve a converged solution. One approach is to apply the NB algorithm as described in Algorithm 3 or, replace the following terms with there Taylor expansion series.

$$g(\mathbf{W}_2, \gamma_2) \approx -\frac{\mathbf{W}_2^{(k)}}{\gamma_2^{(k)}} - \frac{\mathbf{W}_2 - \mathbf{W}_2^{(k)}}{\gamma_2^{(k)}} + \frac{\mathbf{W}_2^{(k)}(\gamma_2 - \gamma_2^{(k)})}{\left(\gamma_2^{(k)}\right)^2}, \tag{5.38a}$$

$$f(\mathbf{W}_1, \gamma_1) \approx -\frac{\mathbf{W}_1^{(k)}}{\gamma_1^{(k)}} - \frac{\mathbf{W}_1 - \mathbf{W}_1^{(k)}}{\gamma_1^{(k)}} + \frac{\mathbf{W}_1^{(k)}(\gamma_1 - \gamma_1^{(k)})}{\left(\gamma_1^{(k)}\right)^2}, \tag{5.38b}$$

$$y(\mathbf{W}_1, u_2) \approx -\frac{\mathbf{W}_1^{(k)}}{u_2^{(k)}} - \frac{\mathbf{W}_1 - \mathbf{W}_1^{(k)}}{u_2^{(k)}} + \frac{\mathbf{W}_1^{(k)}(u_2 - u_2^{(k)})}{\left(u_2^{(k)}\right)^2}. \tag{5.38c}$$

5.3.2.2 HD Cooperative NOMA with MRC and without MRC

On the other hand, when the HD transmission scheme is applied the problem will be

$$\mathbf{P18}: \max_{t,\gamma_2,\gamma_1,\mathbf{W}_1,\mathbf{W}_2,P_R} t \tag{5.39a}$$

$$s.t. \quad \log_2(1+\gamma_2)+\log_2(1+\gamma_1)\geq t, \tag{5.39b}$$

$$\min_{\Delta\hat{\mathbf{h}}_2^H\mathbf{I}\Delta\hat{\mathbf{h}}_2\leq\varepsilon_2^2} -\rho_2\Delta\hat{\mathbf{h}}_2^H\mathbf{W}_2\Delta\hat{\mathbf{h}}_2-2\rho_2\mathrm{Re}\{\Delta\hat{\mathbf{h}}_2^H\mathbf{W}_2\hat{\mathbf{h}}_2\}-\rho_2\hat{\mathbf{h}}_2^H\mathbf{W}_2\hat{\mathbf{h}}_2+\gamma_2\leq 0, \tag{5.39c}$$

$$\min_{\Delta\hat{\mathbf{h}}_2^H\mathbf{I}\Delta\hat{\mathbf{h}}_2\leq\varepsilon_2^2} \rho_2\Delta\hat{\mathbf{h}}_2^H(\mathbf{W}_2-\frac{\mathbf{W}_1}{\gamma_1})\Delta\hat{\mathbf{h}}_2+2\rho_2\mathrm{Re}\{\Delta\hat{\mathbf{h}}_2^H(\mathbf{W}_2-\frac{\mathbf{W}_1}{\gamma_1})\hat{\mathbf{h}}_2\}$$
$$+\rho_2\hat{\mathbf{h}}_2^H(\mathbf{W}_2-\frac{\mathbf{W}_1}{\gamma_1})\hat{\mathbf{h}}_2+1\leq 0, \tag{5.39d}$$

$$\rho_{1,R}|h_3|^2P_R\geq\gamma_1, \tag{5.39e}$$

$$\min_{\Delta\hat{\mathbf{h}}_2^H\mathbf{I}\Delta\hat{\mathbf{h}}_2\leq\varepsilon_2^2} \rho_2\Delta\hat{\mathbf{h}}_2^H(\delta^{HD}\mathbf{W}_2-\mathbf{W}_1)\Delta\hat{\mathbf{h}}_2+2\rho_2\mathrm{Re}\{\Delta\hat{\mathbf{h}}_2^H(\delta^{HD}\mathbf{W}_2-\mathbf{W}_1)\hat{\mathbf{h}}_2\}$$
$$+\rho_2\hat{\mathbf{h}}_2^H(\delta^{HD}\mathbf{W}_2-\mathbf{W}_1)\hat{\mathbf{h}}_2+\delta^{HD}\leq 0, \tag{5.39f}$$

$$\mathrm{Tr}(\mathbf{W}_1+\mathbf{W}_2)\leq P_{\max}, \tag{5.39g}$$

$$P_R\leq P_{R_{\max}}, \tag{5.39h}$$

$$\mathrm{rank}(\mathbf{W}_n)=1, \tag{5.39i}$$

and the problem for the MRC case will be

$$\mathbf{P19}: \max_{t,\gamma_2,\gamma_1,u_1,u_2,\mathbf{W}_1,\mathbf{W}_2,P_R} (5.39a),$$

$$s.t. \quad (5.39b),(5.39c),(5.39d),$$

$$u_1+u_2 \geq \gamma_1, \tag{5.40a}$$

$$\rho_{1,R}|h_3|^2 P_R \geq u_1, \tag{5.40b}$$

$$\min_{\Delta\hat{\mathbf{h}}_1^H \mathbf{I} \Delta\hat{\mathbf{h}}_1 \leq \varepsilon_1^2} \rho_1 \Delta\hat{\mathbf{h}}_1^H (\mathbf{W}_2 - \frac{\mathbf{W}_1}{u_2}) \Delta\hat{\mathbf{h}}_1 + 2\rho_1 \mathrm{Re}\{\Delta\hat{\mathbf{h}}_1^H (\mathbf{W}_2 - \frac{\mathbf{W}_1}{u_2})\hat{\mathbf{h}}_1\}$$
$$+ \rho_1 \hat{\mathbf{h}}_1^H (\mathbf{W}_2 - \frac{\mathbf{W}_1}{u_2})\hat{\mathbf{h}}_1 + 1 \leq 0, \tag{5.40c}$$

$$(5.39f),(5.39g),(5.39h),(5.39i).$$

By applying $\mathcal{S}$-procedure the problems will be reformulated as follows:

$$\mathbf{P20}: \max_{t,\gamma_2,\gamma_1,\mathbf{W}_1,\mathbf{W}_2,P_R,\lambda_1,\lambda_2,\lambda_3} t \tag{5.41a}$$

$$s.t. \quad \log_2(1+\gamma_2) + \log_2(1+\gamma_1) \geq t, \tag{5.41b}$$

$$\begin{bmatrix} -\rho_2 \mathbf{W}_2 - \lambda_1 \mathbf{I} & -\rho_2 \mathbf{W}_2 \hat{\mathbf{h}}_2 \\ -\hat{\mathbf{h}}_2^H \rho_2 \mathbf{W}_2 & -\rho_2 \hat{\mathbf{h}}_2^H \mathbf{W}_2 \hat{\mathbf{h}}_2 + \gamma_2 + \lambda_1 \varepsilon_2^2 \end{bmatrix} \preceq 0, \tag{5.41c}$$

$$\begin{bmatrix} \rho_2(\mathbf{W}_2 - \frac{\mathbf{W}_1}{\gamma_1}) - \lambda_2 \mathbf{I} & \rho_2(\mathbf{W}_2 - \frac{\mathbf{W}_1}{\gamma_1})\hat{\mathbf{h}}_2 \\ \hat{\mathbf{h}}_2^H \rho_2 (\mathbf{W}_2 - \frac{\mathbf{W}_1}{\gamma_1}) & \rho_2 \hat{\mathbf{h}}_2^H (\mathbf{W}_2 - \frac{\mathbf{W}_1}{\gamma_1})\hat{\mathbf{h}}_2 + 1 + \lambda_2 \varepsilon_2^2 \end{bmatrix} \preceq 0, \tag{5.41d}$$

$$\rho_{1,R}|h_3|^2 P_R \geq \gamma_1, \tag{5.41e}$$

$$\begin{bmatrix} \rho_2(\delta^{HD}\mathbf{W}_2 - \mathbf{W}_1) - \lambda_3 \mathbf{I} & \rho_2(\delta^{HD}\mathbf{W}_2 - \mathbf{W}_1)\hat{\mathbf{h}}_2 \\ \hat{\mathbf{h}}_2^H \rho_2 (\delta^{HD}\mathbf{W}_2 - \mathbf{W}_1) & \rho_2 \hat{\mathbf{h}}_2^H (\delta^{HD}\mathbf{W}_2 - \mathbf{W}_1)\hat{\mathbf{h}}_2 + 1 + \lambda_3 \varepsilon_2^2 \end{bmatrix} \preceq 0 \tag{5.41f}$$

$$\mathrm{Tr}(\mathbf{W}_1 + \mathbf{W}_2) \leq P_{\max}, \tag{5.41g}$$

$$P_R \leq P_{R_{\max}}, \tag{5.41h}$$

$$\mathrm{rank}(\mathbf{W}_n) = 1, \tag{5.41i}$$

and

$$\mathbf{P21}: \max_{t,\gamma_2,\gamma_1,u_1,u_2,\mathbf{W}_1,\mathbf{W}_2,P_R,\lambda_1,\lambda_2,\lambda_3,\lambda_4} (5.41a),$$

$$s.t. \quad (5.41b),(5.41c),(5.41d),$$

$$u_1 + u_2 \geq \gamma_1, \tag{5.42a}$$

$$\rho_{1,R}|h_3|^2 P_R \geq u_1, \tag{5.42b}$$

$$\begin{bmatrix} \rho_1(\mathbf{W}_2 - \frac{\mathbf{W}_1}{u_2}) - \lambda_4\mathbf{I} & \rho_1(\mathbf{W}_2 - \frac{\mathbf{W}_1}{u_2})\hat{\mathbf{h}}_1 \\ \hat{\mathbf{h}}_1^H\rho_1(\mathbf{W}_2 - \frac{\mathbf{W}_1}{u_2}) & \rho_1\hat{\mathbf{h}}_1^H(\mathbf{W}_2 - \frac{\mathbf{W}_1}{u_2})\hat{\mathbf{h}}_1 + 1 + \lambda_4\varepsilon_1^2 \end{bmatrix} \preceq 0, \tag{5.42c}$$

$$(5.41f),(5.41g),(5.41h),(5.41i).$$

Then, use the approaches explained earlier to achieve a converged solution. Which are either NB algorithm as described in Algorithm 3 or, replace the following terms by there Taylor expansion series in (5.38).

5.4 Simulation Result

A single cell downlink transmission is considered where a multi-antenna BS serves randomly distributed single antenna users within one kilometre radius. In the simulations, it is assumed that the BS is equipped with two antennas ($M = 2$) and it serves two users ($K = 2$) in the cell. The channel coefficients between the BS and the users are generated as $\mathbf{h}_n = \chi_n \sqrt{d_n^{-\beta_n}}$ where $\chi_n \sim \mathcal{CN}(0, I)$, it is assumed that the path-loss exponent $\beta_1 = 4$ for the far user, $\beta_2 = 2$ for the near user and d_n is the distance between U_n and the BS.

In Table 5.1 the average number of iteration to achieve a solution using AO with the minimum achievable data rate that satisfies SIC constraint $R_{th} = 0.1\ Bit/s/Hz$ for FD cooperative NOMA system model is presented. As the transmitted SNR or the maximum relay power are increased the average number of iteration requires more processing to achieve a solution. Also, this data is represented for the GP algorithm in Table 5.2. However, this algorithm needs more computational processing to achieve a solution comparing to AO. This table shows the computational complexity of each algorithm where NB is more complex compared to GP and AO. In Table 5.3 Number of rank one solution for each algorithm in the FD cooperative NOMA system model.

The achievable rate for users within the individual beam with $P_{R_{max}} = 0.2\ W$ and $R_{th} = 0.1\ Bit/s/Hz$ for FD cooperative NOMA system model using different algorithms in Fig. 5.5. Where the simulation results show that there is a trade-off between using AO, GP and NB. AO provides more data rate for the near user then the GP get a lower data rate than the NB. On the other hand, NB provides more data rate for the far user then the GP get a lower data rate than the AO. The rate for the

far user at different relay power level for FD cooperative NOMA in Fig. 5.6 is displayed.

In Fig. 5.7 the achievable rate for the far user at different R_{th} is illustrated. The allocated power of each user within the beam for the FD cooperative NOMA system model is depicted in Fig. 5.8 for different algorithms. Also, it is shown in Fig. 5.9 the allocated power for each user within the beam at different R_{th}.

Table 5.1: The average number of iteration in order to achieve a solution using AO with $R_{th} = 0.1\ Bit/s/Hz$ for FD cooperative NOMA system model.

$P_{R_{max}}$ \ SNR	0	5	10	15	20	25
0.001 W	3.0033	3.3246	3.1589	3.8264	4.345	6.6458
0.2 W	4.0567	5.8721	7.8604	10.2981	12.0549	17.015
1 W	5.57	8.5861	10.6438	14.511	15.5382	21.0144

Table 5.2: The average number of iteration to achieve a solution using GP with $R_{th} = 0.1\ Bit/s/Hz$ for FD cooperative NOMA system model.

$P_{R_{max}}$ \ SNR	0	5	10	15	20	25
0.001 W	7.6213	8.34	9.0891	9.7417	10.4934	12.2835
0.2 W	7.851	9.7649	12.7841	16.7815	17.7674	20.3871
1 W	9.4323	12.9536	15.0533	18.5908	18.3223	20.5839

Table 5.3: Number of rank one solution for each algorithm in FD cooperative NOMA system model.

Algo \ SNR	0	5	10	15	20	25
AO	300/300	300/300	300/300	300/300	300/300	300/300
GP	300/300	300/300	300/300	300/300	300/300	300/300
NB	6/300	12/300	35 /300	132 /300	233 /300	236/300

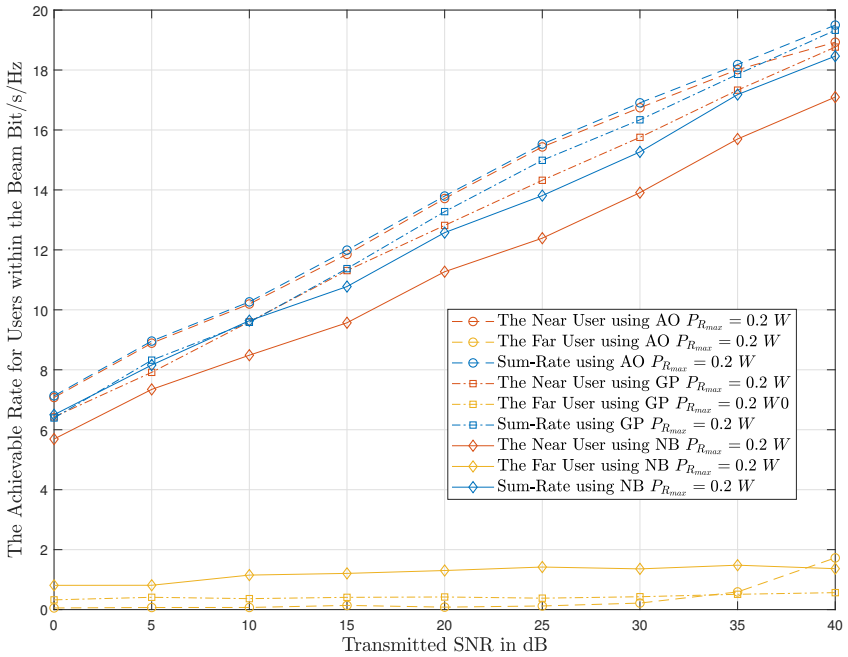

Figure 5.5: The achievable rate for users within the beam with $P_{R_{max}} = 0.2\ W$ and $R_{th} = 0.1\ Bit/s/Hz$ for FD cooperative NOMA system model.

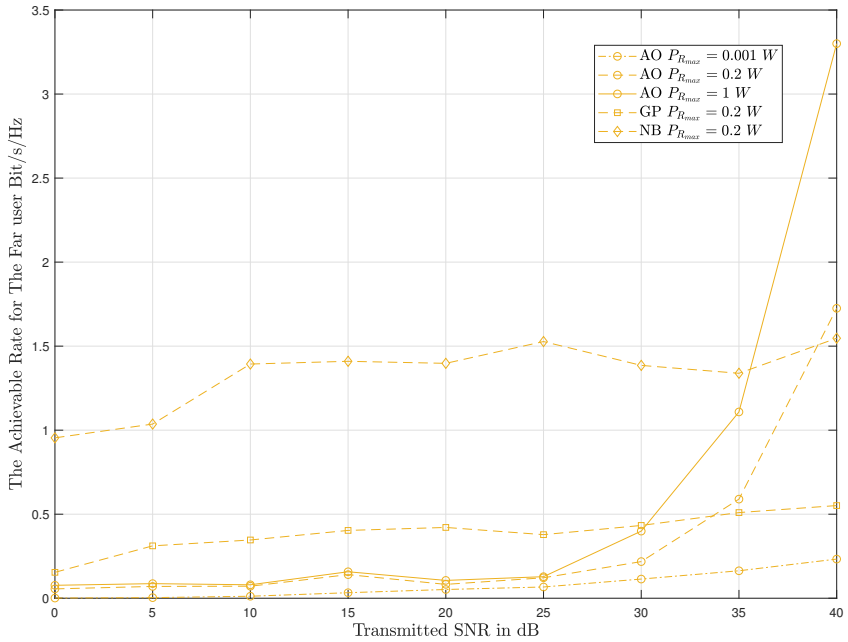

Figure 5.6: The rate for the far user at different relay power for FD cooperative NOMA.

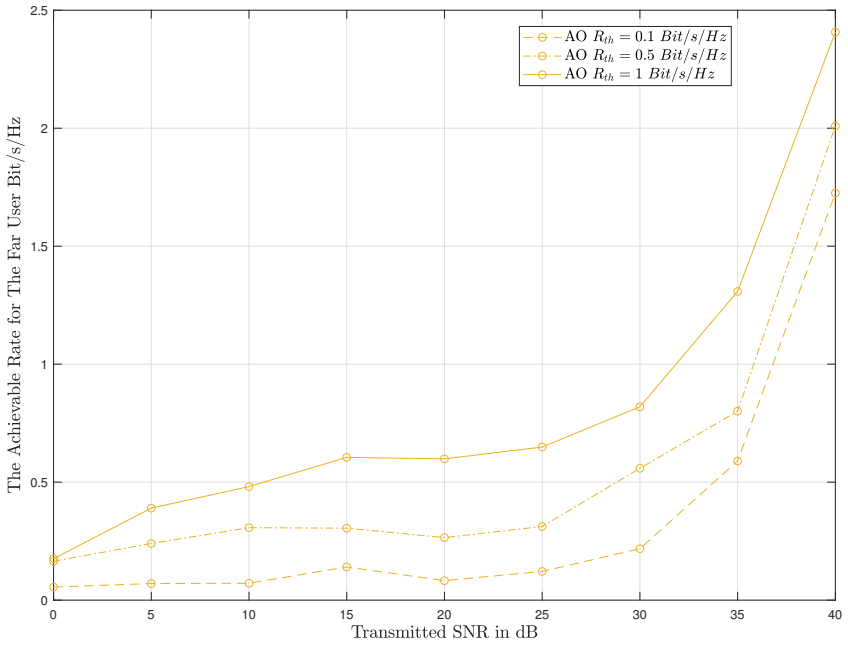

Figure 5.7: The achievable rate for the far user at different R_{th} for FD cooperative NOMA system model.

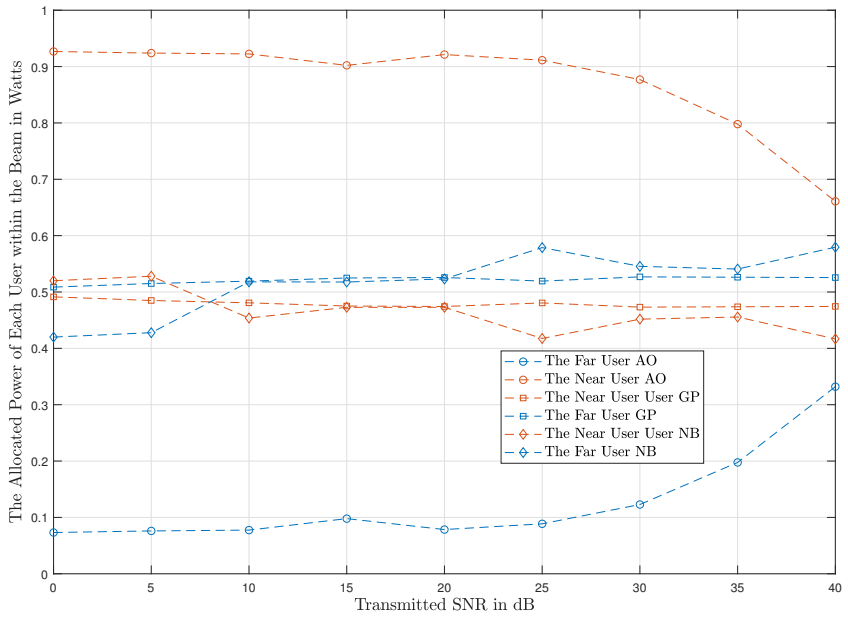

Figure 5.8: The allocated power of each user within the beam for FD cooperative NOMA system model.

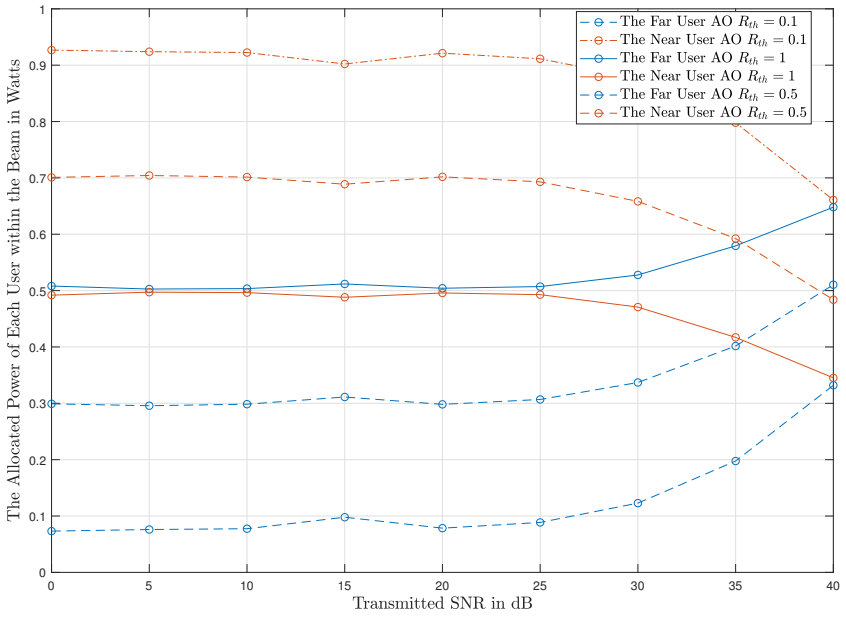

Figure 5.9: The allocated power of each user within the beam at different R_{th} for FD cooperative NOMA system model.

Then the MRC constraint is included in the problem formulation for the FD cooperative NOMA system model. The achievable rate for users within the beam with $P_{R_{max}} = 0.2$ for the FD cooperative NOMA system model considering MRC at the far user in Fig. 5.10. In Fig. 5.11 the allocated power of each user within the beam. In Table 5.4 a comparison is conducted between the FD cooperative NOMA system model with and without considering MRC at the weak user for the average number of iteration to achieve a solution at $P_{R_{max}} = 0.2\ W\ R_{th} = 0.5\ Bit/s/Hz$.

Also, the power of the relay for FD cooperative NOMA system with and without considering MRC at the far user is compared with different algorithms in Fig. 5.12. For the near user, the allocated power for FD cooperative NOMA system with and without considering MRC is compared in Fig. 5.13. It shows that when the MRC is used at the weak user the allocated power for the near user decreases as the transmitted SNR level is increased. This comparison is also illustrated for the cell edge user in Fig. 5.14.

Table 5.4: Comparing The average number of iteration to achieve a solution $P_{R_{max}} = 0.2\ W\ R_{th} = 0.5\ Bit/s/Hz$ for FD cooperative NOMA system model with and without considering MRC at the weak user.

SNR / Algo	0	5	10	15	20	25
AO MRC	5.1433	9.0067	13.27	14.1233	14.6844	11.9475
AO	3.43	5.202	7.1895	10.4479	12.0281	18.4521
GP MRC	5.926	10.2174	13.7855	14.4897	12.3907	11.539
GP	7.851	9.7649	12.7841	16.7815	17.7674	20.3871

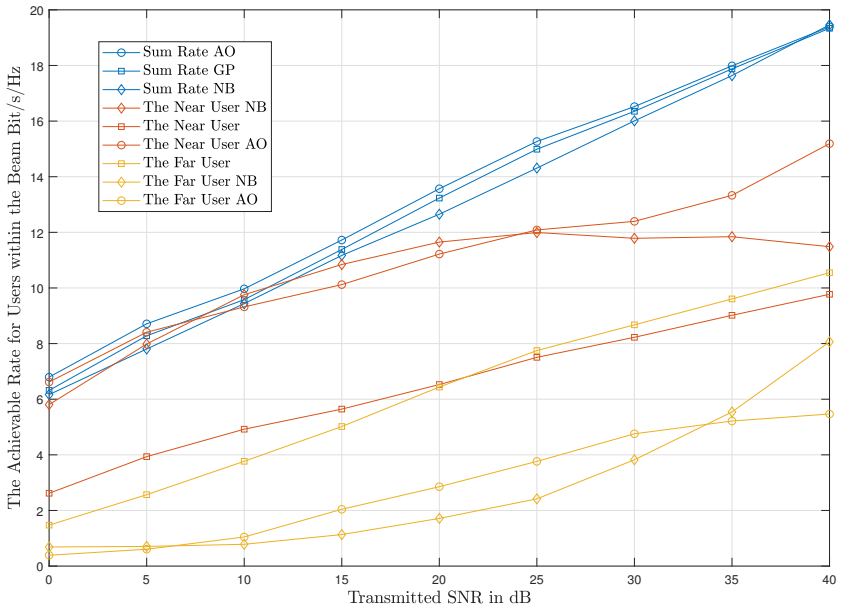

Figure 5.10: The achievable rate for users within the beam with $P_{R_{max}} = 0.2$ for FD cooperative NOMA system model considering MRC at the far user.

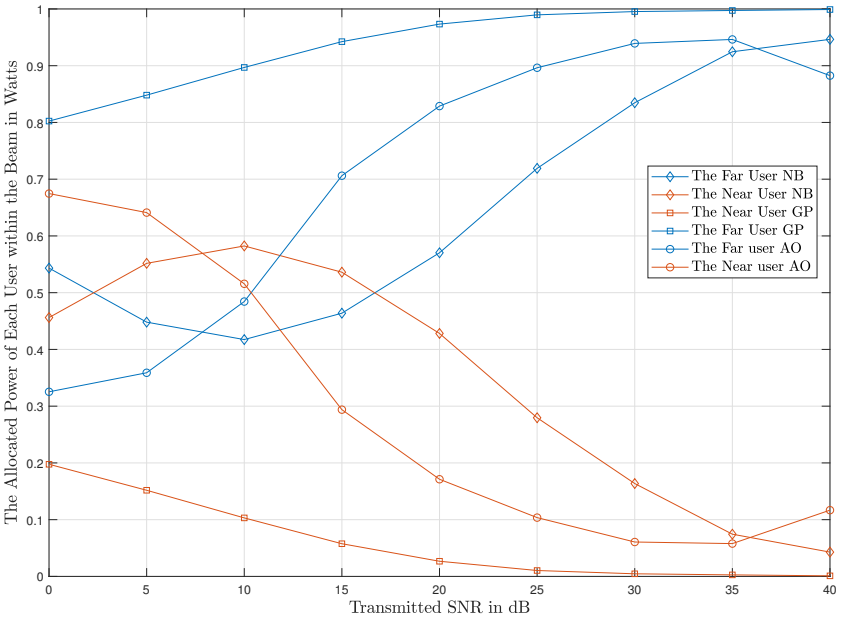

Figure 5.11: The allocated power of each user within the beam for FD cooperative NOMA system model considering MRC at the far user.

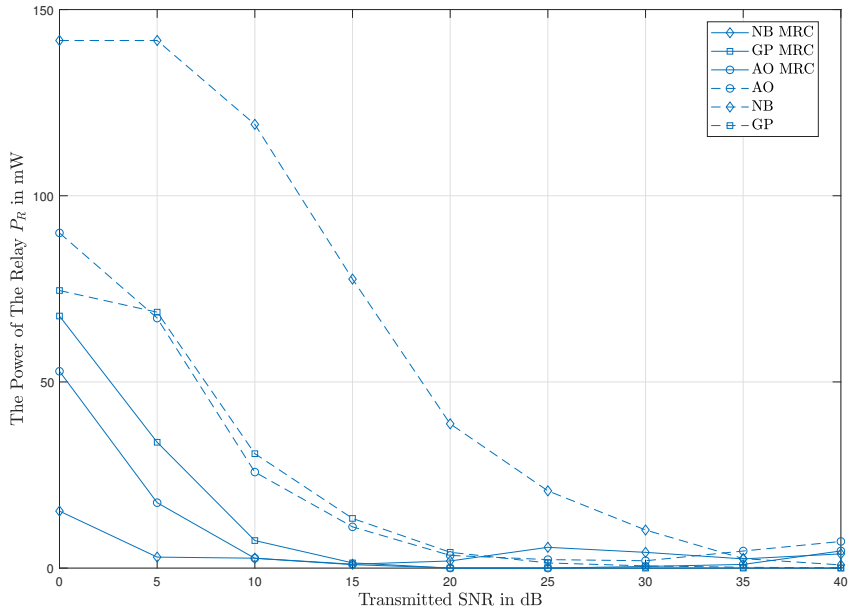

Figure 5.12: Comparing the power of the relay for FD cooperative NOMA system with and without considering MRC at the far user.

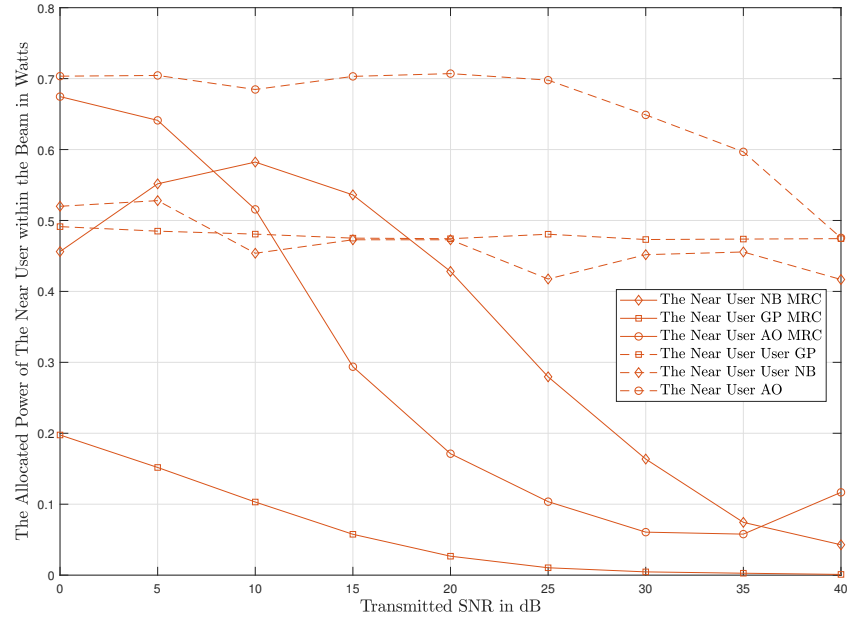

Figure 5.13: Comparing the near user power for FD cooperative NOMA system with and without considering MRC at the far user.

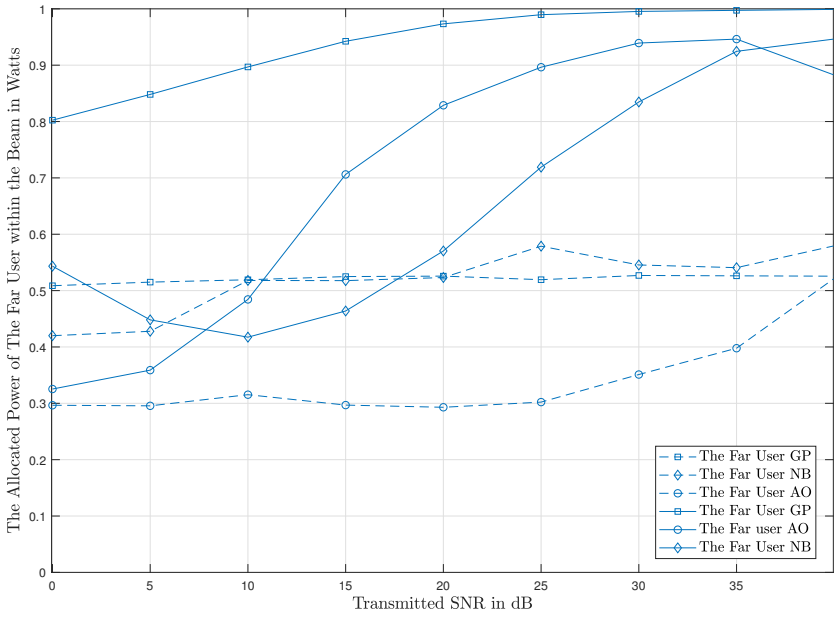

Figure 5.14: Comparing the far user power for FD cooperative NOMA system with and without considering MRC at the far user.

For HD cooperative NOMA scheme the average number of iteration in order to achieve a solution using AO with $R_{th} = 0.1\ Bit/s/Hz$ is presented in Table 5.5 at a different level of relay power. Also, the number of rank one solution for each algorithm in the HD cooperative NOMA system model in Table 5.7 is provided to show that the solutions satisfy the rank one constraint in the problem formulation. In Fig. 5.15 the achievable rate for users within the beam at $P_{R_{max}} = 0.2\ W$ and $R_{th} = 0.1\ Bit/s/Hz$ for HD cooperative NOMA system model is demonstrated for different algorithms.

Fig. 5.16 shows the effect of the relay power level for the cell edge user. Moreover, at different R_{th} rate will affect the achievable rate for far user especially when the AO is used as it is illustrated in Fig. 5.17. The allocated power of each user within the beam is presented in Fig. 5.18. The power allocation is affected by changing different R_{th} as depicted in Fig. 5.19 when AO is used and in Fig. 5.20 when GP is applied.

Table 5.5: The average number of iteration in order to achieve a solution using AO with $R_{th} = 0.1\ Bit/s/Hz$ for HD cooperative NOMA system model.

$P_{R_{max}}$ \ SNR	0	5	10	15	20	25
0.001 W	2.0066	2.6176	2	2.3642	2.3733	3.0733
0.2 W	2.6667	3.64	4.4633	5.4433	6.4934	6.8586
1 W	4.18	4.87	5.8333	6.7	7.3675	8.25

Table 5.6: The average number of iteration in order to achieve a solution using GP with $R_{th} = 0.1\ Bit/s/Hz$ for HD cooperative NOMA system model.

$P_{R_{max}}$ \ SNR	0	5	10	15	20	25
0.001 W	6.01	6.6433	7.08	7.6424	8.457	8.9414
0.2 W	5.97	6.7033	7.2333	7.9103	8.6469	8.2967
1 W	6.05	6.7233	7.64	7.9367	7.66	8.206

In Fig. 5.21 the achievable rate for users within the beam with $P_{R_{max}} = 0.2$ for HD cooperative NOMA system model considering MRC at the far user is illus-

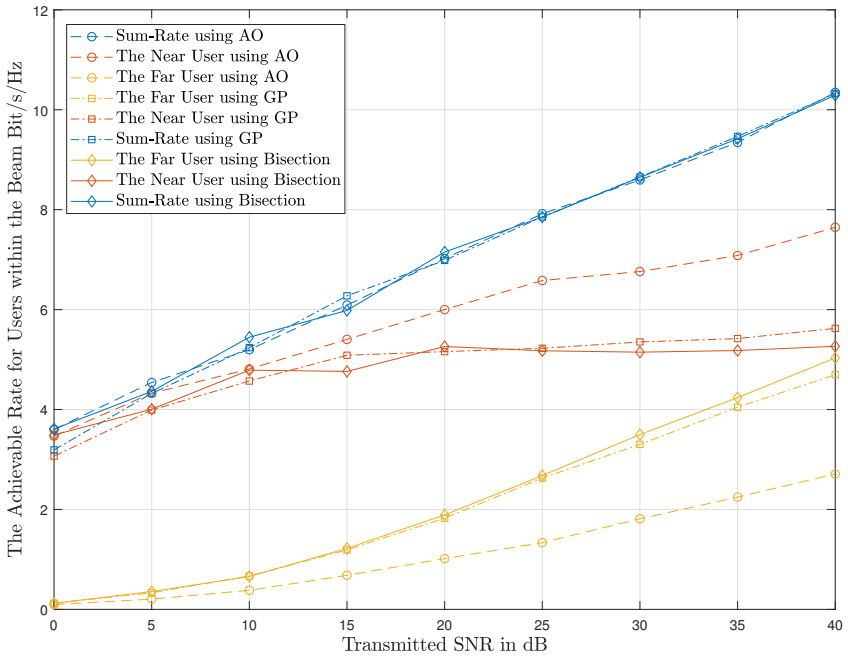

Figure 5.15: The achievable rate for users within the beam with $P_{R_{max}} = 0.2\ W$ and $R_{th} = 0.1\ Bit/s/Hz$ for HD cooperative NOMA system model.

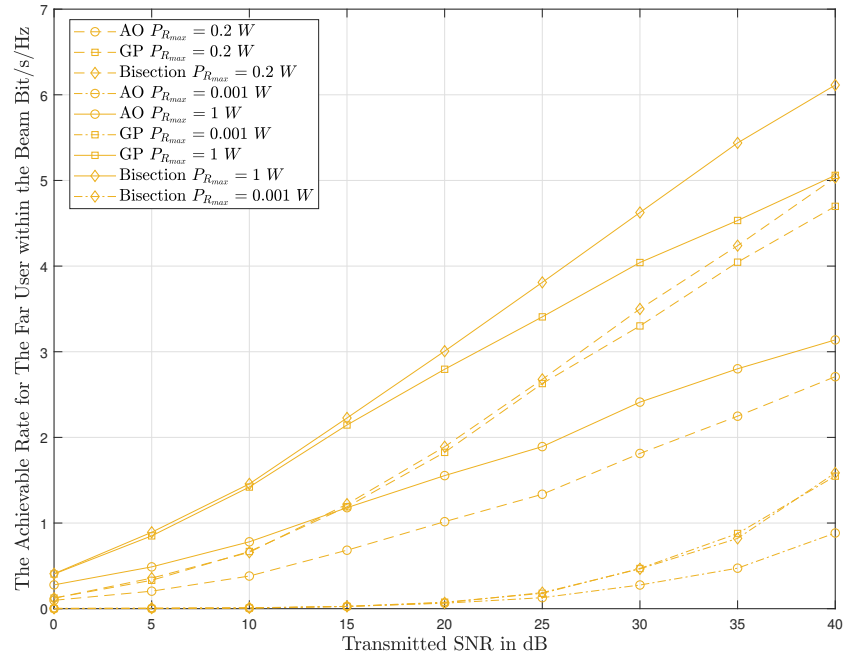

Figure 5.16: The rate for the far user at different relay power for HD cooperative NOMA.

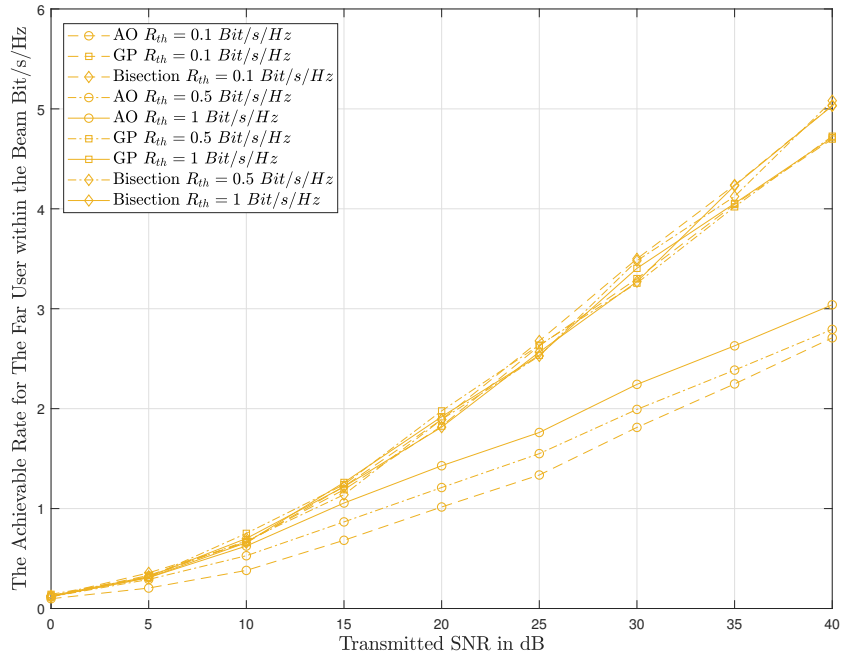

Figure 5.17: The achievable rate for the far user at different R_{th} for HD cooperative NOMA system model.

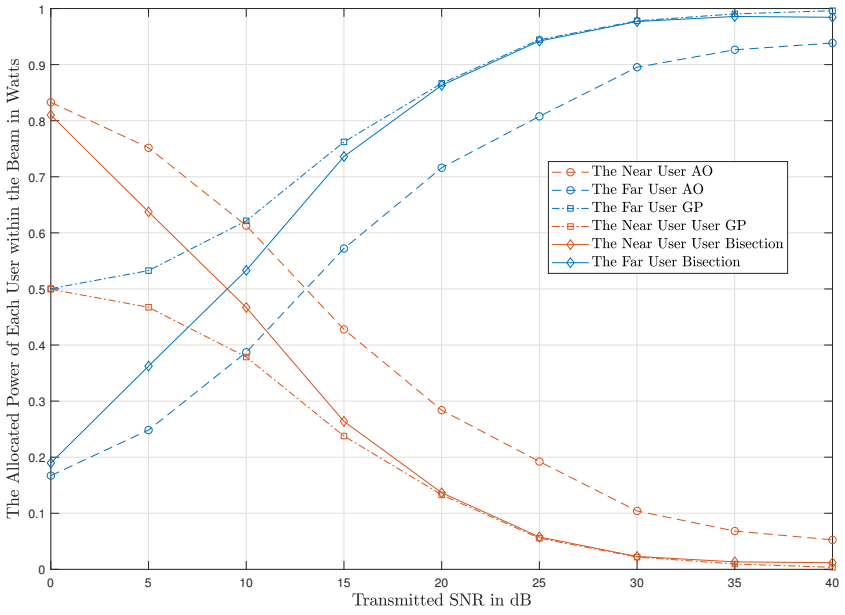

Figure 5.18: The allocated power of each user within the beam for HD cooperative NOMA system model.

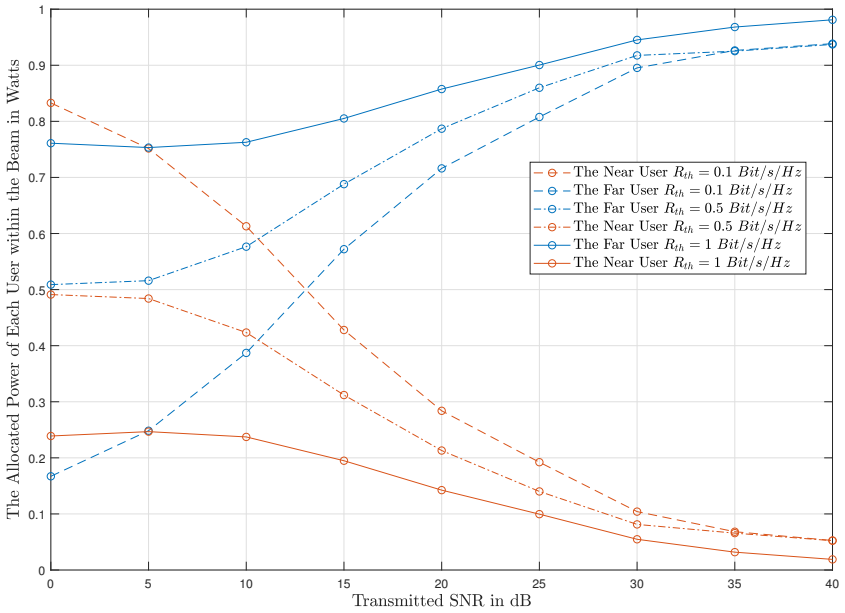

Figure 5.19: The allocated power of each user within the beam at different R_{th} using AO for HD cooperative NOMA system model.

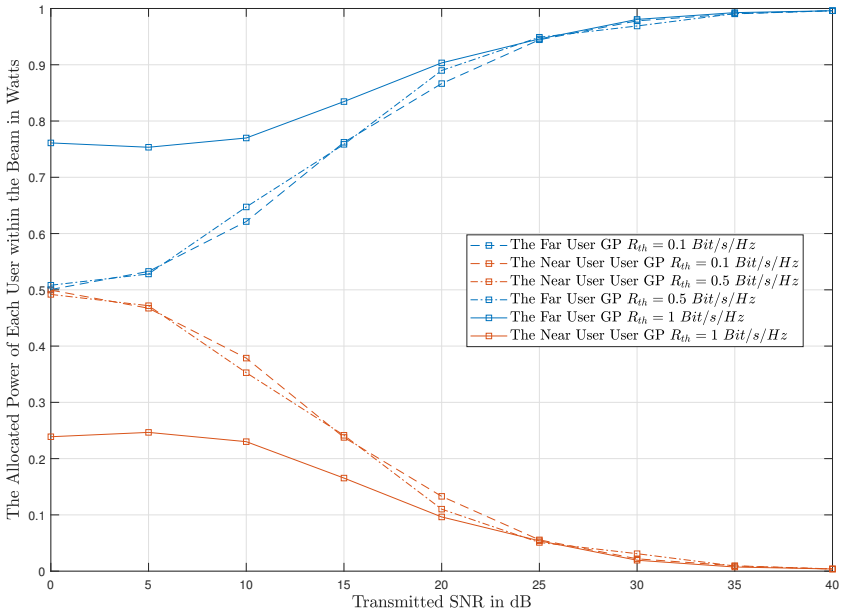

Figure 5.20: The allocated power of each user within the beam at different R_{th} using GP for HD cooperative NOMA system model.

Table 5.7: Number of rank one solution for each algorithm in HD cooperative NOMA system model.

Algo \ SNR	0	5	10	15	20	25
AO	300/300	300/300	300/300	300/300	300/300	300/300
GP	300/300	300/300	300/300	300/300	300/300	300/300
Bisection	299/300	299/300	300/300	300/300	300/300	298/300

trated. The comparison of the average number of iteration to achieve a solution $P_{R_{max}} = 0.2\ W\ R_{th} = 0.5\ Bit/s/Hz$ for HD cooperative NOMA system model with and without considering MRC at the weak user in Table 5.8. Also, Fig. 5.22 compares the power of the relay when the far user applies the MRC and without applying MRC. In addition to that, Fig. 5.23 and Fig. 5.24 compare the allocated power within the beam for the near and far user respectively.

Table 5.8: Comparing The average number of iteration to achieve a solution $P_{R_{max}} = 0.2\ W\ R_{th} = 0.5\ Bit/s/Hz$ for HD cooperative NOMA system model with and without considering MRC at the weak user.

Algo \ SNR	0	5	10	15	20	25
AO MRC	3.7667	5.34	6.0367	6.3046	6.8538	7.2791
AO	2.0367	2.3933	3.4100	4.7409	5.8006	6.7871
GP MRC	5.926	10.2174	13.7855	14.4897	12.3907	11.539
GP	5.7855	6.4752	7.2182	7.6863	8.096	8.2848

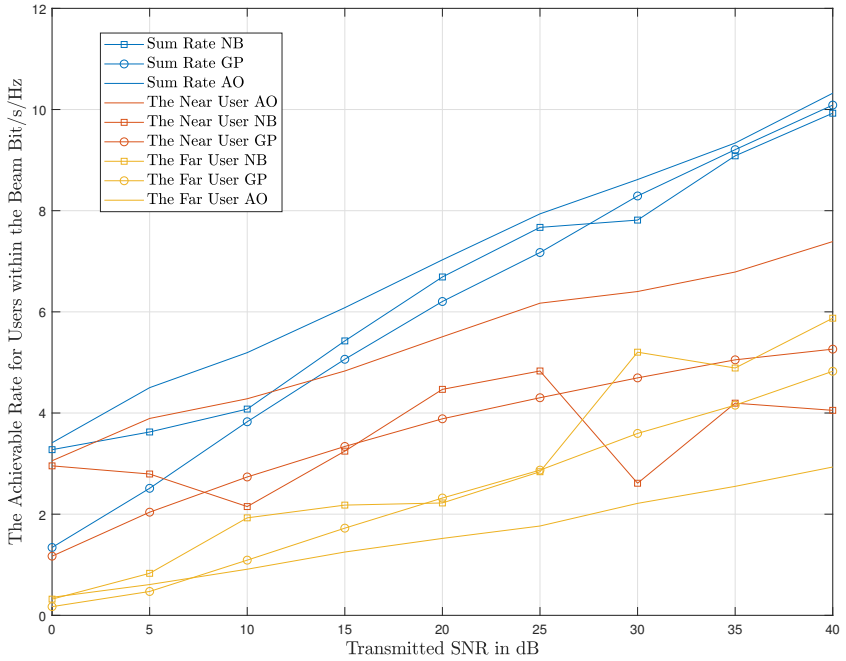

Figure 5.21: The achievable rate for users within the beam with $P_{R_{max}} = 0.2$ for HD cooperative NOMA system model considering MRC at the far user.

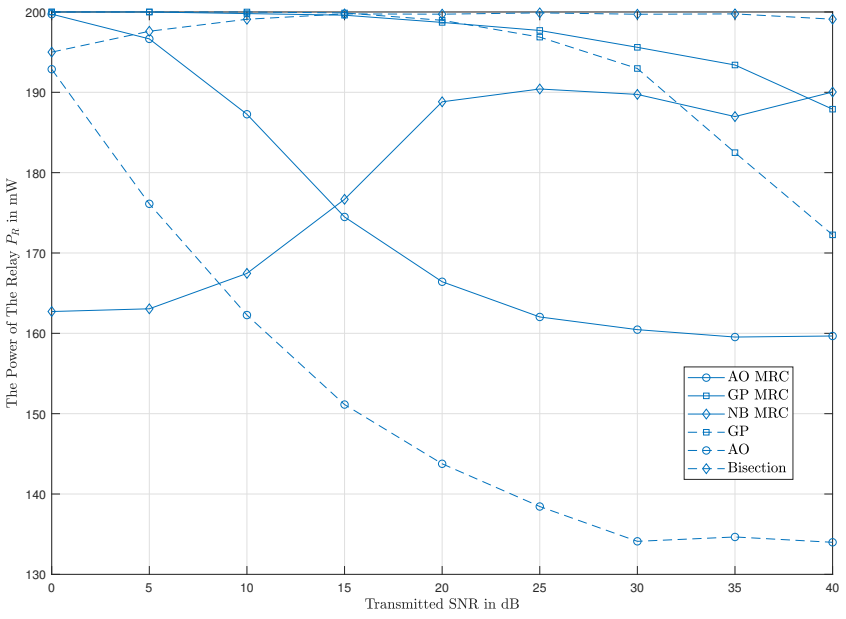

Figure 5.22: Comparing the power of the relay for HD cooperative NOMA system with and without considering MRC at the far user.

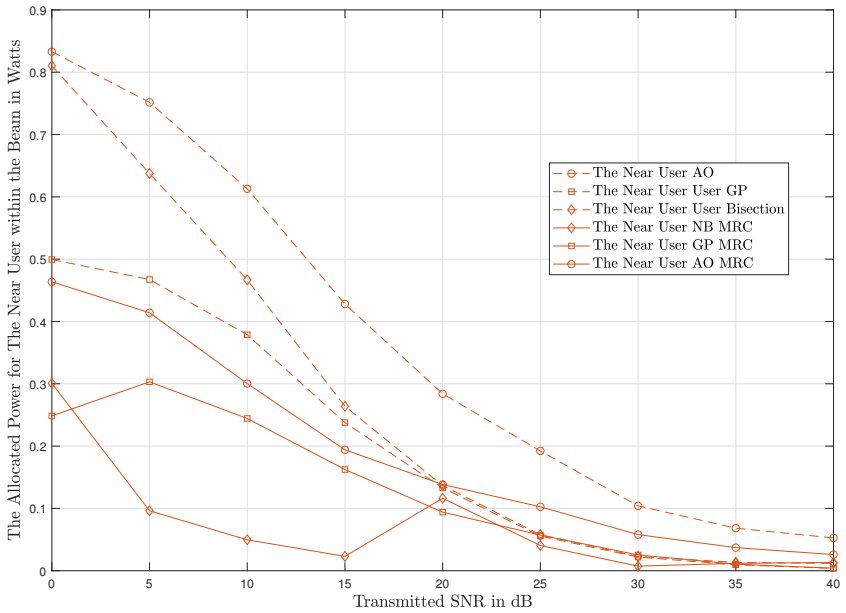

Figure 5.23: Comparing the near user power for HD cooperative NOMA system with and without considering MRC at the far user.

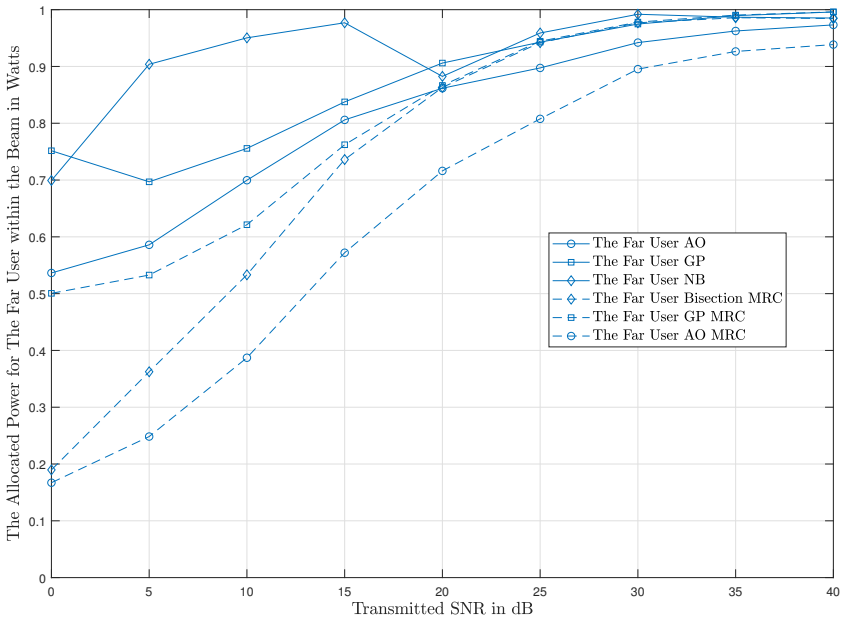

Figure 5.24: Comparing the far user power for HD cooperative NOMA system with and without considering MRC at the far user.

5.5 Conclusion

In this paper, a jointly optimizing beamformer and relay power are investigated for FD/HD cooperative NOMA with several optimization techniques. The study covers both perfect channel state information and the bounded imperfect channel state information. The objective is to maximize the achievable sum-rate for users within the beam. However, the original problem formulation is not convex. Therefore, reformulating the original problem into SDP form is required then several algorithms are applied to find a solution for the optimization problem.

Chapter 6

Conclusions and Directions for Future Work

6.1 Summary

This thesis focuses on applying convex optimization in non-orthogonal multiple access systems. NOMA is an essential enabling technology for the beyond of 5G wireless networks to meet the heterogeneous demands on low latency, high reliability, massive connectivity, improved fairness and high throughput. In this work, various practical constraints, such as grouping based on their QoS requirements and imperfect channel station information have been taken into consideration.

In Chapter 3 the joint design of beamforming and power allocation in the downlink of the NOMA MIMO multiuser system is investigated, where the users are grouped based on their QoS requirements. For the sake of practicality, the problem is formulated where the sum rate of the users who expect to be served with the best efforts

is maximized under the rate constraints of the users with strict QoS requirements and the maximum transmit power constraint at the BS. We then eliminated the inter-beam interference by applying the ZF beamforming. To solve the non-convex optimization problem, the SDR is adopted to approach and showed that the optimal solutions are always rank one using simulation results. Also, a SCA algorithm is proposed based on the AGM inequality to perform the joint design of the beamforming vectors and the power allocation coefficients. Simulation results were presented to show the performance advantage of our proposed algorithm over existing algorithms and the impact of system parameters on the convergence speed of our proposed algorithm.

Chapter 4 has addressed the worst-case robust beamforming design for the MISO-NOMA downlink systems by taking into account the norm-bounded channel uncertainties. The objective was to balance the users SINRs with the constraints of the total transmit power of the other users and the received interference power at the users. However, the original robust problem formulation is not convex due to the imperfect CSI. To tackle the non-convexity with this challenge, the S-procedure is exploited to reformulate the original non-convex problem into the SDP form by recasting the original non-convex constraints into the LMI form. A bisection based algorithm has been devised to obtain robust beamforming solutions with rank relaxation.

In Chapter 5 a jointly optimizing beamformer and relay power are investigated for FD/HD cooperative NOMA with several optimization techniques. The study covers both perfect channel state information and the bounded imperfect channel state information. The objective is to maximize the achievable sum-rate for users within the beam. However, the original problem formulation is not convex therefore, reformulating the original problem into SDP form is required then several algorithms are applied to

approach the solution for the optimization problem.

6.2 Conclusions

- Applying AGM algorithm performs better convergency over other algorithms such as GP and AO as it is shown in Chapter 3.
- There is a performance advantage of the joint design of the beamforming vectors and the power allocation for the NOMA MIMO multiuser system as can be realized in Chapter 3.
- The deterministic error bound which has been applied in Chapter 4 and Chapter 5 shows a reliable lower bound for the performance of the MISO NOMA system.
- There is a trade-off between FD and HD in cooperative NOMA systems in the achievable rate performance as it is demonstrated in Chapter 5 that can be applied in a hybrid system.
- Processing MRC at the cell edge user in HD cooperative NOMA system performs better sum rate over applying MRC for FD system.

6.3 Future Works

6.3.1 Extensions of Current Works

In this part, the possible extensions of the works in this thesis are suggested as following.

- Investigate the performance analysis for the manual pairing in Chapter 3 and examine how it will affect the system.
- Apply the deterministic error bound for imperfect channel state information to the NOMA MIMO multiuser system that grouped based on their QoS in Chapter 3.
- To add multiple base stations to the system model in Chapter 3 and Chapter 4. This will add to the problem formulation several objective functions such as energy efficiency of the system model and the sum-rate of the overall all users in multiple cells.
- Use the probabilistic approach model for the imperfect channel state information to compare it with the deterministic approach which has been used in Chapter 4 and Chapter 5. This requires calculating the outage probability for the proposed system model in this thesis, then add them to the constraint of the problem formulation to be optimized.
- The proposed two-user scenario for cooperative NOMA FD/HD schemes in Chapter 5 can be expanded to a multi-user scenario by using the matching theory [89]. Especially, by applying one-to-one matching, $2K$ users can be divided into K groups, and two users are paired in each group.

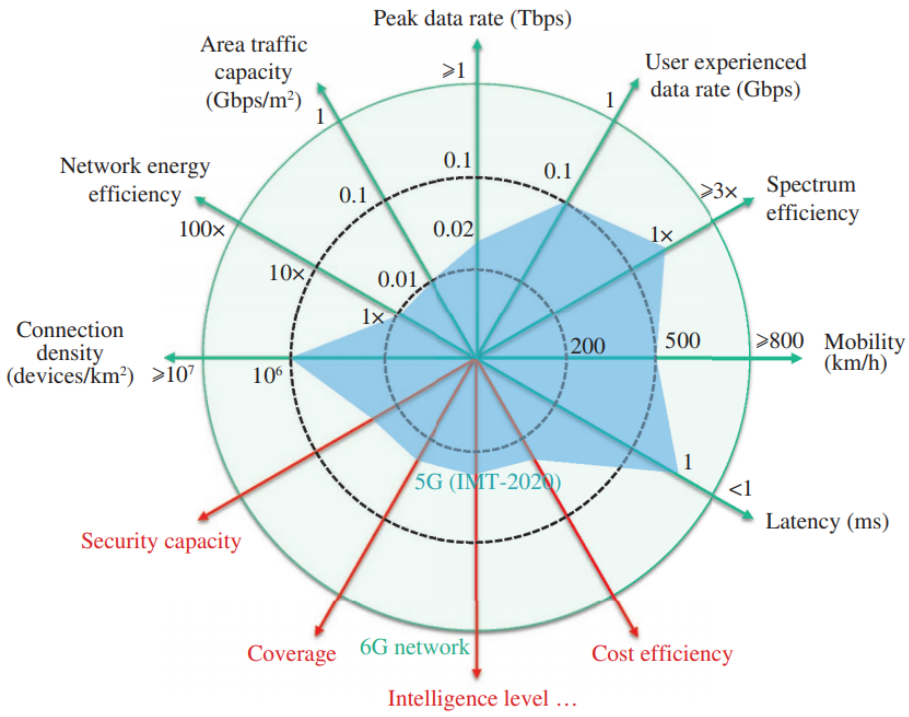

Figure 6.1: 6G performance requirements [1].

6.3.2 Promising Future Directions

Some promising future directions for the research to achieve the 6G performance metric requirements in Fig. 6.1 are presented as follows:

- Applying stochastic convex optimization for advance NOMA systems such as BackCom-NOMA [90], hybrid SIC [91, 92] and NOMA-MEC [93]. Since stochastic optimization is a very effective tool in machine learning episcopally when it is combined with multiple objective optimizations [94].

- Machine learning for NOMA systems, where machine learning is considered as one of the key technologies for the upcoming wireless networks. By observing the environment and data then the machine learns to decide the optimal solu-

tion as it is applied for CR-NOMA [95]. Where, a deep reinforcement learning approach, termed deep deterministic policy gradient (DDPG), is applied to the studied long-term throughput maximization problem.

Bibliography

[1] X. You et al. Towards 6G wireless communication networks: Vision, enabling technologies, and new paradigm shifts. *SCIENCE CHINA Information Sciences*, 2021.

[2] N. Rajatheva et al. White Paper on Broadband Connectivity in 6G, 2020.

[3] Y. Liu et al. Nonorthogonal Multiple Access for 5G and Beyond. *Proceedings of the IEEE*, 105(12):2347–2381, 2017.

[4] E. K. L. Hanzo, L.-L. Yang and K. Yen. *Single-and multi-carrier DS-CDMA: multi-user detection, space-time spreading, synchronisation, standards and networking.* Wiley, 2006.

[5] J. Guey. To 4G mobile communication and beyond. pp. 1–2, 2013.

[6] A. Al-Dulaimi et al. *Standardization: The Road to 5G*, pp. 691–708. 2018.

[7] Yuanwei et al. *Non-Orthogonal Multiple Access for Massive Connectivity.* Springer, 2020.

[8] Y. Cai et al. Modulation and Multiple Access for 5G Networks. *IEEE Communications Surveys Tutorials*, 20(1):629–646, 2018.

[9] L. Hanzo et al. Near-Capacity Wireless Transceivers and Cooperative Communications in the MIMO Era: Evolution of Standards, Waveform Design, and Future Perspectives. *Proceedings of the IEEE*, 99(8):1343–1385, 2011.

[10] R. Steele and L. Hanzo. *Mobile Radio Communications: Second and Third Generation Cellular and WATM Systems*. IEEE Press - John Wiley, May 1999. Address: Chichester, UK.

[11] A. J. Viterbi and R. Padovani. Implications of mobile cellular CDMA. *IEEE Communications Magazine*, 30(12):38–41, 1992.

[12] J. Korhonen. *Introduction to 4G Mobile Communications*. 2014.

[13] M. Vaezi et al. *Multiple Access Techniques for 5G Wireless Networks and Beyond*. Springer, 2019.

[14] J. Zhang et al. Turbo Multi-User Detection for OFDM/SDMA Systems Relying on Differential Evolution Aided Iterative Channel Estimation. *IEEE Transactions on Communications*, 60(6):1621–1633, 2012.

[15] Z. Ding et al. Application of Non-Orthogonal Multiple Access in LTE and 5G Networks. *IEEE Communications Magazine*, 55(2):185–191, 2017.

[16] Y. Saito et al. Non-orthogonal multiple access (NOMA) for cellular future radio access. In *Proc. IEEE VTC Spring*, pp. 1–5, Dresden, Germany, June 2013.

[17] A. Benjebbour et al. Non-orthogonal multiple access (NOMA): Concept, performance evaluation and experimental trials. In *Proc. WINCOM*, pp. 1–6, Marrakech, Morocco, Oct. 2015.

[18] A. Benjebbour et al. NOMA: From concept to standardization. In *Proc. IEEE CSCN*, pp. 18–23, Tokyo, Japan, Oct. 2015.

[19] Z. Ding et al. On the performance of non-orthogonal multiple access in 5G systems with randomly deployed users. 21(12):1501–1505, Dec. 2014.

[20] M. Al-Imari et al. Uplink non-orthogonal multiple access for 5G wireless networks. In *Proc. ISWCS*, pp. 781–785, Barcelona, Spain, Aug. 2014.

[21] Q. Sun et al. On the Ergodic Capacity of MIMO NOMA Systems. *IEEE Wireless Commun. Lett.*, 4(4):405–408, Aug. 2015.

[22] Z. Ding et al. The application of MIMO to non-orthogonal multiple access. 15(1):537–552, Jan. 2016.

[23] Z. Ding et al. A general MIMO framework for NOMA downlink and uplink transmission based on signal alignment. 15(6):4438–4454, June 2016.

[24] M. Hanif et al. A Minorization-Maximization Method for Optimizing Sum Rate in the Downlink of Non-Orthogonal Multiple Access Systems. 64(1):76–88, Jan. 2016.

[25] J. Choi. Minimum power multicast beamforming with superposition coding for multiresolution broadcast and application to NOMA systems. 63(3):791–800, Mar. 2015.

[26] X. Sun et al. Non-orthogonal Multiple Access with Weighted Sum-Rate Optimization for Downlink Broadcast Channel. In *Proc. IEEE MILCOM*, pp. 1176–1181, Tampa, FL, Oct. 2015.

[27] Z. Ding and H. Poor. Design of massive-MIMO-NOMA with limited feedback. 23(5):629–633, May 2016.

[28] T. Takeda and K. Higuchi. Enhanced User Fairness Using Non-Orthogonal Access with SIC in Cellular Uplink. In *2011 IEEE Vehicular Technology Conference (VTC Fall)*, pp. 1–5, Sept 2011.

[29] S. Tomida and K. Higuchi. Non-orthogonal access with SIC in cellular downlink for user fairness enhancement. In *2011 International Symposium on Intelligent Signal Processing and Communications Systems (ISPACS)*, pp. 1–6, Dec 2011.

[30] Z. Ma et al. A General Framework for MIMO Uplink and Downlink Transmissions in 5G Multiple Access. In *2016 IEEE 83rd Vehicular Technology Conference (VTC Spring)*, pp. 1–4, May 2016.

[31] Y. Saito et al. System-level performance evaluation of downlink non-orthogonal multiple access (NOMA). In *2013 IEEE 24th Annual International Symposium on Personal, Indoor, and Mobile Radio Communications (PIMRC)*, pp. 611–615, Sept 2013.

[32] B. Kimy et al. Non-orthogonal Multiple Access in a Downlink Multiuser Beamforming System. In *MILCOM 2013 - 2013 IEEE Military Communications Conference*, pp. 1278–1283, Nov 2013.

[33] Q. Zhang et al. Robust Beamforming for Nonorthogonal Multiple-Access Systems in MISO Channels. *IEEE Transactions on Vehicular Technology*, 65(12):10231–10236, Dec 2016.

[34] F. Alavi et al. Robust Beamforming Techniques for Non-Orthogonal Multiple Access Systems with Bounded Channel Uncertainties. *IEEE Communications Letters*, PP(99):1–1, 2017.

[35] Z. Luo et al. Semidefinite Relaxation of Quadratic Optimization Problems. 27(3):20–34, May 2010.

[36] C. Shen et al. Wireless Information and Energy Transfer in Multi-Antenna Interference Channel. *IEEE Trans. Signal Process.*, 62(23):6249–6264, Dec. 2014.

[37] 5G concept, 5G key technology-novel multiple access. White Paper, Feb. 2015.

[38] B. Makki et al. A Survey of NOMA: Current Status and Open Research Challenges. *IEEE Open Journal of the Communications Society*, 1:179–189, 2020.

[39] 5G Access: Requirements, concept and technologies. White Paper, July 2014.

[40] T. Cover. Broadcast channels. 18(1):2–14, Jan. 1972.

[41] Y. Saito et al. Non-Orthogonal Multiple Access (NOMA) for Cellular Future Radio Access. In *2013 IEEE 77th Vehicular Technology Conference (VTC Spring)*, pp. 1–5, 2013.

[42] R. Zhang and L. Hanzo. A unified treatment of superposition coding aided communications: Theory and practice. *IEEE Communications Surveys Tutorials*, 13(3):503–520, 2011.

[43] D. Tse and P. Viswanath. Cambridge Univ. Press, 2005.

[44] A. Benjebbovu et al. System-level performance of downlink NOMA for future LTE enhancements. In *2013 IEEE Globecom Workshops (GC Wkshps)*, pp. 66–70, 2013.

[45] Z. Ding et al. On the performance of non-orthogonal multiple access in 5G systems with randomly deployed users. *IEEE Signal Processing Letters*, 21(12):1501–1505, 2014.

[46] P. Xu et al. A New Evaluation Criterion for Non-Orthogonal Multiple Access in 5G Software Defined Networks. *IEEE Access*, 3:1633–1639, 2015.

[47] S. Timotheou and I. Krikidis. Fairness for Non-Orthogonal Multiple Access in 5G Systems. *IEEE Signal Processing Letters*, 22(10):1647–1651, Oct 2015.

[48] M. Al-Imari et al. Uplink non-orthogonal multiple access for 5G wireless networks. In *2014 11th International Symposium on Wireless Communications Systems (ISWCS)*, pp. 781–785, 2014.

[49] M. Al-Imari et al. Receiver and resource allocation optimization for uplink noma in 5G wireless networks. In *2015 International Symposium on Wireless Communication Systems (ISWCS)*, pp. 151–155, Aug 2015.

[50] S. Chen et al. A suboptimal scheme for uplink noma in 5G systems. In *2015 International Wireless Communications and Mobile Computing Conference (IWCMC)*, pp. 1429–1434, 2015.

[51] K. HIGUCHI and A. BENJEBBOUR. Non-orthogonal Multiple Access (NOMA) with Successive Interference Cancellation for Future Radio Access. *IEICE Transactions on Communications*, E98.B(3):403–414, 2015.

[52] Q. Sun et al. On the Ergodic Capacity of MIMO NOMA Systems. *IEEE Wireless Communications Letters*, 4(4):405–408, 2015.

[53] J. Choi. Minimum Power Multicast Beamforming With Superposition Coding for Multiresolution Broadcast and Application to NOMA Systems. *IEEE Transactions on Communications*, 63(3):791–800, March 2015.

[54] Z. Ding et al. A General MIMO Framework for NOMA Downlink and Uplink Transmission Based on Signal Alignment. *IEEE Transactions on Wireless Communications*, 15(6):4438–4454, 2016.

[55] Z. Ding et al. MIMO-NOMA Design for Small Packet Transmission in the Internet of Things. *IEEE Access*, 4:1393–1405, 2016.

[56] K. Higuchi and Y. Kishiyama. Non-Orthogonal Access with Random Beamforming and Intra-Beam SIC for Cellular MIMO Downlink. In *2013 IEEE 78th Vehicular Technology Conference (VTC Fall)*, pp. 1–5, Sept 2013.

[57] A. Benjebbour and Y. Kishiyama. Combination of NOMA and MIMO: Concept and Experimental Trials. In *2018 25th International Conference on Telecommunications (ICT)*, pp. 433–438, 2018.

[58] J. Men and J. Ge. Performance analysis of non-orthogonal multiple access in downlink cooperative network. *IET Communications*, 9(18):2267–2273, 2015.

[59] J. Men and J. Ge. Non-Orthogonal Multiple Access for Multiple-Antenna Relaying Networks. *IEEE Communications Letters*, 19(10):1686–1689, 2015.

[60] Z. Ding et al. Cooperative Non-Orthogonal Multiple Access in 5G Systems. *IEEE Communications Letters*, 19(8):1462–1465, 2015.

[61] Z. Ding et al. Relay Selection for Cooperative NOMA. *IEEE Wireless Communications Letters*, 5(4):416–419, 2016.

[62] Z. Yang et al. Novel Relay Selection Strategies for Cooperative NOMA. *IEEE Transactions on Vehicular Technology*, 66(11):10114–10123, 2017.

[63] M. Zeng et al. Cooperative NOMA: State of the Art, Key Techniques, and Open Challenges. *IEEE Network*, 34(5):205–211, 2020.

[64] Z. Yang et al. The Impact of Power Allocation on Cooperative Non-orthogonal Multiple Access Networks With SWIPT. *IEEE Transactions on Wireless Communications*, 16(7):4332–4343, 2017.

[65] Y. Tian et al. On the Performance of Opportunistic NOMA in Downlink CoMP Networks. *IEEE Communications Letters*, 20(5):998–1001, 2016.

[66] Z. Ding et al. Impact of User Pairing on 5G Nonorthogonal Multiple-Access Downlink Transmissions. *IEEE Transactions on Vehicular Technology*, 65(8):6010–6023, Aug 2016.

[67] M. Shirvanimoghaddam et al. Massive Non-Orthogonal Multiple Access for Cellular IoT: Potentials and Limitations. *IEEE Communications Magazine*, 55(9):55–61, 2017.

[68] Z. Ding et al. A Survey on Non-Orthogonal Multiple Access for 5G Networks: Research Challenges and Future Trends. *IEEE Journal on Selected Areas in Communications*, 35(10):2181–2195, 2017.

[69] C.-Y. Chi et al. *Convex Optimization for Signal Processing and Communications*. Boca Raton: CRC Press, 2017.

[70] D. P. Palomar and Y. C. Eldar. *Convex optimization in signal processing and communications*. Cambridge university press, 2010.

[71] H. Hindi. A tutorial on convex optimization. In *Proceedings of the 2004 American Control Conference*, volume 4, pp. 3252–3265. IEEE, 2004.

[72] S. Boyd and L. Vandenberghe. *Convex Optimization*. Cambridge University Press, New York, 2004.

[73] A. Beck. *Introduction to Nonlinear Optimization*. Society for Industrial and Applied Mathematics, Philadelphia, PA, 2014.

[74] H. Hindi. A tutorial on convex optimization II: duality and interior point methods. In *2006 American Control Conference*, pp. 11–pp. IEEE, 2006.

[75] Z. Luo et al. Semidefinite Relaxation of Quadratic Optimization Problems. *IEEE Signal Processing Magazine*, 27(3):20–34, 2010.

[76] A. B. Gershman et al. Convex Optimization-Based Beamforming. *IEEE Signal Processing Magazine*, 27(3):62–75, 2010.

[77] Y. Huang and D. P. Palomar. Rank-Constrained Separable Semidefinite Programming With Applications to Optimal Beamforming. *IEEE Transactions on Signal Processing*, 58(2):664–678, 2010.

[78] S. Boyd et al. *Linear Matrix Inequalities in System and Control Theory*. Society for Industrial and Applied Mathematics, 1994.

[79] T. Cover and J. Thomas. *Elements of Information Theory*. Wiley, New York, NY, 2006.

[80] M. Grant and S. Boyd. CVX: Matlab software for disciplined convex programming, version 2.1. `http://cvxr.com/cvx`, 2014.

[81] B. Kim et al. Non-orthogonal Multiple Access in a Downlink Multiuser Beamforming System. In *Proc. IEEE MILCOM*, pp. 1278–1283, San Diego, CA, Nov. 2013.

[82] Y. Huang and D. Palomar. Rank-Constrained Separable Semidefinite Programming With Applications to Optimal Beamforming. 58(2):664–678, Feb. 2010.

[83] H. Tuy. *D.C. Optimization: Theory, Methods and Algorithms*, pp. 149–216. Springer US, Boston, MA, 1995.

[84] S. Hong et al. Applications of self-interference cancellation in 5G and beyond. *IEEE Communications Magazine*, 52(2):114–121, 2014.

[85] J. Gong et al. Transmission Optimization for Hybrid Half/Full-Duplex Relay With Energy Harvesting. *IEEE Transactions on Wireless Communications*, 17(5):3046–3058, 2018.

[86] Z. Zhang et al. Full-Duplex Device-to-Device-Aided Cooperative Nonorthogonal Multiple Access. *IEEE Transactions on Vehicular Technology*, 66(5):4467–4471, 2017.

[87] G. Liu et al. Hybrid Half-Duplex/Full-Duplex Cooperative Non-Orthogonal Multiple Access With Transmit Power Adaptation. *IEEE Transactions on Wireless Communications*, 17(1):506–519, 2018.

[88] Y. Yuan et al. Energy Efficiency Optimization in Full-Duplex User-Aided Cooperative SWIPT NOMA Systems. *IEEE Transactions on Communications*, 67(8):5753–5767, 2019.

[89] W. Liang et al. User Pairing for Downlink Non-Orthogonal Multiple Access Networks Using Matching Algorithm. *IEEE Transactions on Communications*, 65(12):5319–5332, 2017.

[90] Z. Ding and H. V. Poor. On the Application of BAC-NOMA to 6G umMTC, 2021.

[91] Z. Ding et al. Unveiling the Importance of SIC in NOMA Systems—Part 1: State of the Art and Recent Findings. *IEEE Communications Letters*, 24(11):2373–2377, 2020.

[92] Z. Ding et al. Unveiling the Importance of SIC in NOMA Systems: Part II: New Results and Future Directions, 2020.

[93] Z. Ding et al. Joint Power and Time Allocation for NOMA–MEC Offloading. *IEEE Transactions on Vehicular Technology*, 68(6):6207–6211, 2019.

[94] M. Mahdavi et al. Stochastic convex optimization with multiple objectives. *Advances in Neural Information Processing Systems*, 26:1115–1123, 2013.

[95] Z. Ding et al. No-Pain No-Gain: DRL Assisted Optimization in Energy-Constrained CR-NOMA Networks. 12 2020.

[96] X.-D. Zhang. *Matrix Analysis and Applications*. Cambridge University Press, 2017.

Appendix A

A.1 $\mathcal{S}$-lemma

$\mathcal{S}$-lemma is an alternative method to represent the $\mathcal{S}$-procedure, which can be proven via strong duality. It is stated as following,

$\mathcal{S}$-lemma: *Let* $\mathbf{Q}_1,\ \mathbf{Q}_2 \in \mathbb{S}^n$ *and assume that* $\mathbf{y}^T\mathbf{Q}_1\mathbf{y} > 0$ *for some vector* $\mathbf{y} \in \mathbb{R}^n$. *Then, the implication*

$$\mathbf{z}^T\mathbf{Q}_1\mathbf{z} \geq 0 \Rightarrow \mathbf{z}^T\mathbf{Q}_2\mathbf{z} \geq 0 \tag{A.1}$$

is valid if and only if

$$\mathbf{Q}_2 \succeq \lambda\mathbf{Q}_1 \text{ for some } \lambda \geq 0. \tag{A.2}$$

Where,

$$\mathbf{Q}_1 = -\begin{bmatrix} \mathbf{A}_1 & \mathbf{b}_1 \\ \mathbf{b}_1^T & h_2 \end{bmatrix},\ \mathbf{Q}_2 = -\begin{bmatrix} \mathbf{A}_2 & \mathbf{b}_2 \\ \mathbf{b}_2^T & h_2 \end{bmatrix}, \tag{A.3}$$

and $\mathbf{A}_i$, $\mathbf{b}_i$ and h_i are the corresponding parameters mentioned in the S-procedure. Then the implication including the two quadratic inequalities in (2.21) accords to (A.1) with $\mathbf{z} = (\mathbf{x}, \mathbf{1})$; the assumption $\hat{\mathbf{x}}^T\mathbf{A}_1\hat{\mathbf{x}} + 2\mathbf{b}_1^T\hat{\mathbf{x}} + h_1 > 0$ corresponds to $\mathbf{y}^T\mathbf{Q}_1\mathbf{y} > 0$ with $\mathbf{y} = (\hat{\mathbf{x}}, 1)$; the LMI given by (2.18) corresponds to (A.2).

Proof: To prove the sufficient condition (A.2) $\Rightarrow$ (A.1). Caused by $\mathbf{Q}_2 - \lambda\mathbf{Q}_1 \succeq$

$\mathbf{0}$ for some $\lambda \geq 0$ and $\mathbf{z}^T\mathbf{Q}_1\mathbf{z} \geq 0$, then

$$\mathbf{z}^T(\mathbf{Q}_2 - \lambda\mathbf{Q}_1)\mathbf{z} \geq 0 \text{ and } \mathbf{z}^T\mathbf{Q}_1\mathbf{z} \geq 0 \Rightarrow \mathbf{z}^T\mathbf{Q}_2\mathbf{z} \geq \lambda\mathbf{z}^T\mathbf{Q}_1\mathbf{z} \geq 0. \tag{A.4}$$

Subsequently, the sufficient condition is proved.

Next, to prove the sufficient condition (A.1) $\Rightarrow$ (A.2). So, look at the coming convex problem:

$$s^\star = \max_{s,\lambda\in\mathbb{R}} \quad s \tag{A.5a}$$

$$\text{s.t.} \quad \mathbf{Q}_2 - \lambda\mathbf{Q}_1 \succeq s\mathbf{I}_n, \tag{A.5b}$$

$$\lambda \geq 0. \tag{A.5c}$$

If $s^\star \geq 0$ then the statement of (A.2) is true. Thus, it satisfies to demonstrate that $s^\star$ is nonnegative, provided that $\mathbf{z}^T\mathbf{Q}_1\mathbf{z} \geq 0 \Rightarrow \mathbf{z}^T\mathbf{Q}_2\mathbf{z} \geq 0$ holds true. As there occurs some vector $\mathbf{y} \in \mathbb{R}^n$ such that $\mathbf{y}^T\mathbf{Q}_1\mathbf{y} > 0$, the matrix $\mathbf{Q}_1$ must have a positive eigenvalue. As an illustration, there exists $a > 0$ and $\mathbf{v} \in \mathbb{R}^n$ with $\|\mathbf{v}\|_2$ so $\mathbf{A}\mathbf{v} = a\mathbf{v}$. Then, $\mathbf{v}^T(\mathbf{Q}_2 - \lambda\mathbf{Q}_1)\mathbf{v} = \mathbf{v}^T\mathbf{Q}_2\mathbf{v} - \lambda a \leq \mathbf{v}^T\mathbf{Q}_2\mathbf{v}$, from (A.5b) $s \leq \mathbf{v}^T\mathbf{Q}_2\mathbf{v}$, imposing that the optimal value of (A.5) is bounded above $s^\star < \infty$.

Since (A.5) is convex and satisfies Slater's condition strong duality holds true. So the optimal value $s^\star$ of problem (A.6) which is also feasible as well

$$s^\star = \min_{\mathbf{X}\in\mathbb{S}^n} \quad \text{Tr}(\mathbf{Q}_2\mathbf{X}) \tag{A.6a}$$

$$\text{s.t.} \quad \text{Tr}(\mathbf{Q}_1\mathbf{X}) \geq 0, \tag{A.6b}$$

$$\text{Tr}(\mathbf{X}) = 1, \tag{A.6c}$$

$$\mathbf{X} \succeq 0. \tag{A.6d}$$

Let $\mathbf{X}^\star = \mathbf{D}\mathbf{D}^T$ be an optimal solution to problem (A.6) Then, the identified constraint (A.6b) and the optimal value can be written as

$$0 \leq \text{Tr}(\mathbf{Q}_1\mathbf{X}^\star) = \text{Tr}(\mathbf{D}\mathbf{Q}_1\mathbf{D}^T), \tag{A.7a}$$

$$s^\star = \text{Tr}(\mathbf{Q}_2\mathbf{X}^\star) = \text{Tr}(\mathbf{D}\mathbf{Q}_2\mathbf{D}^T). \tag{A.7b}$$

Assuming $s^\star < 0$ and $\mathbf{K} = \mathbf{D}\mathbf{Q}_1\mathbf{D}^T$and $\mathbf{P} = \mathbf{D}\mathbf{Q}_2\mathbf{D}^T$, so $\text{Tr}(\mathbf{K}) \geq 0$ and $\text{Tr}(\mathbf{P}) = s^\star$.

Giving by Lemma3, there exists a vector $\mathbf{x}$ such that

$$\mathbf{x}^T\mathbf{K}\mathbf{x} = (\mathbf{D}\mathbf{x})^T\mathbf{Q}_1(\mathbf{D}\mathbf{x}) \geq 0 \text{ and } \mathbf{x}^T\mathbf{P}\mathbf{x} = (\mathbf{D}\mathbf{x})^T\mathbf{Q}_2(\mathbf{D}\mathbf{x}) < 0,$$

which contradicts the assumption $\mathbf{z}^T\mathbf{Q}_1\mathbf{z} \geq 0 \Rightarrow \mathbf{z}^T\mathbf{Q}_2\mathbf{z} \geq 0$ where $\mathbf{z} = \mathbf{D}\mathbf{x}$. Therefore, $s^\star \geq 0$ and the proof of S-lemma is complete [69].

Lemma 3 *Let* $\mathbf{K}, \mathbf{P} \in \mathbb{S}^n$ *with* $Tr(\mathbf{K}) \geq 0$ *and* $Tr(\mathbf{P}) < 0$. *Then, there exists a vector* $\mathbf{x}\mathbf{in}\mathbb{R}^\mathbf{n}$ *such that* $\mathbf{x}^T\mathbf{K}\mathbf{x} \geq 0$ *and* $\mathbf{x}^T\mathbf{P}\mathbf{x} < 0$.

Proof: Let $\mathbf{K} = \mathbf{U}\mathbf{\Lambda}\mathbf{U}^T$ where $\mathbf{U}$is an orthogonal matrix and $\mathbf{\Lambda} = \mathbf{Diag}(\lambda_\mathbf{1}, \ldots, \lambda_\mathbf{n})$ is a diagonal matrix formed by its eigenvalues. Let $\mathbf{w} \in \mathbb{R}^n$ be a discrete random vector with i.i.d. entries taking on values of 1 or -1 with equal probability (1/2). Then,

$$(\mathbf{U}\mathbf{w})^T\mathbf{K}(\mathbf{U}\mathbf{w}) = (\mathbf{U}\mathbf{w})^T\mathbf{U}\mathbf{\Lambda}\mathbf{U}^T(\mathbf{U}\mathbf{w}) = \mathbf{w}^T\mathbf{\Lambda}\mathbf{w} = \mathrm{Tr}(\mathbf{K}) < 0 \tag{A.8}$$

$$(\mathbf{U}\mathbf{w})^T\mathbf{P}(\mathbf{U}\mathbf{w}) = \mathbf{w}^T(\mathbf{U}^T\mathbf{P}\mathbf{U})\mathbf{w} \tag{A.9}$$

Taking expectation of the quadratic function of $\mathbf{w}$ in (A.9) yields

$$\mathbb{E}\{(\mathbf{U}\mathbf{w})^T\mathbf{P}(\mathbf{U}\mathbf{w})\} = \mathrm{Tr}(\mathbf{U}^T\mathbf{P}\mathbf{U}\ \mathbb{E}\{\mathbf{w}\mathbf{w}^\mathbf{T}\}) = \mathrm{Tr}(\mathbf{P}) \geq \mathbf{0}, \tag{A.10}$$

where $\mathbb{E}\{\mathbf{w}\mathbf{w}^T\} = \mathbf{I}_n$. By (A.8) and (A.10), there exists at least one vector $\mathbf{w} \in \mathbb{R}^n$ such that $(\mathbf{U}\mathbf{w})^T\mathbf{K}(\mathbf{U}\mathbf{w}) < 0$ and $(\mathbf{U}\mathbf{w})^T\mathbf{P}(\mathbf{U}\mathbf{w}) \geq 0$, i.e., there exists an $\mathbf{x} = \mathbf{U}\mathbf{w}$ such that $\mathbf{x}^T\mathbf{K}\mathbf{x} \geq 0$ and $\mathbf{x}^T\mathbf{P}\mathbf{x} < 0$.

Appendix B

Proposition 1 *If a block Hermition matrix* $\mathbf{B} = \begin{bmatrix} \mathbf{B_1} & \mathbf{B}_2 \\ \mathbf{B}_3 & \mathbf{B}_4 \end{bmatrix} \succeq 0$ *then the main diagonal matrices* $\mathbf{B_1}$ *and* $\mathbf{B_4}$ *must be positive definite (PSD) matrices [96].*

PROOF of *Lemma* 2

To prove (4.16) is a rank(1), the Karush-Kuhn-Tucker (KKT) conditions are examined. First, let $\mathbf{Y}_l \in \mathbb{C}^{M\times M}$,$\mathbf{T}_l, \mathbf{T}_{il} \in \mathbb{C}^{(M+1)\times(M+1)}$ and , $\mu_l\mu_t \in \mathbb{R}_+$ denote the dual variable of the constraints in (4.16), respectively. Then, the Lagrangian dual function of (4.16) can be written as

$$\begin{aligned}\mathcal{L}(t, \mathbf{W}_l, \lambda_l, \mathbf{T}_l, \lambda_{il}, \mathbf{T}_{il}, \mu_l, \mu_t) &= -t + \sum_l \mathrm{Tr}(\mathbf{T}_l\mathbf{C}_l) \\ &+ \sum_{il} \mathrm{Tr}(\mathbf{T}_{il}\mathbf{D}_{il}) - \mu_t(\mathrm{Tr}(\sum_l \mathbf{W}_l) - P_T) \\ &+ \sum_l \mathrm{Tr}(\mathbf{Y}_l\mathbf{W}_l) + \sum_l \mathrm{Tr}(\mathbf{W}_l), \end{aligned} \tag{B.1}$$

let $\mathbf{A}_1 = \begin{pmatrix} \lambda_l \mathbf{I} & 0 \\ 0 & -\lambda_l \epsilon^2 - \sigma_l^2 \end{pmatrix}$,

$\mathbf{A}_2 = \begin{pmatrix} -\sum_{m=1}^{l} \mathbf{W}_m & 0 \\ 0 & 0 \end{pmatrix}$, and $\mathbf{H}_l = \begin{bmatrix} \mathbf{I} & h_l \end{bmatrix}$. then

$$\mathcal{L}(t, \mathbf{W}_l, \lambda_l, \mathbf{T}_l, \lambda_{il}, \mathbf{T}_{il}, \mu_l, \mu_t) = -t + \sum_l \mathrm{Tr}(\mathbf{T}_l \mathbf{A_1})$$

$$+ \sum_l \mathrm{Tr}(\mathbf{T}_l \mathbf{H}_l^{\mathbf{H}} (\frac{\mathbf{W}_l}{t} - \sum_{m=l+\mathbf{1}}^{K} \mathbf{W}_m) \mathbf{H}_l) + \sum_l \mathrm{Tr}(\mathbf{T}_l \mathbf{A_2})$$

$$\sum_{il} \mathrm{Tr}(\mathbf{T}_{il} \mathbf{D}_{il}) - \mu_t (\mathrm{Tr}(\sum_l \mathbf{W}_l) - P_T) + \sum_l \mathrm{Tr}(\mathbf{Y}_l \mathbf{W}_l)$$

$$+ \sum_l \mathrm{Tr}(\mathbf{W}_l). \tag{B.2}$$

The following KKT conditions hold for (4.16)

$$\frac{\partial \mathcal{L}}{\partial \mathbf{W}_l} = 0, \tag{B.3}$$

$$\Rightarrow \sum_{j=l}^{l-1} \mathbf{H}_l^H \mathbf{T}_j (\frac{\mathbf{1}}{t} - \mathbf{1}) \mathbf{H}_l - \sum_{j=l+\mathbf{1}}^{K} \mathbf{T}_j - \mu_t + \mathbf{Y}_l + \mathbf{I} = \mathbf{0}, \tag{B.4}$$

$$\mathbf{Y}_l \mathbf{W}_l = 0, \tag{B.5}$$

$$\mathbf{T}_l (\mathbf{A_1} + \mathbf{H}_l^{\mathbf{H}} (\frac{\mathbf{W}_l}{t} - \sum_{m=l+\mathbf{1}}^{K} \mathbf{W}_m) \mathbf{H}_l + \mathbf{A_2}), \tag{B.6}$$

$$\mu_t (\mathrm{Tr}(\sum_l \mathbf{W}_l) - P_T) = 0. \tag{B.7}$$

by pre-multiplying (B.4) by $\mathbf{W}_l$, i.e,

$$\mathbf{H}_l^H \mathbf{T}_j \frac{\mathbf{W}_l}{t} \mathbf{H}_l = \mathbf{W}_l (\sum_{\mathbf{j=l}}^{l-\mathbf{1}} \mathbf{H}_l^{\mathbf{H}} \mathbf{T}_j \mathbf{H}_l + \sum_{j=l+\mathbf{1}}^{K} \mathbf{T}_j - \mathbf{I}), \tag{B.8}$$

then the rank relation can be written as following

$$\mathrm{rank}(\mathbf{W}_l) = \mathrm{rank}[\mathbf{W}_l (\sum_{\mathbf{j=l}}^{l-\mathbf{1}} \mathbf{H}_l^{\mathbf{H}} \mathbf{T}_j \mathbf{H}_l + \sum_{j=l+\mathbf{1}}^{K} \mathbf{T}_j - \mathbf{I})], \tag{B.9}$$

$$= \mathrm{rank}(\mathbf{W}_l \mathbf{H}_l^H \mathbf{T}_l \mathbf{H}_l), \tag{B.10}$$

$$\leq \min \left\{ \mathrm{rank}(\mathbf{H}_l^H \mathbf{T}_l \mathbf{H}_l), \mathrm{rank}(\mathbf{W}_l) \right\}. \tag{B.11}$$

Based on (B.11), it is required to show $\text{rank}(\mathbf{H}_l^H \mathbf{T}_l \mathbf{H}_l) \leq \mathbf{1}$ if $\text{rank}(\mathbf{W}_l) \leq \mathbf{1}$ is claimed. The following equations and *Proposition* 1 should be considered:

$$[\ \mathbf{I}\quad \mathbf{0}\ ]\mathbf{H}_l^H = \mathbf{I}, [\ \mathbf{I}\quad \mathbf{0}\ ]\mathbf{A}_1 = \lambda_l(\mathbf{H}_l - [\ \mathbf{0}_M \quad \mathbf{h}_l\ ]),$$
$$[\ \mathbf{I}\quad \mathbf{0}\ ]\mathbf{A}_2 = -\sum_{m=1}^{l} \mathbf{W}_m(\mathbf{H}_l - [\ \mathbf{0}_M \quad \mathbf{h}_l\ ]). \tag{B.12}$$

Then pre-multiply $[\ \mathbf{I}\quad \mathbf{0}\ ]$ and post-multiply $\mathbf{H}_l^H$ by (B.6), respectively,and applying the equalities in (B.12):

$$\lambda_l(\mathbf{H}_l - [\ \mathbf{0}_M \quad \mathbf{h}_l\ ])\mathbf{T}_l\mathbf{H}_l^H - \sum_{m=\mathbf{1}}^{l} \mathbf{W}_m(\mathbf{H_l}$$
$$- [\ \mathbf{0}_M \quad \mathbf{h_l}\ ])\mathbf{T}_l\mathbf{H}_l^H + (\frac{\mathbf{W}_l}{t} - \sum_{m=l+\mathbf{1}}^{K} \mathbf{W}_m)\mathbf{H}_l\mathbf{T}_l\mathbf{H}_l^H = \mathbf{0}$$
$$\Rightarrow (\lambda_l\mathbf{I} - \sum_{m=l+\mathbf{1}}^{K} \mathbf{W_m} + (\frac{\mathbf{W}_l}{t} - \sum_{m=l+\mathbf{1}}^{K} \mathbf{W}_m))\mathbf{H}_l\mathbf{T}_l\mathbf{H}_l^H$$
$$= (\lambda_l\mathbf{I} - \sum_{m=\mathbf{1}}^{l} \mathbf{W}_m)[\ \mathbf{0}_M \quad \mathbf{h}_l\ ]\mathbf{T}_l\mathbf{H}_l^H. \tag{B.13}$$

By applying *Proposition* 1 to (4.14), $(\lambda_l \mathbf{I} + (\frac{\mathbf{W}_l}{t} - \sum_{m=l+\mathbf{1}}^{K} \mathbf{W}_m) - \sum_{m=\mathbf{1}}^{l} \mathbf{W}_m) \succeq \mathbf{0}$ and is nonsingular; thus, multiplying by a nonsingular matrix will not change the matrix rank. Thus the following rank relation holds:

$$\begin{aligned} \text{rank}(\mathbf{H}_l \mathbf{T}_l \mathbf{H}_l^H) &= \text{rank}((\lambda_\mathbf{l} \mathbf{I} - \sum_{m=\mathbf{1}}^{l} \mathbf{W}_m)[\ \mathbf{0}_M \quad \mathbf{h}_l\ ] \mathbf{T}_l \mathbf{H}_l^H) \\ &\leq \text{rank}([\ \mathbf{0}_M \quad \mathbf{h}_l\ ]) \leq 1. \end{aligned} \tag{B.14}$$

This completes the proof of *Lemma* 2 there always exists a rank-one optimal solution $\mathbf{W}_l^*$